

ZFP36L3: A Unique Member of the Tristetraprolin Family
of RNA-Binding CCCH Tandem Zinc Finger Proteins

by

Elizabeth Dawn Frederick

Department of Biochemistry
Duke University

Date: _____

Approved:

Perry Blackshear, Supervisor

Kenneth Kreuzer

Christopher Newgard

Christian Raetz

Barbara Shaw

Dissertation submitted in partial fulfillment of
the requirements for the degree of Doctor
of Philosophy in the Department of
Biochemistry in the Graduate School
of Duke University

2009

ABSTRACT

ZFP36L3: A Unique Member of the Tristetraprolin Family
of RNA-Binding CCCH Tandem Zinc Finger Proteins

by

Elizabeth Dawn Frederick

Department of Biochemistry
Duke University

Date: _____

Approved:

Perry Blackshear, Supervisor

Kenneth Kreuzer

Christopher Newgard

Christian Raetz

Barbara Shaw

An abstract of a dissertation submitted in partial
fulfillment of the requirements for the degree
of Doctor of Philosophy in the Department of
Biochemistry in the Graduate School
of Duke University

2009

Copyright by
Elizabeth Dawn Frederick
2009

Abstract

Members of the tristetraprolin (TTP) family of CCCH tandem zinc finger proteins bind to AU-rich elements in the 3' untranslated regions of certain cellular mRNAs, leading to their deadenylation and destabilization. Studies in knockout mice have demonstrated roles for three of the family members, TTP, ZFP36L1 (L1), and ZFP36L2 (L2), in inflammation, chorioallantoic fusion, and hematopoiesis, respectively. However, little is known about a recently-discovered TTP family member, ZFP36L3 (L3). Although L3 exhibits similar general biochemical functions to other members of the TTP family, initial studies of this family member revealed a number of unique characteristics.

First, L3 does not shuttle between the nucleus and cytoplasm like TTP, L1, and L2. Through studies of L3 deletion mutants, we determined that a nuclear localization signal that resides within the conserved tandem zinc finger domain was functional, although the C-terminal nuclear export sequence was non-functional. We then demonstrated that the unique repeat domain of L3 was responsible for the “full-time” cytoplasmic localization of the protein and was able to override the ability of the nuclear localization signal to direct transport into the nucleus.

In addition, L3 is specifically expressed in rodent yolk sac and placenta, while the other members of the TTP family exhibit relatively ubiquitous expression. We

further examined the expression of L3 at both the RNA and protein level. Through northern and western blotting, we demonstrated the expression of L3 during mid-to-late gestation in mouse placenta. We also performed immunostaining of placental sections to demonstrate that this protein is exclusively expressed in the cytoplasm of the labyrinthine trophoblast cells and trophoblast giant cells of the placenta.

L3 most likely binds to and promotes the decay of a certain set of mRNA transcripts. Because of its specific sites of expression, we hypothesized that L3 may regulate the decay of a set of mRNAs that are important for the development or physiology of the placenta. We employed the ribonucleoprotein immunoprecipitation-microarray analysis of mouse placenta lysates to identify possible mRNA targets of L3. Our study identified approximately 400 transcripts that were enriched in immunoprecipitates using a highly specific L3 antibody. Some of these transcripts could be bound and downregulated by L3 in a physiological setting. Our top candidate transcript, based on relative enrichment and sequence analysis, was B-type natriuretic peptide, a hormone well-known for its role in cardiac physiology. We confirmed the expression of B-type natriuretic peptide in mouse placenta through northern blotting and in situ hybridization histochemistry. We also verified the ability of L3 to directly bind to and promote the degradation of this transcript in electrophoretic mobility shift assays and co-transfection assays, respectively.

Lastly, L3 demonstrates a unique migration characteristic in denaturing polyacrylamide gel electrophoresis as compared to TTP, L1, and L2. It migrates as two distinct species of M_r ~90,000 and ~100,000. We investigated the basis for this unusual migration in studies of deletion mutants and serine mutants. We found that both phosphorylation and the presence of the conserved C-terminus are required for the existence of the slower-migrating species. We then focused our study on phosphorylation of the C-terminus and discovered that the phosphorylation of Ser721 may play a role in creating the slower-migrating species. We also identified four other phosphorylated residues with mass spectrometry. Finally, we examined the effect of the C-terminus on the function of L3 and determined that this conserved region is not required for mRNA binding or to promote mRNA deadenylation or degradation in our assays.

The work described in this dissertation increases our understanding of this unique tristetraprolin family member, L3. Additional study of this protein is required to further elucidate its role in the physiology of rodent placenta, and to determine whether this role is subsumed by one of the other TTP family members in the placentas of other mammals.

Dedication

To my Mom and Dad for all of their love, support, and encouragement.

Contents

Abstract	iv
Contents.....	viii
List of Tables.....	xii
List of Figures	xiii
List of Abbreviations	xv
Acknowledgements	xviii
1. Introduction	1
1.1 Regulation of gene expression in eukaryotes.....	1
1.2 Messenger RNA decay.....	4
1.3 AU-rich elements and their binding proteins	8
1.4 Tristetraprolin family.....	11
1.4.1 Mammalian proteins of the tristetraprolin family.....	13
1.4.2 Binding the AU-rich element.....	23
1.4.3 Tristetraprolin family members & disease.....	25
1.5 Aim of research.....	27
2. A unique C-terminal repeat domain maintains the cytosolic localization of ZFP36L3	28
2.1 Introduction.....	28
2.2 Methods	31
2.2.1 Plasmids.....	31
2.2.2 Cell culture and transfections.....	35

2.2.3 Fluorescence microscopy.....	35
2.2.4 Leptomycin B treatment.....	36
2.2.5 Analysis of mRNA binding.....	36
2.2.6 Northern blotting and immunoblotting for endogenous L3.....	37
2.2.7 Immunofluorescence of placental sections.....	39
2.3 Results.....	39
2.3.1 Identification of a functional nuclear localization sequence within the TZF domain of L3.....	39
2.3.2 Evaluation of a potential nuclear export sequence within the C-terminus of L3.....	44
2.3.3 Effect of the repeat domain on the subcellular localization of L3.....	47
2.3.4 Subcellular localization of endogenous L3 in mouse placenta.....	49
2.4 Discussion.....	52
3. Identification of candidate mRNA targets of ZFP36L3 using ribonucleoprotein immunoprecipitation-microarray analysis.....	57
3.1 Introduction.....	57
3.2 Methods.....	60
3.2.1 Ribonucleoprotein immunoprecipitation-microarray analysis.....	60
3.2.2 Northern blotting for endogenous BNP mRNA.....	64
3.2.3 In situ hybridization histochemistry.....	64
3.2.4 Plasmids.....	66
3.2.5 Cell culture and transfection.....	68
3.2.6 Analysis of BNP mRNA binding.....	68

3.2.7 Analysis of BNP mRNA degradation.....	70
3.3 Results	71
3.3.1 Identification of potential physiological targets of L3	71
3.3.2 Analysis of BNP mRNA expression in mouse placenta	77
3.3.3 Binding of L3 to the BNP ARE	79
3.3.4 Effect of L3 on the degradation of BNP RNA.....	81
3.4 Discussion.....	84
4. Identification of phosphorylation sites and functional analysis of the conserved C-terminus of ZFP36L3	90
4.1 Introduction.....	90
4.2 Methods	93
4.2.1 Plasmids.....	93
4.2.2 Cell culture and transfection.....	96
4.2.3 Preparation of cell lysates.....	97
4.2.4 Detection of L3 protein by immunoblotting.....	97
4.2.5 Phosphatase treatment of native L3 and serine mutants.....	98
4.2.6 Purification of FLAG-L3 fusion proteins	98
4.2.7 Mass spectrometry	99
4.2.8 Analysis of mRNA binding.....	99
4.2.9 Analysis of mRNA degradation.....	100
4.2.10 <i>In vitro</i> deadenylation assay.....	101
4.3 Results	102

4.3.1 Detection of L3 with various L3 antibodies	102
4.3.2 Phosphatase treatment of full length L3	103
4.3.3 Analysis of deletion mutants	106
4.3.4 Analysis of serine mutants	108
4.3.5 Identification of phosphorylated residues via mass spectrometry	111
4.3.6 Functional activity of full length and truncated L3.....	112
4.4 Discussion.....	120
5. Conclusions and future directions.....	124
5.1 Contributions of the nuclear localization signal, nuclear export signal, and unique repeat domain to the subcellular localization of L3	125
5.2 The role of L3 in placental mRNA decay	127
5.3 The conserved C-terminus and the phosphorylation of L3.....	130
5.4 Concluding remarks.....	132
Appendix.....	134
References	135
Biography	145

List of Tables

Table 1: Potential physiological RNA targets of L3 identified by RIP-Chip analysis of mouse placenta.....	75
Table 2: Primers used in site-directed mutagenesis to create serine mutants.....	95
Table 3: Phosphopeptides analyzed by mass spectrometry	112

List of Figures

Figure 1: RNA translation and degradation pathways	5
Figure 2: Regulation of mRNA decay by ARE binding proteins	10
Figure 3: The conserved tandem zinc finger domain of the tristetraprolin family	11
Figure 4: Alignment of mouse TTP protein family members	20
Figure 5: L3 constructs used to characterize the NLS, NES, and repeat domain.....	32
Figure 6: NLSs and NESs in mouse TTP family members	40
Figure 7: Subcellular distribution of L3 TZF arginine mutants.....	42
Figure 8: Binding activity of L3 TZF and full length L3 arginine mutants.....	43
Figure 9: Effect of LMB on the subcellular localization of full length L2 and L3 and their nuclear export sequences	46
Figure 10: Subcellular distribution of full length L3 and deletion mutants	48
Figure 11: Developmental expression of L3 mRNA and protein in mouse placenta.....	50
Figure 12: Cellular and subcellular localization of endogenous L3.....	51
Figure 13: Design of L3 RIP-Chip experiment	73
Figure 14: BNP as a target of L3.....	76
Figure 15: Expression of BNP RNA in mouse placenta.....	78
Figure 16: Binding of L3 to a BNP ARE probe	80
Figure 17: L3-promoted degradation of BNP RNA	83
Figure 18: Analysis of the two characteristic species of L3	105
Figure 19: Analysis of L3 deletion mutants.....	107
Figure 20: Analysis of L3 serine mutants.....	110

Figure 21: Conservation of the C-terminus within the TTP family	113
Figure 22: Binding activity of truncated L3.....	114
Figure 23: Ability of truncated L3 to promote mRNA degradation	115
Figure 24: Ability of truncated L3 to promote mRNA deadenylation	117
Figure 25: Analysis of reaction rate for deadenylation promoted by truncated L3	119

List of Abbreviations

AM	Adrenomedullin
ANOVA	Analysis of Variance
ANP	A-type Natriuretic Peptide
ARE	AU-rich Element
ARE BP	AU-Rich Element Binding Protein
BNP	B-type Natriuretic Peptide
C	Carboxyl
CIAP	Calf Intestinal Alkaline Phosphatase
CNP	C-type Natriuretic Peptide
DTT	Dithiothreitol
E	Embryonic Day
ECL	Enhanced Chemiluminescence
GFP	Green Fluorescent Protein
GM-CSF	Granulocyte Macrophage-Colony Stimulating Factor
H & E	Hematoxylin & Eosin
HEK	Human Embryonic Kidney
HRP	Horseradish Peroxidase
Ier3	Immediate Early Response 3

IL	Interleukin
iNOS	Inducible Nitric Oxide Synthase
IP	Immunoprecipitation
L1	ZFP36L1
L2	ZFP36L2
L3	ZFP36L3
LMB	Leptomycin B
LPS	Lipopolysaccharide
m ⁷ G	7-Methylguanosine
miRNA	MicroRNA
MK2	Mitogen Activated Protein Kinase Activated Protein Kinase 2
MEM	Minimal Essential Medium
MLP	Marcks-like Protein
N	Amino
NES	Nuclear Export Sequence
NGS	Normal Goat Serum
NLS	Nuclear Localization Sequence
NMD	Nonsense Mediated Decay
PAGE	Polyacrylamide Gel Electrophoresis
PARN	PolyA Ribonuclease

P-bodies	Processing Bodies
PCR	Polymerase Chain Reaction
PBS-CMF	Phosphate Buffered Saline-Calcium Magnesium Free
RIP-Chip	Ribonucleoprotein Immunoprecipitation-Microarray
RISC	RNA-Induced Silencing Complex
SDS	Sodium Dodecyl Sulphate
StAR	Steroidogenic Acute Regulatory
SSC	Saline-Sodium Citrate
SV40	Simian Virus 40
TBS	Tris Buffered Saline
TNF- α	Tumor Necrosis Factor-Alpha
TTP	Tristetraprolin
TZF	Tandem Zinc Finger
UTR	Untranslated Region

Acknowledgements

In many ways, graduate school is like a long-distance hike. With bug bites and twisted ankles, yet also summits and beautiful sunsets, my journey's end is finally in sight. I would like to express my gratitude to all those who have helped me along my way.

First, I would like to thank my advisor, Perry Blackshear, for his guidance. Perry has trained me to think critically and to aptly communicate my data and ideas. My work in Perry's lab has provided me with many skills and experiences that have defined me as a scientist and will aid me in my future career.

I would also like to thank my committee, Ken Kreuzer, Chris Newgard, Chris Raetz, and Barbara Shaw. Over the past six years, they have taken the time to follow my research and to offer their guidance. Their useful advice has helped me to develop my project and to strengthen my training.

I am grateful to all of the members of the Blackshear lab, both past and present. To Betsy Kennington, for knowing the answer to practically everything and for always being available to help. To Wi Lai, for her advice on all things RNA and for sharing many of her reagents and plasmids. To Debbie Stumpo, for teaching me many lab techniques and for providing tissues, RNA, and slides. To Melissa Adkins, for her work on the deadenylation assays, for getting me to think, and for trying to make me tougher.

To Toni Ward, for all of our chats on science and on life. To Michelle Higgin and Silvia Ramos, for taking me under their wing during my first years in the lab and for becoming great mentors and friends. To Wendy Montague, Chris Ellis, Daniel Brown, Thierry Horner, Brandon Cuthbertson, Sri Diah, Vish Kedar, Nihal Cakmakci, Donghui Zhang, Youn-Jeong Choi, and Nishadi Rajapakse, for all of their scientific advice and for making lab fun. I will miss all of you!

I would also like to thank many of the core laboratories at the NIEHS for their work and guidance, specifically, John Ostot in the DNA sequencing core, Bob Petrovich in the protein expression core, Jeff Reece and Jeff Tucker in the confocal microscopy core, Jason Williams in the mass spectrometry core, and Sherry Grissom and Kevin Gerrish in the microarray core.

Finally, I would like to thank my family and friends. Thank you, Mom, Dad, and Abbie, for always being there for me, for believing in me, and for helping me to become the person I am today. Thanks to Heather Wieman, my “tall friend”, my partner in crime, and my hiking and running buddy; to Liz Finger, “the other” Liz, a giver of great advice, my dance partner, and a woman of many facts; and to Kayla Capps, the best roommate anyone could ask for, the biggest Duke basketball fan, and the most selfless person I know. I’ve had the best time with you girls and I want to thank you for being such great friends. Thank you to my very best friend, Will Gersch, for all of your love and for supporting me in many ways, whether proofreading a paper, listening to a

practice seminar, or taking my mind off work with a trip to the Nickel. We've had so many great adventures and I can't wait for more. I love you all very much.

1. Introduction

1.1 Regulation of gene expression in eukaryotes

While some genes are constitutively expressed, others are induced or repressed in response to intra- or extra-cellular signals. The regulation of gene expression is required to control the levels of their encoded products so that the cell may survive in its environment. This regulation is accomplished through the cooperation and interaction of both *cis*- and *trans*-acting factors and can occur at the DNA, RNA, and protein level.

Transcription is one of the best explored stages at which genes can be regulated. Because transcriptional initiation occurs at the beginning of the pathway from DNA to protein, it is also an efficient place for regulation. In eukaryotes, regulation at this level can be attained by a number of mechanisms. For example, the arrangement of chromatin and differential levels of histone acetylation affect the condensation of the gene and the physical availability of the DNA for the transcriptional machinery (Munshi et al., 2009). In addition, the activity of transcription factors aid in positioning RNA polymerase II at the start of the coding sequence by binding to sequences within the promoter, or even within the introns or transcript coding region. A variety of transcription factors work in concert to either repress or enhance the progress of RNA polymerase II along the promoter towards the start site.

Although regulation of gene expression is often thought to be primarily accomplished at the level of transcription, research pertaining to post-transcriptional gene regulation has uncovered the significance of this level of control. Post-transcriptional processes, such as mRNA processing, transport, surveillance, silencing, and turnover, play critical roles in providing the necessary quantity of the appropriate mRNAs to the translational machinery [reviewed in (Moore, 2005)].

After a gene is effectively transcribed, the primary mRNA transcript is processed through splicing, and through addition of a 5' 7-methylguanosine (m⁷G) cap and a 3' polyA tail. Alternative splicing of the transcript through the removal of introns can alter the expression levels of different sequence isoforms and can result in expression of proteins with differing activities or functions (Kornblihtt, 2007). The addition of the 5' m⁷G cap protects the transcript from 5' to 3' exonuclease activity and also binds eukaryotic initiation factor 4E to promote recruitment of the ribosome (Sonenberg, 2008). The addition of the 3' polyA tail shields the mRNA from 3' to 5' exonuclease activity and promotes export of the mRNA from the nucleus (Dreyfus and Regnier, 2002). Both the m⁷G cap and polyA tail are critical components in creating circular mRNAs. The cap binding protein complex and members of the polyA binding protein family interact to pull the 5' and 3' ends of the transcript together, resulting in a circular mRNA that can be more efficiently translated, and also protects the mRNA from degradation (Mangus et

al., 2003). Thus, the stability of the mRNA, the rate of translation, and the activity of the encoded protein may be regulated through mRNA processing.

The export of mRNA from the nucleus into the cytoplasm is largely controlled by the components of nuclear pore complexes and their interacting proteins (Kohler and Hurt, 2007). Once mRNA has been exported into the cytoplasm, it can be transported to processing bodies (P-bodies) or stress granules where it can be sequestered or degraded (Anderson and Kedersha, 2009). Thus, these intra-cellular transport processes can affect the availability of mRNA to the translational machinery.

Finally, post-transcriptional gene regulation can occur during translation through the modulation of initiation, elongation, and termination factors and by *cis*-acting elements within the RNA. At this step in the central dogma, initiation of translation is the principal target of regulation. For example, post-translational modification of initiation factors, specifically phosphorylation, affects the activity of these proteins which, in turn, hinders the ability of the small subunit of the ribosome to bind the RNA (Pierrat et al., 2007). The presence of secondary structures between the m⁷G cap and the start codon can also prevent the ribosome from scanning along the 5' untranslated region (UTR) to begin translation (van der Velden and Thomas, 1999).

Through regulation of gene expression at each step of the pathway from DNA to RNA to protein, the cell is provided with the necessary tools to survive and function in

its constantly changing environment. This precise regulation is accomplished with the concerted efforts of many proteins and enzymes which are themselves also regulated through these processes.

1.2 Messenger RNA decay

As mRNAs enter the cytoplasm, they can be translated, stored, or degraded in response to the physiological needs of the cell (Fig. 1). The decay of mRNA plays an important role in gene regulation because the control of the steady-state level of mRNA is achieved through both the rate of synthesis, through transcription, and the rate of decay. The half-life of mRNA can vary from minutes to days in eukaryotes. Short-lived mRNAs usually encode proteins that require tight control over their expression, such as regulatory proteins or proteins needed in response to extra-cellular stimuli.

The rate of mRNA decay is controlled largely through the action of proteins that directly bind to sequence elements within the UTRs of the mRNA. Various UTRs can be produced through the use of alternative transcription start sites, polyA sites, or splicing sites. These UTRs can vary between tissues or developmental stages and can affect the pattern of gene expression by containing different regulatory sequence elements. In fact, mRNAs that encode proteins involved in development have been shown to have longer, more complex UTRs, possibly to allow for more complex regulation (Ji et al., 2009). Upon binding to a sequence element in the UTR, RNA binding proteins can act to either

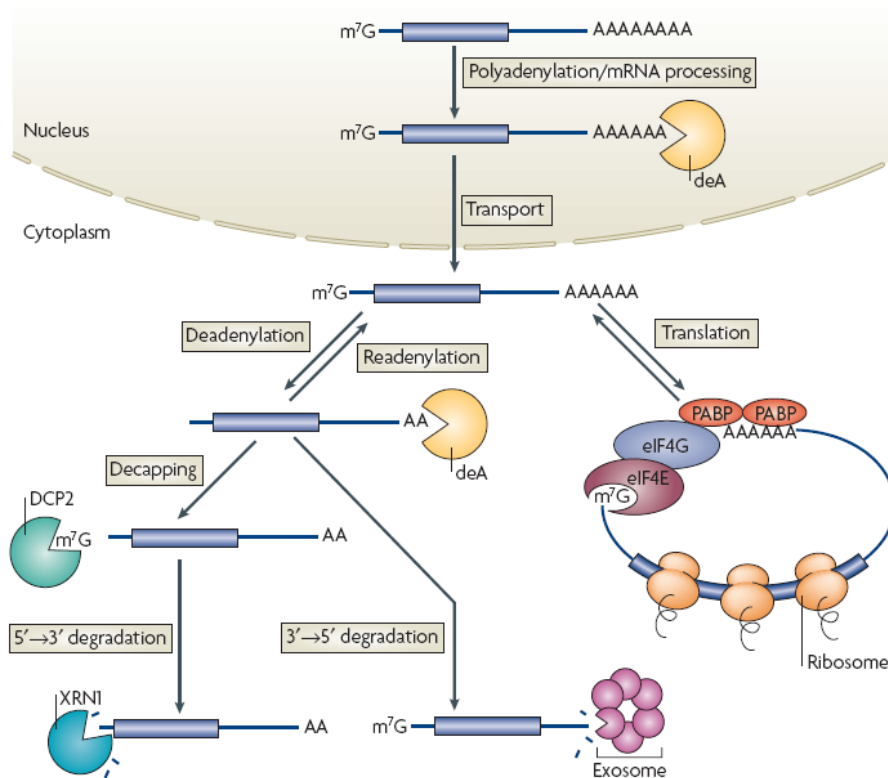


Figure 1: RNA translation and degradation pathways

Upon transcription, mRNAs are processed and transported out of the nucleus where they can be translated or degraded. The association of the cap binding proteins and members of the polyA tail binding protein family promote translation through the formation of circular RNA. Removal of the polyA tail results in RNA degradation through two common pathways. Adapted from (Goldstrohm and Wickens, 2008).

stabilize or destabilize the transcript by preventing or promoting the recruitment of decay enzymes and/or controlling transport to P-bodies or stress granules.

Decay of mRNA is also mediated by the activity of microRNA (miRNA), short, non-coding RNAs that bind to mRNA targets, usually in their 3'UTRs [reviewed in

(Carthew and Sontheimer, 2009)]. According to the needs of the cell, certain miRNAs are processed by Drosha and Pasha in the nucleus and then exported into the cytoplasm. The characteristic stem-loop of the pre-miRNA is cleaved by Dicer to result in a mature miRNA of approximately 22 nucleotides with 3' overhangs. Dicer also promotes the incorporation of one strand of the miRNA into the RNA-induced silencing complex (RISC). The miRNA guides RISC to the target mRNA and forms a duplex. The degree of complementarity between the miRNA and its target sequence dictates the fate the target mRNA. The target will be degraded if the miRNA is highly complementary, while the translation of the target will be repressed if the miRNA is only partially complementary.

Additional regulation of mRNA decay can be achieved through a quality-control mechanism called nonsense mediated decay (NMD) [reviewed in (Matsuda et al., 2008)]. Surveillance through NMD prevents aberrant mRNAs, such as those containing premature stop codons, from being translated into truncated proteins. Aberrant mRNAs are recognized due to the existence of exon-junction protein complexes found downstream of premature stop codons, which are normally removed by the ribosome during translation. Decay enzymes are then recruited to degrade the targeted mRNA.

Two major eukaryotic decay pathways have been described [reviewed in (Goldstrohm and Wickens, 2008)]. In mammals, Pan2/Pan3, the CCR4-NOT complex,

and PARN deadenylate the 3' polyA tail in the first, rate limiting step of both pathways. In the deadenylation-dependent pathway, the 5' m⁷G cap on an incompletely deadenylated mRNA is hydrolyzed to form m⁷GDP and a transcript containing a 5' monophosphate by Dcp1/Dcp2. The resultant transcript is accessible to further degradation by the 5' to 3' exonuclease Xrn1. In the 3' decay pathway, a fully deadenylated transcript is degraded by the exosome, a complex of 3' exonucleases and their associated polypeptides, and the cap is hydrolyzed to produce m⁷GMP by DcpS. These pathways occur within cytoplasmic foci, such as P-bodies.

A third, less common pathway involves endonucleolytic decay. When an mRNA is cleaved by an endonuclease, the 5' product can be degraded by 3' exonucleases as its 3' end is accessible and resembles a deadenylated transcript. The 3' product, on the other hand, can be degraded by 5' exonucleases in a manner similar to a decapped transcript.

While there is evidence that mRNA decay and transcription occur simultaneously, mRNA decay and translation must occur independently since the m⁷G cap and the polyA tail are required for initiation of translation (Sachs and Varani, 2000). This division may exist to prevent mRNA decay intermediates from being translated into truncated proteins that could have a negative effect on the cell.

1.3 AU-rich elements and their binding proteins

The life of an mRNA depends greatly on both key regulatory elements contained within its UTRs, and the activity and availability of their binding proteins. An AU-rich element (ARE) is a *cis*-element located in 3'UTR of many short-lived mRNAs that consists of a region rich in adenosine and uridine nucleotides. In humans, between 5 and 8% of genes code for mRNAs that have putative AREs in their 3'UTRs (Bakheet et al., 2003). Messenger RNAs that contain this repetitive element require specific control over their expression both spatially and temporally. The protein products of many of these mRNAs are required for cell proliferation or response to a stimulus.

The ARE was first identified as a nucleotide sequence that was common in the 3'UTRs of mRNAs encoding proteins important in the inflammatory response, but was rare in mRNAs in general (Caput et al., 1986). This sequence was conserved across humans and rodents for mRNAs such as those encoding tumor necrosis factor-alpha (TNF- α) interleukin (IL)-1, and interferon. The role of the ARE in mRNA decay was demonstrated soon thereafter by studying the stability of a rabbit β -globin reporter containing the ARE of granulocyte macrophage-colony stimulating factor (GM-CSF) within its 3'UTR (Shaw and Kamen, 1986).

AREs are classified into three major groups according to the presence of the pentamer AUUUA (Xu et al., 1997). Class I AREs have one or more pentamers within a

generally U-rich region. This class of ARE can be found in mRNAs such as those encoded by the *c-fos*, *c-myc*, and *IL-4* genes. Class II AREs have multiple overlapping pentamers and a U-rich region. Messenger RNAs with these AREs also usually have the nonamer UUAUUUAUU, which is the minimal sequence that can stimulate decay in reporter systems (Zubiaga et al., 1995). The mRNAs of GM-CSF, IL-2, TNF- α , and interferon- α contain AREs that belong to this class. Class III AREs have no pentamers, but still possess a U-rich region. The ARE sequence in the mRNA of *c-jun* falls into this class.

ARE-containing mRNAs undergo decay in a mechanism that is dependent on initial deadenylation of the transcript [reviewed in (Barreau et al., 2005)]. The polyA tail of RNAs with class I and class III AREs is degraded synchronously, while those of mRNAs with class II AREs are degraded asynchronously, producing transcripts with polyA tails of intermediate lengths. The deadenylated mRNAs are then further degraded by exonucleases and perhaps endonucleases as described earlier.

The mRNA instability that is associated with the presence of an ARE is controlled by proteins that bind to this sequence element. ARE binding proteins (ARE BPs) regulate the turnover of their ARE-containing mRNA targets by promoting or inhibiting their degradation and by influencing translation. ARE BPs can compete for the ARE site in order to exert their functions. For example, some ARE BPs promote the

decay of their ARE-containing RNA targets by recruiting decay complexes, while others inhibit this decay by physically protecting the ARE from binding to decay-promoting proteins (Fig. 2). The destabilizing binding proteins elements primarily exert their regulatory effect by promoting deadenylation (Chen and Shyu, 1995), which will consequently promote the complete degradation of the transcript.

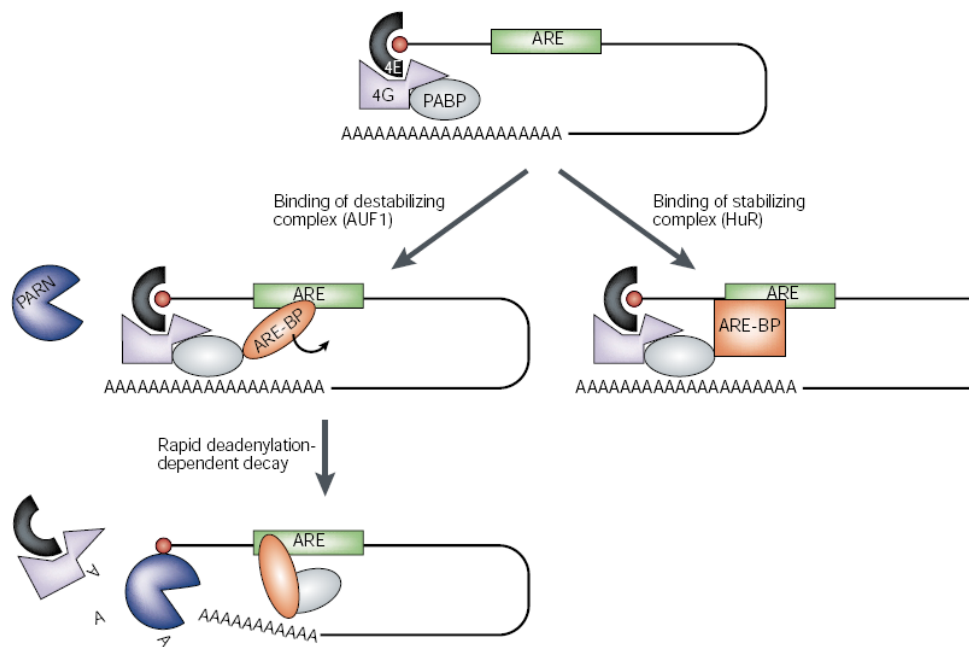


Figure 2: Regulation of mRNA decay by ARE binding proteins

An mRNA can be stabilized through its interaction with ARE binding proteins, such as HuR, which support its circular structure. Conversely, an mRNA can be destabilized through interactions with ARE binding proteins, like AUF1, which promote deadenylation and decay. Adapted from (Wilusz et al., 2001).

It has been suggested that groups of RNA binding proteins regulate post-transcriptional operon networks in eukaryotes. In these networks, RNA binding proteins co-regulate multiple related mRNAs by orchestrating their splicing, transport, and stability. The RNA binding proteins themselves are regulated and may act in concert or in opposition, providing complex control over gene expression (Keene and Tenenbaum, 2002).

1.4 *Tristetraprolin family*

The TTP family was discovered in the early 1990s and is composed of RNA-binding CCCH tandem zinc finger (TZF) proteins. All TTP family members share high percentages of amino acid sequence identity within their TZF domains. This domain contains two independently folding protein motifs, each of which contains three cysteines and one histidine that coordinate a zinc ion. This domain also retains characteristic intra- and inter-finger spacing, and defined “lead-in” sequences (Fig. 3).

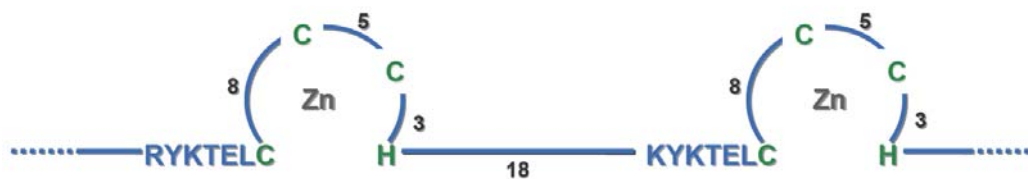


Figure 3: The conserved tandem zinc finger domain of the tristetraprolin family

Each member of the TTP family is distinguished by the conserved intra-finger spacing of C-X8-C-X5-C-X3-H, inter-finger spacing of 18 residues, and the lead-in sequences (R/K)YKTEL. The cysteine and histidine residues that coordinate zinc in each of the two fingers are shown in green.

The TZF domain is responsible for high-affinity binding to AREs found in the 3' UTRs of target mRNAs. The binding of the proteins, in turn, promotes deadenylation and destabilization of the targeted mRNAs (Lai and Blackshear, 2001; Lai et al., 1999; Lai et al., 2000) in a still unclear process that appears to involve decapping and nucleolytic decay.

The mammalian members of the TTP family include TTP, ZFP36L1 (L1), ZFP36L2 (L2), and ZFP36L3 (L3). Similarities among TTP, L1, and L2 in their RNA binding and destabilizing properties suggest functional overlap among the family members, although the differences in transcriptional regulation and cell- and tissue-specific expression suggest different target mRNAs. Interactions between these CCCH TZF proteins and their mRNA targets provide an important regulatory control on gene expression at the post-transcriptional level.

TTP is evolutionarily conserved, with orthologues present in many mammals and other species. Proteins of the TTP family are also present in yeast, flies, frogs, and fish. CTH1 and CTH2 were cloned from budding yeast, *Saccharomyces cerevisiae* (Thompson et al., 1996). These CCCH TZF proteins are expressed during iron deficiency and promote the decay of certain mRNAs in order to alter glucose metabolism under these conditions (Puig et al., 2008). Zfs1, the TTP family member in fission yeast, *Schizosaccharomyces pombe*, could play a role in mating and the coordination of mitosis

(Kano et al., 1995). Zfs1 has been shown to bind and promote the degradation of the mRNA of *arz1*, which contains multiple AREs but encodes a protein of unknown function (Cuthbertson et al., 2008).

Insects such as *Drosophila melanogaster* also express a single TTP family member, DTIS11 (Ma et al., 1994). In unpublished data, our laboratory has found that this protein can also bind to and promote the decay of ARE-containing mRNAs. Its role in insect physiology remains to be determined.

In frogs, three CCCH tandem zinc finger proteins, XC3H-1, XC3H-2, and XC3H-3, are orthologues of mammalian TTP, L1, and L2, respectively. *Xenopus laevis* also expresses a fourth CCCH protein, XC3H-4, that contains the two characteristic conserved zinc fingers of the TTP family but also contains two additional zinc fingers that are more distantly related. The expression of XC3H-4 was demonstrated to be restricted to oocytes, ovaries, eggs, and early embryos, suggesting that it could be involved in regulating the decay of mRNAs that are important for oocyte maturation and early embryonic development (De et al., 1999).

1.4.1 Mammalian proteins of the tristetraprolin family

TTP (also known as ZFP36, TIS11, Nup475, and GOS24) was identified in a screen for genes whose transcription was rapidly stimulated by growth factors and mitogens (Lai et al., 1990). It was first thought to be a transcription factor due to its

immediate early response gene characteristics and the fact that zinc fingers are a common structural motif in DNA binding proteins. Since its discovery, the ability of TTP to bind to and promote the decay of ARE-containing mRNA has been fully established and this protein has become one of the most well studied ARE-BPs. There are still suggestions that TTP could also act as a transcription factor, as initially assumed, although it seems to function primarily in the regulation the stability of a set of mRNAs.

The role of TTP in mRNA turnover and in innate immunity was determined upon the development and analysis of TTP knockout mice (Carballo et al., 1998; Taylor et al., 1996a). These mice developed a phenotype that included myeloid hyperplasia, cachexia, and arthritis that was consistent with TNF- α excess. This association was confirmed in that the TTP knockout phenotype could be rescued by treatment of the mice with an antibody against TNF- α . TTP was later shown to regulate the stability of the TNF- α transcript by directly binding to its ARE and promoting its deadenylation and destabilization (Lai et al., 1999). Since TNF- α was determined to be the primary physiological target of TTP, its ARE has become a common tool used in RNA binding and degradation experiments for other TTP family members.

The ability of TTP to promote the degradation of a β -globin reporter containing the ARE of GM-CSF in co-transfection experiments was examined and confirmed. Further characterization of TTP knockout mice and experiments conducted with TTP-

deficient cells from these animals identified GM-CSF mRNA as another physiological target of TTP (Carballo et al., 2000). Excess levels of GM-CSF in the TTP knockout mice could contribute to the myeloid hyperplasia phenotype.

TTP has been shown to control the decay of a number of other ARE-containing mRNAs through a variety of methods, although only some of these have been validated as true physiological targets. For example, the ARE sequence of IL-2 was found to bind TTP after induction by TCR and CD28 co-receptor stimulation in lymphocytes, using gel supershift assays. A β -globin reporter could be destabilized upon insertion of the IL-2 ARE into its 3' UTR and addition of TTP. This regulation was then verified through analysis of IL-2 mRNA stability in wild type and TTP-deficient splenocytes (Ogilvie et al., 2005).

In another example, a microarray experiment was conducted to identify transcripts with different decay rates in wild type and TTP-deficient fibroblasts (Lai et al., 2006). The mRNA encoding immediate early response gene 3 (*Ier3*), which has a possible role in blood pressure regulation, was the most stabilized transcript in the TTP-deficient cells. The ability of TTP to bind to ARE sites on the *Ier3* mRNA to regulate its decay was confirmed through gel electrophoretic mobility shift assays and co-transfection assays.

In an mRNA immunoprecipitation-microarray (RIP-Chip) experiment, macrophages were stimulated with lipopolysaccharide (LPS) to promote the expression of TTP (Stoecklin et al., 2008). TTP-RNA complexes were immunoprecipitated and the associated mRNAs were identified. The decay rate of IL-10 mRNA, one of the top candidate transcripts, was then determined to be lower in primary macrophages from TTP knockout mice as compared to wild type. This study can be criticized because the primary target of TTP, TNF- α , was not recognized through this method. Nonetheless, if TTP targets IL-10 along with TNF- α , it could function in both the activation and inactivation of the inflammatory response due to the ability of IL-10 to inhibit the synthesis of TNF- α .

Other putative targets have been identified through TTP knockdown and over-expression experiments. For instance, TTP was suggested to target the inducible nitric oxide synthase (iNOS) mRNA, not through direct binding to the ARE, but through an indirect action with KH-type splicing regulatory protein in which the iNOS mRNA is stabilized (Fechir et al., 2005). This work suggests that TTP could act in mRNA stabilization as well as in its well-known role in destabilization.

Jing et al introduced another interesting and atypical role for TTP. TTP was shown to interact, not directly with the ARE, but with RISC complex proteins and a specific miRNA, mi16 (Jing et al., 2005). Through this interaction, TTP was suggested to

assist in the binding of miRNA and the ARE of TNF- α . Consequently, TTP may play a role in the turnover of this mRNA by the miRNA pathway.

L1 (also known as cMG1, TIS11B, ERF1, BRF1, and Berg36) was actually the first member of the TTP family in which the existence of a novel proposed tandem zinc finger domain was identified. It was discovered as an immediate early response gene, like TTP, by differential screening of epithelial cells activated by epidermal growth factor (Gomperts et al., 1990). This family member is 71% identical to TTP within its TZF domain, and 93% identical to that of L2. L1 performs similarly to TTP in assays of mRNA binding and decay using TNF ARE target sequences (Lai et al., 2000).

Although the physiological mRNA targets for L1 have not yet been identified, creation of L1 knockout mice provide some understanding of the role of this protein in mammals (Stumpo et al., 2004). Disruption of *Zfp3611* results in embryonic lethality; about two-thirds of the knockout mice die before embryonic day (E) 11. This outcome is largely due to failure of chorioallantoic fusion, a necessary event in the development of a functional umbilical circulation. In the rare instances in which the chorion and allantois were able to fuse, decreased cell proliferation and atrophy of the trophoblast layers of the placenta were apparent by E10.5. Other characteristic traits of these mice include runting, neural tube opening in the forebrain, and apoptosis in the neural tube, although

these defects seem to be secondary to the circulatory insufficiency. Hence, L1 has been shown to play a crucial role in formation of the feto-placental circulation.

L1 has also been linked to a variety of other cellular processes, including myogenesis (Busse et al., 2008), bone remodeling (Reppe et al., 2004), and cholesterol metabolism (Duan et al., 2009). In a very recent study, the steriodogenic acute regulatory (StAR) mRNA was identified as a possible target of L1 (Duan et al., 2009). The StAR protein mediates transport of cholesterol in the mitochondria. L1 was shown to directly bind to the StAR ARE sequence. Turnover of the StAR transcript that contains an extended 3'UTR was enhanced by L1, and knockdown of L1 resulted in increased levels of this mRNA. Therefore, L1 was suggested to downregulate StAR mRNA to lead to increased cholesterol metabolism.

L2 (also known as TIS11D, ERF2, and BRF2) was originally identified through a search for TTP-like TZF domain sequences (Varnum et al., 1991), although the original published sequence was incorrect at both ends. L2 exhibits a high level of sequence conservation within the TZF, with 73% of residues identical to those of TTP in this region. L2 can also bind to and promote the deadenylation and degradation of ARE-containing RNAs (Lai et al., 2000), similar to the other TTP family members.

Insight into the biological significance of this protein has been suggested by study of its knockout mouse (D.J. Stumpo, unpublished data). L2 knockout mice die,

apparently from hemorrhage, at about two weeks of age. Further analysis revealed defects in hematopoiesis in surviving mice, and a decrease in hematopoietic progenitors in yolk sac and liver during gestation. Mice have also been created in which the *Zfp3612* gene was disrupted to produce decreased levels of a truncated protein that lacked the 29 amino (N)-terminal residues (Ramos et al., 2004). This gene disruption was suggested to be a partial loss of function mutation. These mice exhibited complete female infertility due to a block of cell proliferation at the embryonic two-cell stage. Both gene disruption experiments provide evidence for the involvement of L2 in hematopoiesis and early embryonic development.

L3 was recently discovered as the fourth mammalian member of the TTP family by BLASTing the mouse genome for TTP family TZF sequences (Blackshear et al., 2005). It exhibits a high percentage of sequence similarity to the other three family members within the TZF domain and the extreme carboxyl (C)-terminus (Fig. 4). The TZF domain of L3 is 76% identical to that of TTP in mouse and exhibits the distinguishing characteristics of the TTP family: identical intra-finger spacing of the cysteine and histidine residues and exact inter-finger spacing, as well as the presence of the conserved “lead-in” sequences to the zinc fingers.

We began the work described in this dissertation directly following the discovery and initial analysis of this TTP family member in 2005. Functional studies showed that

L3 could mimic the RNA binding and destabilizing activities of TTP, L1, and L2. For example, L3 was found to bind a TNF-based RNA probe in a cell-free system, and to promote decay of an ARE-containing RNA target in intact cell transfection experiments (Blackshear et al., 2005). Thus, this new family member presumably retains the general biological functions of TTP, L1, and L2, i.e., the ability to downregulate certain ARE-containing mRNAs; however, this concept remains to be proven in a physiological setting.

Further study revealed qualities that were unique to L3 within the TTP family. While TTP, L1, and L2 are cytoplasmic at steady state, they have been found to shuttle between the nucleus and cytoplasm using the importin CRM1 and standard nuclear export and nuclear localization signals (Murata et al., 2002; Phillips et al., 2002). L3, in contrast, does not shuttle but exists solely in the cytoplasm (Blackshear et al., 2005).

The expression of L3 is highly specific as compared to TTP, L1, and L2. While TTP, L1, and L2 are expressed relatively ubiquitously, the expression of L3 is limited to placental tissue and yolk sac in rodents. In sequence database searches and screens of total RNA for the presence of L3, L3 was not found in non-rodents, but was found in mouse, rat, and hamster (Blackshear et al., 2005)(R.S. Philips, D.J. Stumpo, and P.J. Blackshear, P.J., unpublished data). In mouse placenta in particular, expression of the

2.4 kb transcript was detected during mid-to-late gestation, between E 8.5 and E18.5, and peaked between E13.5 and E14.5 (Blackshear et al., 2005).

Other general characteristics of L3 also differ from those of the other TTP family members. L3 is composed of 725 amino acids and, thus, is about twice the size of the other family members. This increase in size is largely due to the existence of a repeat domain in L3 that is lacking in TTP, L1, and L2 (Fig. 4). The unique repeat domain may play an important role in the life of this protein. Another difference can be observed in the second lead-in sequence within the TZF domain. In L3, a proline replaces a leucine in the most common sequence, KYKTEL, yielding KYKTEP. This change is also found in TTP family members in other species, such as *Danio rerio*. Finally, the predicted pI of L3 is 5.55, in contrast to the basic pIs of TTP, L1, and L2; this difference is largely contributed by the acidic repeat domain.

Since the initial publication in which L3 was introduced, four other articles have been published in peer-reviewed journals which present data relating to this protein. First, the effect of green tea on the expression of TTP family members was evaluated; L3 could not be detected in the tissues examined in this study (Cao et al., 2007). Second, a study of the subcellular localization of L3 and its mechanisms was described (Frederick et al., 2008), and represents Chapter 2 of this work. Third, the expression of 43 genes, including those encoding the TTP family members, was studied in response to insulin in

mouse 3T3-L1 adipocytes (Cao et al., 2008). This work purported to show L3 mRNA expression in cells other than mouse placenta or extra-embryonic tissues using quantitative real-time polymerase chain reaction (PCR). Finally, *Zfp36l3* was identified as being expressed in mouse cornea, as compared to lens, through a genome-wide analysis of gene expression patterns (Wu et al., 2008); however, these results should be interpreted with caution since the gene is also listed as *Zfp36l1*.

1.4.2 Binding the AU-rich element

The TZF domain of the TTP family is both necessary and sufficient for binding to class II AREs. Mutation of any of the cysteines or histidines that are responsible for coordinating the zinc ion prevents binding activity (Lai et al., 1999). Conversely, mutation of adenosine residues within the ARE of TNF- α also prevents binding (Lai et al., 2000). The TZF of TTP has been demonstrated to bind the nonamer UUAUUUAUU with maximum affinity to TTP *in vitro*, distinguishing this ARE sequence as the canonical binding site (Blackshear et al., 2003; Brewer et al., 2004). The TZF of TTP is able to form more than one complex with an ARE probe, depending on probe length and TZF peptide concentration (Blackshear et al., 2003).

The structure of TTP has been elusive to date partially because of the insolubility of the over-expressed recombinant protein. However, a high-quality NMR structure of the TZF domain bound to the 9-mer UUAUUUAUU has been solved for L2 (Hudson et

al., 2004). The TZF domain without zinc is unstructured, although when zinc is present, this domain folds into a pair of identical CCCH zinc fingers. When a synthetic UUAUUUAUU nonamer is then added, the conformation of each of the fingers is slightly altered in order to bind the RNA while the linker remains relatively static. Each finger binds a 5'-UAUU-3' subsite. Binding is accomplished through electrostatic interactions, hydrogen bonds, and stacking between aromatic side chains and the RNA bases. Another ARE-BP, HuD, binds to both class I and II AREs through its two RNA recognition motifs. Like L2, and probably TTP, HuD binds to ARE-containing RNA through hydrogen bonding and aromatic stacking interactions (Wang and Tanaka Hall, 2001).

Sequence specificity of L2 for the ARE nonamer was attributed to hydrogen bonds between main chain functional groups in the protein backbone and the Watson-Crick edges of the RNA bases. To date, it is not known whether binding of TTP family members and other CCCH TZF proteins can preferentially recognize different RNA sequences due to small differences in their primary sequences or changes within the TZF domain linker. It is also possible that RNA secondary structures created by the entire ARE and its sequence context could confer some sequence specificity to TTP family members, but this has not been demonstrated.

1.4.3 Tristetraprolin family members & disease

In cancer, gene expression can be deregulated to affect processes such as cell division, angiogenesis, and apoptosis. Alterations in the expression or activity of RNA binding proteins have been linked to cancer because these changes can affect the stability of mRNAs encoding cell cycle regulators, proto-oncogenes, and cytokines [reviewed in (Audic and Hartley, 2004)].

Decreased TTP expression has been revealed in many tumor types. For example, breast tumors exhibit low levels of TTP expression relative to normal breast tissue, which is accompanied by increased expression of vascular endothelial growth factor (VEGF) and a higher pathological tumor grade (S.E. Brennan, unpublished data). This association suggests that TTP may regulate the decay of VEGF mRNA. The regulation of VEGF mRNA by TTP family members is also supported by RNA binding, mRNA reporter stability, and knockdown experiments (Ciais et al., 2004). It is proposed that, when TTP is downregulated in tumors, the stability of VEGF mRNA increases, increasing the amounts of VEGF and promoting angiogenesis in the tumor.

L1 may also be involved in tumor genesis or cancer progression.

Medroxyprogesterone acetate (MPA) is a drug used in hormonal therapy of metastatic breast cancer that inhibits estrogen-mediated growth in hormone-responsive breast cancer cells. The expression of L1 has been shown to be directly regulated by MPA

(Pennanen et al., 2009), suggesting that MPA may exert its anti-cancer function, in part, through control of L1 expression.

Other disease states can also be achieved by deregulation of gene expression. Sequence variations in the genes of TTP family members could be linked to altered expression or function of TTP proteins, and, hence, secondary effects on the stability of mRNA targets. Increased levels of these mRNA targets and their encoded proteins could lead to disease. For instance, increased levels of TNF could promote the development of an autoimmune disease, such as rheumatoid arthritis. By sequencing the genomic DNA encoding TTP, L1 and L2, polymorphisms could be discovered that may have an effect on the expression or activity of these proteins. In fact, polymorphisms have been identified in *ZFP36*, the gene encoding TTP, that were associated with the autoimmune disease rheumatoid arthritis in African-Americans (Carrick et al., 2006) and obesity (Bouchard et al., 2007).

1.5 Aim of research

The aim of the research included in this dissertation was to study the activity and function of the most-recently discovered TTP family member, L3, with special consideration to the properties that are unique within the TTP family. The questions addressed in the following chapters are outlined below:

Why does L3 not undergo nucleocytoplasmic shuttling?

Where and when is L3 expressed at the RNA and protein level?

What are the physiological mRNA targets of L3?

Is the L3 protein modified, specifically by phosphorylation?

If it is modified, does this affect the ability of L3 to function?

Through this work, we hoped to gather valuable information pertaining to the mechanism of action and biological significance of L3 in the placenta of rodents. We also hoped to be able to apply this knowledge to better our understanding of the roles of the other members of the TTP family in general, as well as their potential “L3-like” functions in the placentas of non-rodent mammals.

2. A unique C-terminal repeat domain maintains the cytosolic localization of ZFP36L3

Portions of this chapter are reproduced from the Journal of Biological Chemistry:

J Biol Chem. 2008; 283: 14792-800.

2.1 Introduction

A significant biochemical distinction between ZFP36L3 (L3) and its relatives within the tristetraprolin (TTP) family of CCCH tandem zinc finger (TZF) proteins concerns its subcellular localization. L3, which is cytoplasmic at steady state when expressed as a green fluorescent protein (GFP)-fusion protein in transfected human embryonic kidney (HEK) 293 cells, does not appear to shuttle between the nucleus and cytoplasm (Blackshear et al., 2005), whereas the other TTP family members exhibit shuttling activity (Murata et al., 2002; Phillips et al., 2002). Like other nucleocytoplasmic shuttling proteins, TTP, ZFP36L1 (L1) and ZFP36L2 (L2) contain both apparent nuclear localization sequences (NLS), which mediate nuclear import, and functional nuclear export sequences (NES), which facilitate nuclear export [reviewed in (Nigg, 1997; Pemberton and Paschal, 2005; Yoneda, 2000)].

NLSs include motifs rich in basic residues that bind to nuclear import receptors, such as the importins, for transport into the nucleus. The NLSs of TTP, L1 and L2 have been mapped to the inter-finger region of their conserved TZF domains; the import of

these proteins into the nucleus requires the TZF domain (Murata et al., 2002; Phillips et al., 2002), and two arginines within the inter-finger spacer have been proposed to be critical for this translocation (Murata et al., 2002). Mouse L3 shows 76% amino acid sequence identity in its TZF domain compared to mouse TTP, and also retains the conserved arginine residues (Blackshear et al., 2005). Therefore, like the other family members, L3 may contain a functional NLS that is able to drive transport of the protein into the nucleus.

The NESs of TTP, L1, and L2 are characterized by hydrophobic regions that bind CRM1, a nuclear membrane export protein that directs transport of proteins from the nucleus to the cytoplasm. The NESs of L1 and L2 are located within their identical carboxyl (C)-termini and contain a leucine-rich cluster, whereas the NES of TTP is located at its extreme amino (N)-terminus (Phillips et al., 2002). A potential NES of L3 is also located at the extreme C-terminus and, although superficially similar to those of the other family members, contains a significant difference in sequence: the fourth hydrophobic residue characteristic of the NESs of L1 and L2 is, instead, an aspartate residue in L3. This difference may lead to failure of the L3 NES to bind the export receptor CRM1; the NES of L3 could, therefore, be non-functional, due to the lack of a conserved hydrophobic residue that is essential for export.

If L3 contains a functional NLS and a non-functional NES, the protein would be expected to be nuclear. However, L3 has been shown to be cytosolic, at least as a GFP-labeled fusion protein in transfection experiments (Blackshear et al., 2005). Therefore, an additional factor must contribute to its localization. The molecular weight of L3 is much larger than those of the other family members, with a predicted M_r of 72,345 for the mouse protein. This increase in size is largely due to the existence of a unique repeat domain within the C-terminal half of the protein. This domain contains 10 repeats of the sequence AAMAPGAALAPAAALTPA, or close variants, and is predicted to fold into seven hydrophobic alpha helices (Blackshear et al., 2005). In theory, this domain could be responsible for targeting L3 to a membrane and, therefore, could affect the subcellular localization of L3.

In this study we examined the possible cytosolic restriction of L3 by manipulating these predicted localization domains. We addressed the following hypotheses: [1] the TZF domain contains a functional NLS and the aforementioned arginines are critical for NLS activity; [2] the putative C-terminal NES is non-functional; and [3] the unique repeat domain is a cytoplasmic localization domain. We also examined the cellular and subcellular localization of the endogenous L3 protein in the placenta.

2.2 Methods

2.2.1 Plasmids

The plasmid pZfp36l3-ORF (Blackshear et al., 2005), which contains the open reading frame of mouse *Zfp36l3* (GenBank accession number NM_001009549.2), was used as a polymerase chain reaction (PCR) template for each N-terminal GFP fusion construct. See (Fig. 5) for a schematic illustration of the full length and deletion L3 plasmid constructs used in this study.

Plasmid GFP-L3 was created by PCR amplifying bases 150-2327 of GenBank accession number NM_001009549.2, corresponding to amino acids 1-725 of GenPept accession number NP_001009549.1, using the forward primer 5'-ggggacaagttgtacaaaaaagcaggctctATGGGCCAACAACAATCTG-3' and the reverse primer 5'-ggggaccactttgtacaagaaagctgggtcTCATTTTTCAGAGTCTG-3', in which the lower case letters represent recombination sequences for cloning into the Gateway system (Invitrogen). The resulting amplification product was recombined into the pDONR221 entry vector (Invitrogen) and then subsequently recombined into the pcDNA-DEST53 expression vector (Invitrogen). The sequence was confirmed by dRhodamine dye terminator cycle sequencing (Applied Biosystems).

Site directed mutagenesis was performed on the plasmid GFP-L3 according to the QuikChange protocol (Stratagene). Arginines 153 and 157 (from GenPept accession

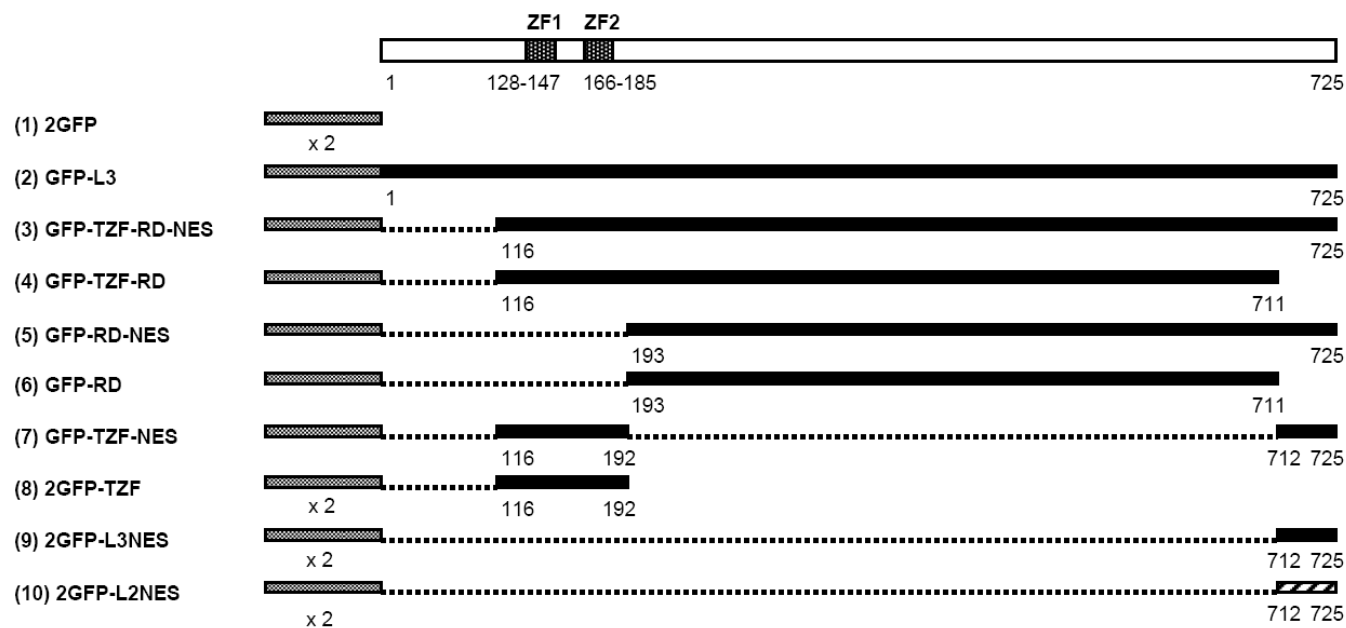


Figure 5: L3 constructs used to characterize the NLS, NES, and repeat domain

The indicated regions of L3 were cloned into the pcDNA-DEST53 expression vector to generate proteins fused downstream of and in frame with N-terminal GFPs. Plasmids GFP-L3 (2) and 2GFP-TZF (8) were subjected to site-directed mutagenesis to change critical arginines within the inter-finger domain of the L3 TZF. Plasmids 2GFP (1), 2GFP-TZF (8), 2GFP-L3NES (9) and 2GFP-L2NES (10) were designed to express fusion proteins containing two tandem GFPs that should be too large to diffuse across the nuclear membrane. Each deleted region is shown by a dotted line. GFP, L3, and L2 sequences are represented by crosshatch, black fill, and diagonal lines, respectively.

number NP_001009549.1) were mutated to alanines both singly and together using the following primer sets: 5'-GGCTACCGCGAACTGGCTACCCTGTCAAGG-3' and 5'-CCTTGACAGGGTAGCCAGTTCGCGGTAGCC-3' for mutation of R153; 5'CGTACCCTGTCAGCGCACCCCAAGTACAAGACG-3' and 5'-CGTCTTGTACTTGGGGTGCCTGACAGGGTTACG-3' for mutation of R157; and 5'-CCGCGAACTGGCTACCCTGTCAGCGCACCCCAAGTACAAGACG-3' and 5'-CGTCTTGTACTTGGGGTGCCTGACAGGGTAGCCAGTTCGCGG-3' for mutation of both simultaneously. All mutations were confirmed by sequencing.

Plasmids for L3 deletion mutants were constructed by a similar method to that described above for plasmid GFP-L3. The appropriate regions of the L3 cDNA were amplified by PCR, followed by recombination into the entry vector pDONR221, and then into the expression vector pcDNA-DEST53. The sequences were confirmed by dRhodamine dye terminator cycle sequencing.

Plasmid GFP-TZF-RD-NES expresses an N-terminal GFP fused to amino acids 116-725 of GenPept accession number NP_001009549.1, corresponding to nucleotides 495-2327 of GenBank accession number NM_001009549.2. Plasmid GFP-TZF-RD expresses GFP fused to amino acids 116-711, corresponding to nucleotides 495-2282. Plasmid GFP-RD-NES expresses GFP fused to amino acids 193-725, corresponding to nucleotides 495-2327. Plasmid GFP-RD expresses GFP fused to amino acids 193-711,

corresponding to nucleotides 726-2282. Plasmid 2GFP-TZF expresses two tandem GFP domains fused to amino acids 116-192, corresponding to nucleotides 495-725; site directed mutagenesis of Arg153 and Arg157 was performed on this plasmid as was described for plasmid GFP-L3. Plasmid 2GFP-L3NES expresses two tandem GFP domains fused to amino acids 712-725, corresponding to nucleotides 2283-2327.

A mutant plasmid was also constructed that expresses an N-terminal GFP-GFP fused to the NES of L2. The C-terminal portion of L2, which contains the NES, corresponding to amino acids 471-484 of accession number NP_001001806.1 and nucleotides 1664-1708 of accession number NM_001001806.2, was used in plasmid 2GFP-L2NES. This plasmid expresses only the C-terminal 14 amino acids of L2 downstream of two tandem GFP domains.

Two plasmids containing the simian virus 40 (SV40) large T antigen NLS were created for comparison of this extensively studied, strong NLS to the putative NLS located in the L3 TZF domain. Plasmid 2GFP-SV40NLS expresses two tandem GFP domains fused to the NLS of SV40, corresponding to the nucleotide sequence 5'-GATCCAAAAAAGAAGAGAAAGGTA-3'. Plasmid GFP-SV40NLS-RD expresses GFP fused to the NLS of SV40 followed by the repeat domain of L3 (amino acids 193-711 of GenPept accession number NP_001009549.1, corresponding to nucleotides 726-2282 of GenBank accession number NM_001009549.2).

pEGFP-N1 (Clontech) and 2GFP, which expresses one or two tandem GFP domains, respectively, were used in control experiments. GFP-TIS11D (Phillips et al., 2002) expresses a C-terminal GFP fused to mouse L2 and was utilized as a positive control in nuclear export assays.

All plasmids that express two tandem GFP domains alone or fused to an L3 domain were designed to increase the size of the protein and therefore prevent passive diffusion across the nuclear membrane. All plasmids that express only one GFP domain fused to the L3 repeat domain should also be larger than the nuclear pore and should not undergo passive diffusion into or out of the nucleus.

2.2.2 Cell culture and transfections

HEK 293 cells were maintained in Minimal Essential Medium (Invitrogen) supplemented with 10% (v/v) fetal bovine serum, 100 U/ml penicillin, 100 µg/ml streptomycin, and 2mM glutamine. Transient transfections were performed with FuGENE 6 Transfection Reagent (Roche Applied Science) according to the manufacturer's protocol with a reagent:DNA ratio of 3:1.

2.2.3 Fluorescence microscopy

HEK 293 cells (1×10^5) were plated in 35 mm glass bottom plates (MatTek Corporation) and transfected with 1 µg of DNA for each of the GFP fusion constructs. Live HEK 293 cells expressing GFP fusion proteins were observed and images were

obtained using a Zeiss LSM510 confocal microscope. The patterns of fluorescence shown in the figures are representative of all cells expressing a given fusion protein.

2.2.4 Leptomycin B treatment

In nucleocytoplasmic shuttling assays, HEK 293 cells were plated and transfected as described above. Leptomycin B (LMB) (Sigma-Aldrich) was added to the medium at a final concentration of 10 ng/ml in 0.18% (final concentration; v/v) methanol 16-20 h after DNA transfection. As a control treatment, an equal amount of methanol was added. Subcellular localization of GFP-labeled proteins was observed 4 -5 h later using fluorescence microscopy of live cells.

2.2.5 Analysis of mRNA binding

To prepare protein for RNA binding analysis, 0.7×10^6 HEK 293 cells were plated on 100 mm plates and transfected with 1 μ g of DNA from the appropriate constructs. After 16 to 20 h, the medium was removed and the cells were washed three times with 10 ml of ice-cold phosphate buffered saline-calcium and magnesium free (PBS-CMF) (pH 7.4). A volume of 300 μ l of ice-cold, freshly-made homogenization buffer (50 mM Tris-HCl [pH 8.0], 1% [v/v] Nonidet-P40, 5 mM EDTA, 100 mM NaCl, 50 mM NaF, 1X complete EDTA-free protease inhibitor cocktail [Roche Applied Science]) was added to the cells, which were then scraped and collected. The cells were subsequently incubated on ice for 20 min to complete cell lysis. Centrifugation at 110 x g for 10 min at 4°C was

then performed to remove cell nuclei and debris. Finally, glycerol was added to 15% (v/v).

To check for recombinant protein expression, 50 or 100 µg of protein from this cell lysate was boiled in loading buffer, subjected to sodium dodecyl sulphate-polyacrylamide gel electrophoresis (SDS-PAGE) on a 10% acrylamide gel and transferred to a nitrocellulose membrane. Western blot analysis was performed with either an anti-GFP-horseradish peroxidase (HRP) conjugate (Santa Cruz Biotechnology) at a dilution of 1:3000 or an anti-GFP antibody (BD Biosciences) at a dilution of 1:2000 followed by a protein A-HRP conjugate (BioRad) at a dilution of 1:4000. Proteins were visualized with enhanced chemiluminescence (ECL) (Pierce).

RNA gel shift assays were performed as described previously (Lai et al., 1999; Lai et al., 2000). Briefly, 15 µg of total protein from the cell lysate was incubated with a ³²P-labeled TNF ARE RNA probe, and the reactions were analyzed on either a 4 or 8% (w/v) non-denaturing polyacrylamide gel followed by autoradiography.

2.2.6 Northern blotting and immunoblotting for endogenous L3

Placentas were collected from pregnant female Crl:CD1(CR) mice (Charles River Laboratories)(Appendix) at embryonic days (E) 9.5, E10.5, E12.5, and E14.5. Half of the tissues were placed in RNAlater and were used for total cellular RNA isolation with the RNeasy Mini Kit (Qiagen) following the manufacturer's instructions. To check for L3

transcript expression, 20 µg of RNA from each sample was fractionated on a 1.2% formaldehyde-agarose gel, transferred to a Nytran SuPer Charge membrane, and hybridized with random-primed, α -³²P-labeled probes. The probe used for detecting L3 transcripts consisted of nucleotides 150 to 585 of GenBank accession number NM_001001806.2. The blot was also hybridized with a full length GAPDH cDNA probe to monitor gel loading. Hybridization was visualized using autoradiography.

The rest of the tissues were rapidly frozen. They were then pulverized in liquid nitrogen, extracts were made in the aforementioned homogenization buffer using a Tissumizer (Tekmar), and the samples were cleared of debris by centrifugation at 12000 x g at 4°C for 20 min. Total protein concentration was determined using the BioRad Protein Assay. To check for endogenous L3 expression, 100 µg of total protein from each extract was subjected to SDS-PAGE on a 10% acrylamide gel and transferred to a nitrocellulose membrane. Western blot analysis was performed with a rabbit antiserum directed against the 16 N-terminal amino acids of mouse L3 (Covance) at a dilution of 1:2000 followed by a protein-A HRP conjugate (BioRad) at a dilution of 1:4000. Proteins were visualized with ECL. The blot was then stripped and re-probed with an anti-actin antibody (Chemicon) at a dilution of 1:10,000 followed by goat anti-mouse HRP conjugate (BioRad) at a dilution of 1:10,000. Immunoreactive proteins were again visualized with ECL.

2.2.7 Immunofluorescence of placental sections

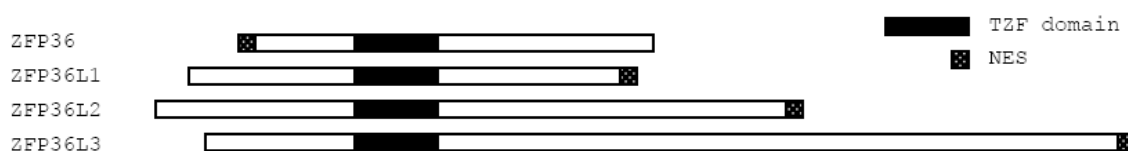
Slides of placental sections from B6(Cg)-*Tyr^{C-2}*/J mice (Jackson Laboratory) (Appendix) at E14.5 were stained with either pre-immune serum or an anti-L3 antibody each diluted to 1:1000 with 0.1M phosphate buffer (pH 7.4)/0.9% NaCl/1% normal goat serum (NGS), as described (Blackshear et al., 2005; Cao et al., 2004). They were then washed two times for 10 min each with 0.2% (v/v) Triton X-100 in Tris buffered saline (TBS), incubated with an Alexa Fluor 488 goat anti-rabbit secondary antibody (Invitrogen) diluted to 1:300 in TBS/25% NGS for 30 min, and washed again repeatedly for 5 min. Sections were blotted and mounted with VectaShield Mounting Medium for Fluorescence with DAPI (Vector). Slides were viewed and images were obtained with an Olympus inverted microscope and a Zeiss 510 LSM510 confocal microscope.

2.3 Results

2.3.1 Identification of a functional nuclear localization sequence within the TZF domain of L3

Because NLSs appear to exist within the TZF domains of TTP, L1, and L2, and because TTP family members from a given animal species exhibit great sequence similarity within their TZF domains (Fig. 6, A and B), we investigated whether there was a functional NLS within the TZF domain of L3. A construct was made which expressed the L3 TZF domain alone fused to an N-terminal GFP-GFP tag. Site directed mutagenesis was then utilized to alter the aforementioned conserved arginines within

A. Mouse TTP family



B. TZF domain

```

          ▼   ▼
ZFP36      RYKTELCRTYSESGRCRYGAKCQFAHGLGELRQANRHPKYKTELCHKFYLQGRCPYGSRCHFII 158
ZFP36L1    RYKTELCRPFEEENGACKYGDCKQFAHGIHELRLSLTRHPKYKTELCRTFHTIGFCPYGPRCHFII 177
ZFP36L2    RYKTELCRPFEEESGTCKYGEKCQFAHGFHELRLSLTRHPKYKTELCRTFHTIGFCPYGPRCHFII 218
ZFP36L3    RYKTELCRPFEEESGICKYGHKCQFAHGYRELRTLRSRHPKYKTEPCRTFHSVGFPCPYGTRCHFII 185
*****.:.* *:* *  *****  ***  .***** *:.*: * ****.*****

```

C. C-terminus

```

          ▼
ZFP36L1    RRLPIFSRLSISDD 338
ZFP36L2    RRLPIFSRLSISDD 484
ZFP36L3    RRLPIFSRFSDEK 725
*****.:.* *:*

```

Figure 6: NLSs and NESs in mouse TTP family members

(A) TZF domains, which contain the NLSs of TTP, L1, L2, and possibly L3, are shown in black. The N-terminal NES of TTP, C-terminal NESs of L1 and L2, and putative C-terminal NES of L3 are shown as dotted boxes. (B) An alignment of the sequence of the TZF domains of TTP, L1, L2, and L3 is shown. The conserved inter-finger arginines are noted with arrows. (C) An alignment of the sequence of the C-termini of L1, L2, and L3 is shown. The fourth hydrophobic residue of the L1 and L2 NES, an aspartic acid in L3, is noted with an arrow. Identical, conserved, and semi-conserved residues are noted with (*), (:), and (.), respectively.

the inter-finger spacer of the TZF domain to alanines. The three mutants that were produced contained R153A alone, R157A alone, or both together. These four constructs were individually transiently transfected into HEK 293 cells and analyzed with confocal microscopy to determine the subcellular localization of the fusion proteins. RNA gel shift experiments were also performed to assess the ability of these mutant TZF proteins to bind to a TNF ARE RNA probe.

The TZF domain alone promoted nuclear localization of 2GFP-TZF in live-cell fluorescence microscopy experiments in transfected HEK 293 cells. Although 2GFP alone was distributed throughout the cell (Fig. 7A), the 2GFP-TZF peptide was observed almost exclusively within the nucleus (Fig. 7B). Mutation of each of the two arginines within the TZF domain to alanine, singly and together, resulted in some, but not complete, loss of nuclear localization (Fig. 7, C-E).

Gel shift analysis revealed that binding of these fusion proteins to an ARE probe was also completely disrupted by mutation of either of these arginines, or both together, while the intact 2GFP-TZF domain caused a typical gel shift with the ARE probe (Fig. 8A). Because of the possibility of abnormal folding of the mutant TZF proteins, RNA binding studies were also performed with full length L3 fusion proteins containing the inter-finger arginine mutations (Fig. 8B). In the context of the intact protein, the single mutants appear to shift the ARE RNA probe to some extent, whereas the double mutant

showed no RNA binding ability. Equivalent levels of wild type and mutant proteins are shown in the lower panel of (Fig. 8).

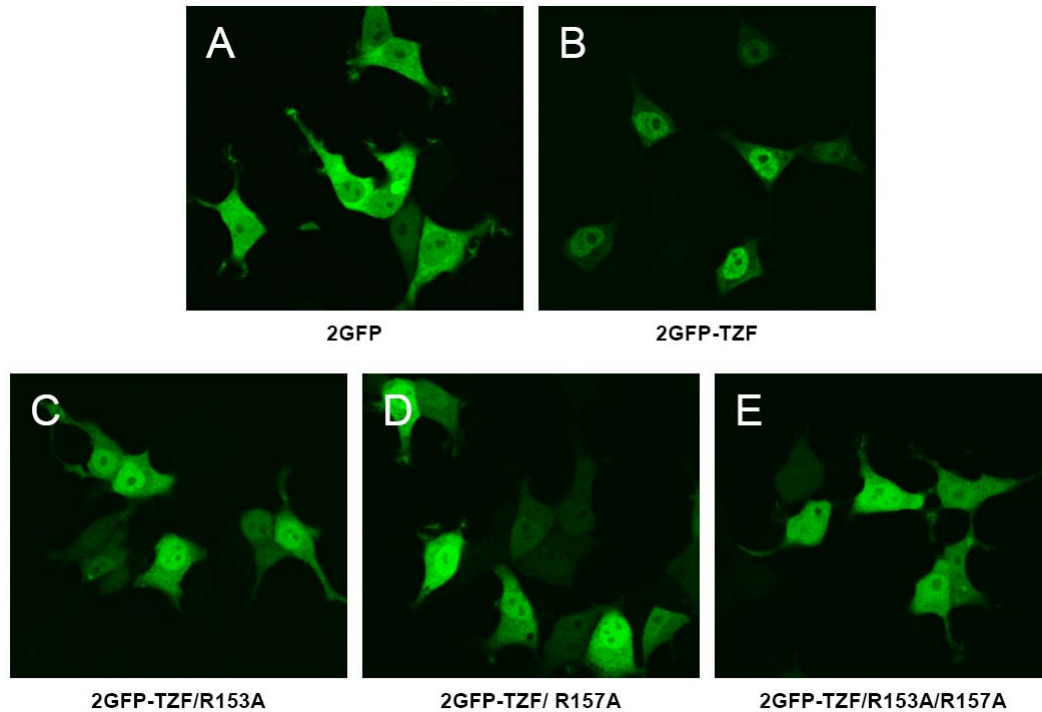


Figure 7: Subcellular distribution of L3 TZF arginine mutants

2GFP-L3 TZF fusion proteins were expressed in HEK 293 cells and observed with confocal microscopy. 2GFP alone (A) localizes throughout both the nucleus and cytoplasm. Note the predominantly nuclear localization of the fusion protein containing the native TZF domain (B) as compared to the increase in cytoplasmic localization of the fusion proteins containing TZF domains altered by mutation of the conserved inter-finger arginines, singly and together (C-E).

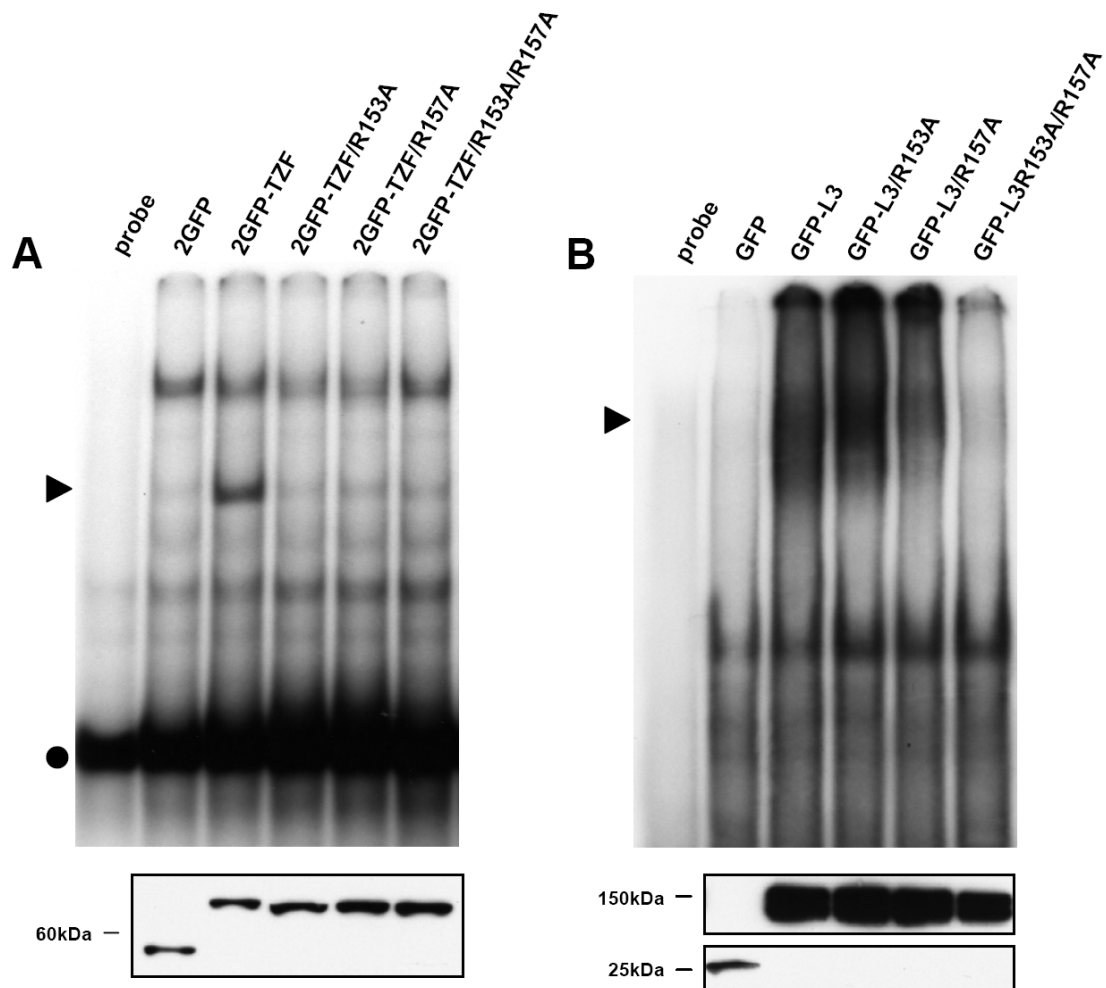


Figure 8: Binding activity of L3 TZF and full length L3 arginine mutants

L3 TZF (A) and full length L3 (B) fusion proteins from extracts of transfected HEK 293 cells were incubated with a TNF ARE RNA probe. (▶) denotes the protein-RNA complex. (●) denotes free probe. Note that while free probe can be seen on the 8% gel in A, it has run off of the 4% gel in B. Western blots with an antibody directed against GFP are shown below to demonstrate fusion protein expression in each of the cell extracts used in these assays.

These data demonstrate that the Arg153 and Arg157 mutations not only inhibited the nuclear uptake of the L3 TZF domain, as well as the intact L3 protein, but at least the double mutant completely disrupted the fundamental structure of the TZF domain in such a way as to prevent RNA binding. The failure of nuclear uptake of these TZF domain mutants might thus be due to alterations in the structure of the TZF domain rather than disruption of a specific nuclear import sequence. To our knowledge, mutants have not yet been identified in any family member in which nuclear uptake is inhibited but normal affinity RNA binding is present.

2.3.2 Evaluation of a potential nuclear export sequence within the C-terminus of L3

L1 and L2 contain functional NESs within their extreme C-termini, whereas TTP contains a functional NES at its extreme N-terminus (Murata et al., 2002; Phillips et al., 2002)(Fig. 6A). The C-terminus of mouse L3 exhibits high sequence similarity with those of L1 and L2, apart from a non-conserved substitution of an acidic residue for a presumed critical hydrophobic residue (Fig. 6C); this same substitution is present in the rat L3 sequence (Blackshear et al., 2005). In order to determine whether the putative NES of L3 is competent to mediate nuclear export, plasmids were prepared that expressed GFP fusion proteins containing full length L2 or L3 and 2GFP fusion proteins containing only the NES from L2 or L3; note that the functional NES sequence for mouse L2 is identical to that for L1. These fusion proteins were expressed in HEK 293 cells,

which were then subjected to either control treatment or treatment with LMB to inhibit the nuclear export receptor CRM1. Upon addition to cells, LMB causes proteins with functional NESs, such as TTP, L1 and L2, to accumulate within the nucleus (Murata et al., 2002; Phillips et al., 2002). Confocal images were obtained 4-5 h after treatment.

Under these conditions, 2GFP alone was found throughout the cytoplasm and nucleus after addition of either the methanol control or LMB (Fig. 9A). As expected, GFP-L2 and 2GFP-L2NES, which contain functional NESs, accumulated in the nucleus after LMB treatment (Fig. 9, B and C). However, no differences were observed between control and LMB treatments when GFP-L3 and 2GFP-L3NES were expressed (Fig. 9, D and E). Furthermore, the subcellular distributions of 2GFP-L2NES and 2GFP-L3NES differed. Whereas 2GFP-L2NES was more abundant in the cytoplasm than in the nucleus, presumably because of its nuclear export activity (Fig. 9C), 2GFP-L3NES was distributed evenly throughout the cell (Fig. 9E), essentially identical to 2GFP alone (Fig. 9A). Taken together, these data indicate that the extreme C-terminus of L3 has no detectable NES activity.

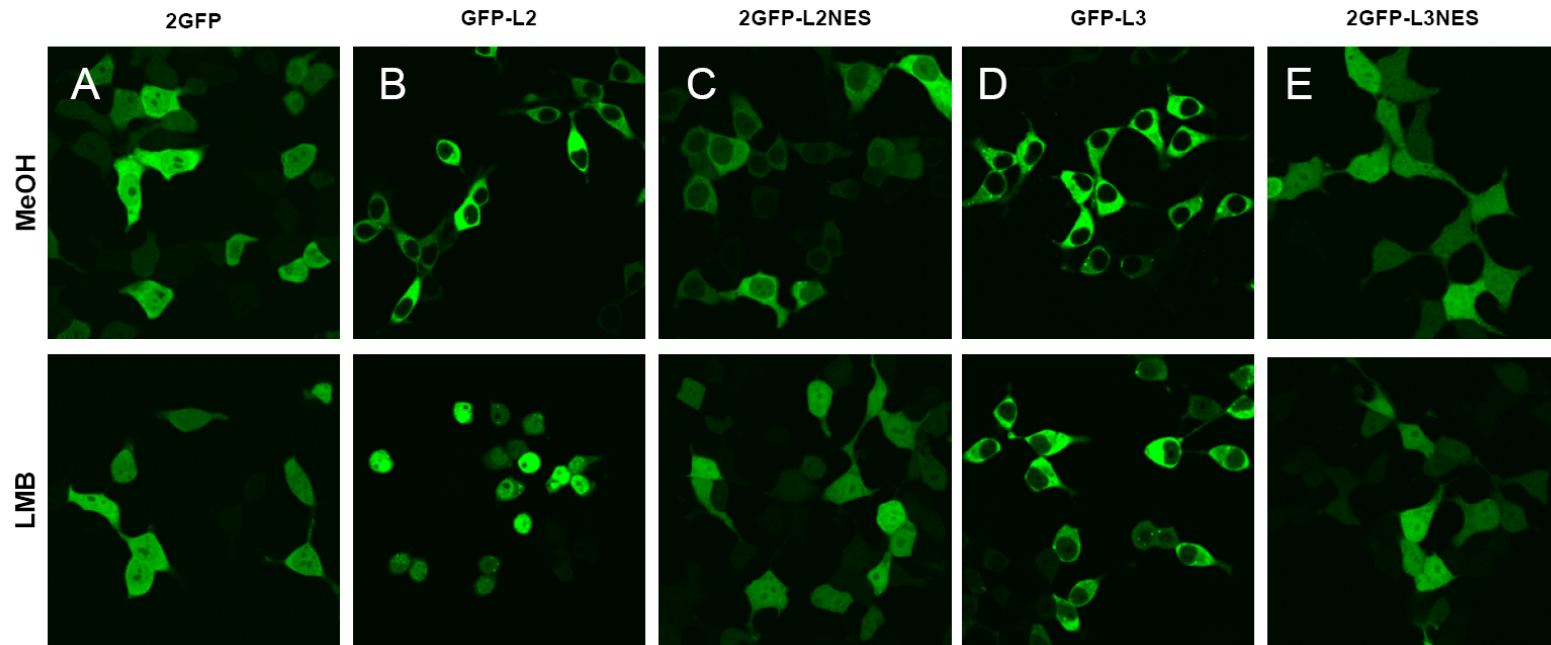


Figure 9: Effect of LMB on the subcellular localization of full length L2 and L3 and their nuclear export sequences

HEK 293 cells were transiently transfected with the indicated plasmids, incubated for 16-20 additional hours, and then treated with either methanol as a control or 10 ng/ml LMB. Confocal images were captured 4-5 h after treatment with LMB. Note the nuclear accumulation of GFP-L2 (B) and 2GFP-L2NES (C) after LMB treatment, compared to the unchanged localization of 2GFP (A), GFP-L3 (D), and 2GFP-L3NES (E).

2.3.3 Effect of the repeat domain on the subcellular localization of L3

Although the TZF of L3 exhibited functional nuclear import activity, and the C-terminus lacks nuclear export activity, this protein is unexpectedly cytoplasmic rather than nuclear (Blackshear et al., 2005). We postulated that the unique C-terminal repeat domain caused L3 to be localized to the cytoplasm. Plasmids were constructed that expressed GFP-fusions containing the L3 repeat domain alone, as well as the L3 repeat domain linked to other portions of the protein. Two additional plasmids were prepared that contained the SV40 NLS to test the ability of the L3 repeat domain to potentially counteract the function of a well known, strong NLS. These fusion proteins were expressed in HEK 293 cells and were analyzed with fluorescence microscopy.

In control experiments, 2GFP alone was distributed throughout the cytoplasm and the nucleus (Fig. 10A), and 2GFP-TZF was predominantly nuclear (Fig. 10B). However, when the L3 C-terminal repeat domain was added to GFP, the fusion protein was detected only in the cytoplasm (Fig. 10C). Furthermore, with the addition of the N-terminus, the TZF, and/or the rest of the C-terminus to the repeat domain, the protein remained cytoplasmic (Fig. 10, D-G). Importantly, this cytoplasmic localization was seen with fusion proteins containing the active nuclear localization activity found within the TZF. Moreover, the L3 repeat domain promoted cytoplasmic localization of GFP in the presence of the strong NLS of SV40 (Fig. 10I); as expected, the 2GFP fusion protein

containing the NLS of SV40 alone was exclusively nuclear (Fig. 10H). These data demonstrate that the repeat domain is a cytoplasmic localization domain and can override the nuclear localization activity of either the L3 or SV40 NLS.

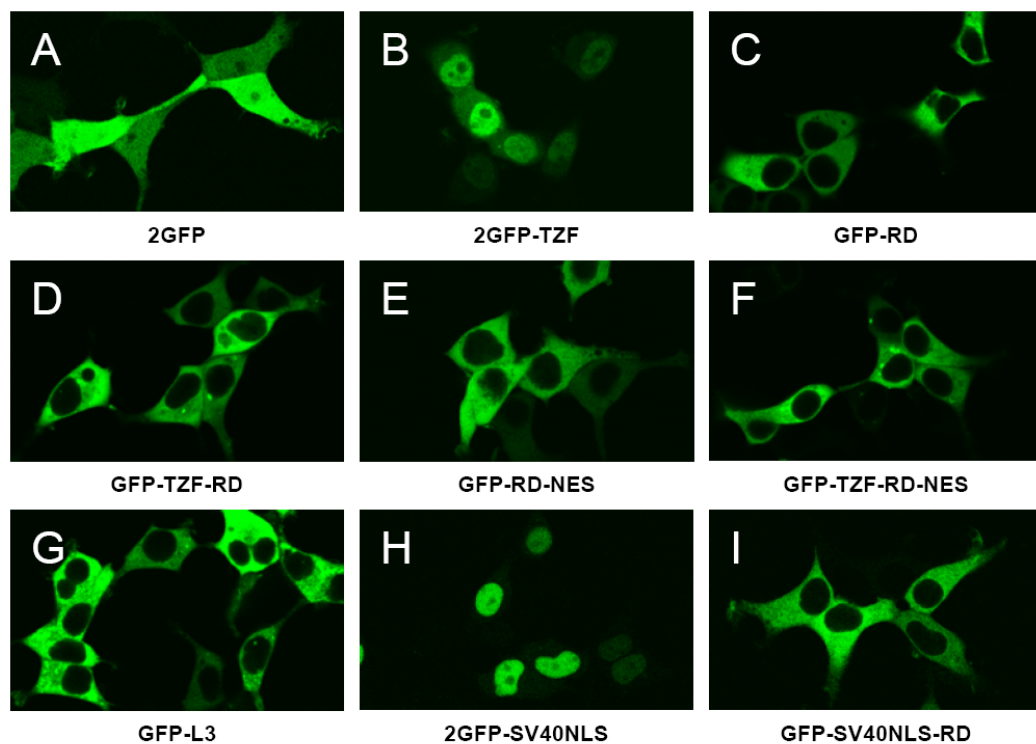


Figure 10: Subcellular distribution of full length L3 and deletion mutants

HEK 293 cells were transiently transfected to express GFP-L3 fusion proteins which were viewed with confocal microscopy. Note the cytosolic localization of all fusion proteins containing the repeat domain (C-G and I), as compared to the 2GFP control (A) as well as 2GFP-TZF (B) and 2GFP-SV40NLS (H).

2.3.4 Subcellular localization of endogenous L3 in mouse placenta

L3 expression in mouse tissue has previously been examined at the RNA level. L3 transcripts were found exclusively in the placenta and yolk sac, where they were detected as early as E8.5, and peaked at E13.5 to E14.5 (Blackshear et al., 2005). Highest levels of mRNA expression were found in the labyrinthine layer of the placenta, with lower levels in the spongiotrophoblast and giant cell layers, and minimal expression was seen in the allantois and maternal decidua (Blackshear et al., 2005). In the present study, we extended these results by investigating the developmental time course of RNA and protein expression, using northern and western blotting. Western blotting of placental extracts was performed with an antibody directed at an N-terminal peptide of L3.

L3 RNA transcripts were first detected at E9.5, and peaked at E12.5 to E14.5 (Fig. 11). L3 protein was first detected at E10.5, and then increased greatly by E14.5 (Fig. 11). The protein was expressed as two discrete bands of M_r ~100,000 and 90,000 that were of approximately equal intensity under these conditions. Further work is underway to determine the biochemical difference between the two species, but it does not seem to be due to alternative translational initiation, premature truncation, or proteolysis, since a separate antibody directed at an extreme C-terminal peptide yielded similar western blotting results (E.D. Frederick and P.J. Blackshear, unpublished data).

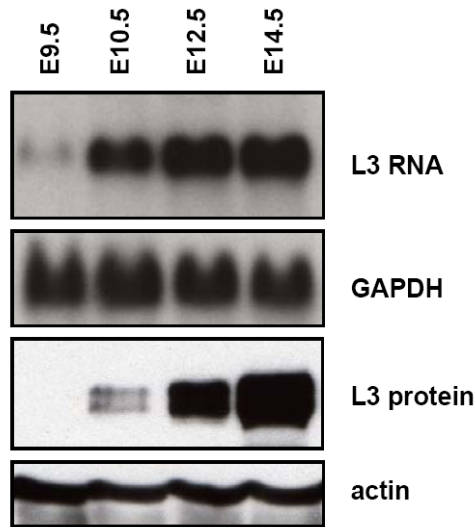


Figure 11: Developmental expression of L3 mRNA and protein in mouse placenta

Placental RNA (20 μ g each) and protein extracts (100 μ g each) from the indicated embryonic days were subjected to northern and western analysis, respectively, to detect L3 mRNA and protein expression. The levels of GAPDH mRNA and actin protein are also shown as loading controls.

Because of the apparently high level of protein expression at E14.5 determined by western blotting, placenta sections from that embryonic day were used for immunofluorescence studies in which the cellular and subcellular localization of the L3 protein was determined. In corroboration with previous studies (Blackshear et al., 2005), the L3 protein was most highly expressed in the labyrinthine trophoblast layer, the primary site of materno-fetal exchange (Fig. 12, A and B), as well as in the trophoblast giant cells (Fig. 12, A and C). In confirmation of the cell transfection experiments, confocal microscopy with a nuclear counterstain confirmed that the protein was

exclusively expressed in the cytoplasm of these cells, and its staining did not overlap with nuclear staining (Fig. 12, B and C).

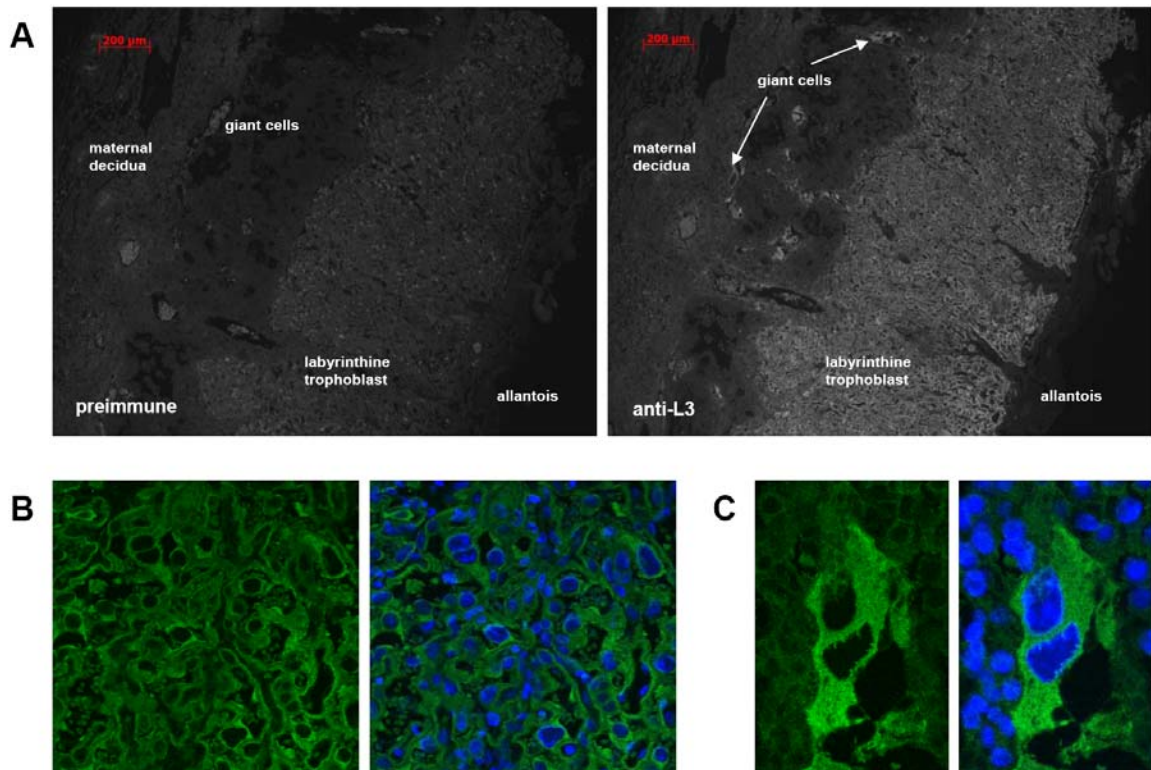


Figure 12: Cellular and subcellular localization of endogenous L3

Mouse placenta sections from E14.5 were incubated with either preimmune serum (A, left panel) or an anti-L3 antibody (A, right panel; B and C) followed by a fluorescent secondary antibody. Nuclei were also stained with DAPI (shown in B, right panel and C, right panel). L3 expression was readily detectable in the cells of the trophoblast layers, including the trophoblast giant cells. At the subcellular level, L3 was expressed exclusively in the cytoplasm of the labyrinthine trophoblast cells (B) and giant cells (C); this expression did not overlap with nuclear staining.

2.4 Discussion

Through examination and modification of predicted subcellular localization domains, we have identified the basis for the apparent cytosolic restriction of the L3 protein. First, we demonstrated that, like the other mammalian members of the TTP family, L3 contains a functional NLS within its TZF domain. We provided evidence that the arginines within the inter-finger spacer that have been proposed to be critical to the NLS activity of TTP, L1, and L2 also affect the NLS activity of the L3 TZF domain. Although these arginines were demonstrated to be important for the import of the TZF domain of L3 into the nucleus, the same mutations in these conserved basic residues that prevented nuclear import had a variable effect on RNA binding, depending on whether the mutations were in the context of the TZF domain alone or in the intact protein. The double arginine mutant clearly exhibited loss of RNA binding activity, suggesting that major structural alterations in the TZF domain occurred as a result of these mutations. Typically, a monopartite or bipartite NLS contains clusters of basic amino acids, allowing for binding to a carrier protein, such as a member of the importin superfamily, and subsequent import to the nucleus; overall, this import is influenced by the Ran-GTP/GDP cycle [reviewed in (Nigg, 1997; Pemberton and Paschal, 2005; Yoneda, 2000)]. The NLS must be exposed on the surface of the protein in order for contact with binding partners, and masked NLSs can be revealed by a variety of mechanisms (Boulikas, 1993).

Further studies are required to determine the specific residues that contribute to the NLS function of the TZF domain of all the TTP family members, including L3, and whether or not this function can be separated from the RNA binding activity of the same domain.

We have also demonstrated that the NES-like sequence that is present at the extreme C-terminus of L3 is non-functional, presumably because of the presence of an acidic amino acid in the mouse and rat L3 sequence in place of a branched chain amino acid in the sequences of the other family members (Blackshear et al., 2005). This non-functional NES would therefore be unable to aid in nuclear export via CRM1. The NES is typically a short, leucine-rich sequence with defined spacing, and conserved hydrophobic residues constituting the NES have been shown to be required for export activity (Bogerd et al., 1996). This sequence was first identified in the viral protein HIV-Rev (Fischer et al., 1995), a viral RNA exporter, and has now been found in many shuttling proteins including TTP, L1, and L2 (Murata et al., 2002; Phillips et al., 2002). The nuclear export receptor CRM1, which is part of the nuclear pore complex, interacts directly with the NES to mediate the transport of NES-containing proteins; the Ran-GTP/GDP cycle also affects export from the nucleus [reviewed in (Nigg, 1997; Pemberton and Paschal, 2005; Yoneda, 2000)]. LMB has been shown to specifically inhibit NES-dependent nuclear export by binding to CRM1 (Kudo et al., 1999; Kudo et al., 1998). We utilized LMB to block export via CRM1 in order to study the ability of the

NES-like sequence of L3 to drive transport out of the nucleus. This sequence, when compared to the C-terminal NES of L2, did not behave like a functional NES. Although the NES of TTP is located at its N-terminus, there is no evidence for a leucine-rich or hydrophobic-rich region characteristic of an NES in this region of L3. No other likely NESs were found in the rest of the L3 sequence, suggesting that it does not contain a functional NES.

Finally, we found that the unusual C-terminal repeat domain, which is unique to L3 within the TTP family, can override the nuclear uptake activity of the L3 TZF domain, causing the protein to be restricted to the cytoplasm. This makes L3 the only family member that apparently does not shuttle between nuclear and cytoplasmic compartments. This cytoplasmic localization was seen not only in cell transfection studies, but also in studies of the subcellular localization of the endogenous protein in placental trophoblast cells. The shuttling of TTP, L1, and L2 could be a means of regulating their mRNA binding and destabilizing activities. It has been shown that TTP translocates from the nucleus to the cytoplasm upon addition of mitogens (Taylor et al., 1996b). Furthermore, the p38 mitogen-activated protein kinase and the extracellular signal-regulated kinase signaling pathways have been implicated in regulating the subcellular localization and stability of the TTP protein (Brook et al., 2006). In the case of TTP, an initial stimulus could be responsible for creating a signal cascade which leads to

shuttling of the protein and, ultimately, could affect the ability of the protein to perform its function.

The mechanism by which the repeat domain confers cytoplasmic localization on the L3 protein is unknown. It is possible that the repeat domain simply prevents nuclear import because of its sheer size, or that it targets L3 to a membrane, organelle, or other protein partners. Additional research is necessary to determine the function of the repeat domain and its contribution to the activities of L3. However, since placental immunofluorescence staining confirms its cytosolic localization *in vivo*, its similarities to and differences from the other family members in terms of activity must take into account this unique localization.

Besides its unique subcellular localization compared to the other TTP family members, and its unique C-terminal repeat domain, L3 differs from the rest of the family in several other respects. First, its gene appears to be intronless (Blackshear et al., 2005), whereas the other members all have a single intron. Second, it appears so far to be expressed only in rodents (Blackshear et al., 2005). Both rat and mouse mRNA sequences are present in GenBank at the respective accession numbers XM_228661.2 and NM_001009549.2. By northern analysis, we have identified mRNA bands of similar size that hybridize to the mouse cDNA probe in placenta samples from golden hamster and gerbil (D.J. Stumpo, unpublished data), but not in other mammals tested, including

guinea pig. Finally, its tissue localization appears to be unique compared to the other family members, with significant expression so far detected only in the placenta and yolk sac of mice (Blackshear et al., 2005). In addition to determining its function in the physiology of these tissues, it will be interesting to uncover the evolutionary events that occurred to allow this gene to develop and remain in rodents, but apparently not in other mammals. It is also appealing from a practical perspective to determine whether one or more of the other family members will have subsumed the role of L3 in yolk sac and placental physiology in other mammalian species.

By analogy to other family members, as well as its activity as revealed in cell transfection experiments (Blackshear et al., 2005), L3 is predicted to act as a regulator of mRNA destabilization in the placenta. We predict that L3 will be found to perform the general functions of a TTP family member in the specific location of placental trophoblast cells. Attempts to determine its physiological targets, as well as its importance in placental development or physiology, are currently underway. The generation of a knockout mouse will be particularly important in this regard, since mice deficient in TTP, L1, and L2 exhibit defects in completely distinct physiological processes: inflammation (Taylor et al., 1996a), chorioallantoic fusion (Stumpo et al., 2004) and hematopoiesis (D.J. Stumpo, unpublished data), respectively.

3. Identification of candidate mRNA targets of ZFP36L3 using ribonucleoprotein immunoprecipitation-microarray analysis

3.1 Introduction

The placenta serves as the major site for exchange of nutrients, wastes, and gases between mother and fetus throughout gestation. The intrauterine environment can have major influences on growth and development of the fetus, including influences on post-natal development. The placenta is also involved in the production of essential, pregnancy-related hormones and growth factors, as well as in the immune protection of the fetus. Problems in the development or functioning of this organ can result in complications in pregnancy, early termination, or other more subtle developmental consequences leading to problems later in life.

ZFP36L3 (L3) is specifically expressed in the labyrinthine trophoblast cells and trophoblast giant cells of rodent placenta during mid-to-late gestation (Blackshear et al., 2005; Frederick et al., 2008). L3 is a member of the tristetraprolin (TTP) family of CCCH tandem zinc finger (TZF) proteins which all contain highly conserved TZF domains. Each TZF domain contains two independently folding protein motifs in which three cysteines and one histidine coordinate a zinc ion. This domain is responsible for binding specific sequences in AU-rich elements (ARE) in the 3'-untranslated region (UTR) of

target mRNAs. The conserved TZF domain is both necessary and sufficient for RNA binding, and mutation of any zinc-coordinating residue within the TZF disrupts this binding (Lai et al., 2002). The binding of a TTP family member to an ARE-containing mRNA can, in turn, promote destabilization of the target message. Similarities in RNA binding and destabilizing properties among TTP family members provide a foundation for the concept of functional overlap across the family. The interactions between this class of CCCH proteins and their mRNA targets may provide an important regulatory control on gene expression at the post-transcriptional level.

By identifying the physiological mRNA targets of each of the TTP family members, we hope to gain insights into their biological relevance. For example, TTP, the first-discovered and best-studied member of this family, has been shown to target tumor necrosis factor alpha (TNF- α) mRNA. TTP is able to bind the TNF- α ARE sequence in electrophoretic mobility shift assays (Carballo et al., 1998). TTP can also promote the degradation and deadenylation of RNA containing the TNF- α ARE in co-transfection experiments and cell-free assays, respectively (Lai et al., 1999). TTP knockout mice exhibit a systemic inflammatory syndrome mainly resulting from excess levels of TNF- α (Taylor et al., 1996b). Hence, TTP targets TNF- α RNA for degradation in a physiological setting and plays an important role in the innate immune response.

Identification of the physiological mRNA targets of L3 will aid in understanding the mechanism of action of L3 and, perhaps, of the TTP family of proteins in general. Determination of L3 targets will also help to delineate the roles of this protein in the normal physiology of the placenta. In addition, this study may assist in the identification of potential physiological roles for one or more of the other TTP family members in the placentas of non-rodent mammals, which do not appear to express the L3 protein. TTP, ZFP36L1 (L1), and ZFP36L2 (L2) are all expressed in the placentas of mice (D.J. Stumpo, unpublished data), and may be expressed in the placentas of non-rodent mammals where one or more of these proteins may subsume the role played by L3.

Although L3 is able to bind to a TNF ARE RNA probe in cell-free assays, and promote degradation of a TNF 3'UTR reporter RNA in a cellular co-transfection assay (Blackshear et al., 2005), its physiological mRNA targets are completely unknown. Because L3 is highly and exclusively expressed in rodent placenta and yolk sac (Blackshear et al., 2005), we predict that it will be found to act as an mRNA destabilizing protein that downregulates target mRNAs that are important for placental integrity or development.

In order to uncover possible physiological targets of L3, we utilized the ribonucleoprotein immunoprecipitation-microarray (RIP-Chip) method developed by

(Keene et al., 2006). This approach allows for identification of interactions between endogenous transcripts and proteins within a cell line or tissue sample, and, therefore, can lead to identification of novel putative mRNA targets. In this study, we immunoprecipitated L3-mRNA complexes from mouse placenta at embryonic day (E) 14.5, using a highly specific antibody directed against L3, and isolated the L3-associated mRNAs. These mRNAs were then identified and quantitated using microarrays. A number of possible L3 targets were found that contained one or more copies of the canonical binding sequence for members of this protein family.

The top candidate target, B-type natriuretic peptide (BNP) mRNA, was increased by eight-fold over control immunoprecipitations. We verified the ability of L3 to bind to and promote the degradation of this novel target transcript. BNP is a peptide hormone that is well-known for its cardiac expression and functions as a regulator of blood pressure and body fluid homeostasis, but its role in the placenta is currently unknown.

3.2 Methods

3.2.1 Ribonucleoprotein immunoprecipitation-microarray analysis

The RIP-Chip assay was performed as described (Keene et al., 2006), using freshly isolated placentas from E14.5 mice of the Crl:CD1(CK) strain (Charles River Laboratories)(Appendix)(Fig. 13A). Briefly, placentas were homogenized with a Tissumizer (Tekmar) in ice-cold polysome lysis buffer (100 mM KCl, 5 mM MgCl₂, 10

mM HEPES [pH 7.0], 0.5% Nonidet-P40, 1 mM dithiothreitol [DTT], 100 U RNase inhibitor [Applied Biosystems], 1x complete EDTA-free protease inhibitor cocktail [Roche Applied Science]), incubated on ice for 5 min, and stored at -80°C. For immunoprecipitation, Protein A Sepharose beads (GE Healthcare) were pre-swollen in ice-cold NT2 buffer (50 mM Tris-HCl [pH 7.4], 150 mM NaCl, 1 mM MgCl₂, 0.05% Nonidet-P40) supplemented with 5% (w/v) bovine serum albumin for 1 h at 4°C and then incubated with an L3 antiserum (Covance) or its corresponding pre-immune serum (Covance) at 1:100, rotating overnight at 4°C. The beads were washed five times with ice-cold NT2 buffer and then resuspended in 850 µL of ice-cold NT2 buffer. 200 U of RNase inhibitor (Applied Biosystems) was added along with 10 µL of 100 mM DTT and 40 µL of 0.5 M EDTA. After thawing and clearing of the placenta lysate by centrifugation (15 min, 15000 x g, 4°C), 2 mg of lysate was added to each tube of beads and the tubes were rotated for 4 h at 4°C. The beads were pelleted by centrifuging briefly at 8000 x g and were then washed five times with ice-cold NT2 buffer. RNA was isolated by incubating the beads in 400 µL of the RNeasy RLT solution (Qiagen) and 30 µg proteinase K (Invitrogen) at 55°C for 20 min, pelleting the beads, and then processing the elution following the manufacturer's instructions for the Qiagen RNeasy Kit.

The microarray experiments and statistical analyses were performed by the National Institute of Environmental Health Sciences microarray core facility. The

quality of each of the ten RNA samples (five sets from paired pre-immune serum and L3 antibody immunoprecipitations) was verified with a Bioanalyzer (Agilent) according to the manufacturer's protocol. Each of the samples was then hybridized to the GeneChip Mouse Expression Set 430 (Affymetrix). This whole mouse genome array set interrogates 34,000 variants and 39,000 transcripts from well-characterized mouse genes using 45,000 probe sets. Total RNA (20 ng) was amplified using the Affymetrix Two-Cycle cDNA synthesis protocol. For each array, 15 μ g of amplified biotin-cRNAs was fragmented and hybridized to the array for 16 h at 45°C in a rotating hybridization oven using the Affymetrix eukaryotic target hybridization controls and protocol. Slides were stained with streptavidin/phycoerythrin using a double-antibody staining procedure and washed using the EukGE-WS2v5 protocol of the Affymetrix fluidics station FS450 for antibody amplification. Arrays were scanned with an Affymetrix scanner 3000, and data were obtained using the GeneChip operating software (GCOS; version 1.2.0.037).

The resulting files (.dat, .cel, and .chp) were imported into the Rosetta Resolver system (version 6.0). Rosetta Resolver performs data preprocessing, normalization, and error modeling. Error weighting in Resolver takes advantage of the technology-specific error model that Affymetrix has generated for use with its arrays. This error model takes into account factors contributing to measurement error, such as sample preparation, labeling, and chip quality variation. Error weighting helps to increase

statistical power despite low numbers of replicates. The intensity profiles from each replicate pair (pre-immune serum and anti-L3 antibody) were combined into ratio experiments as described (Weng et al., 2006). Intensity plots were generated for each ratio experiment, and genes were considered to be possible targets of L3 if the fold change was greater than two and the p-value was consistently less than 0.001 in all five experiments. The sequences of the thirty genes whose transcripts had the highest average enrichment value in all five replicates were then analyzed for the presence of TTP family binding sequences in their 3'UTRs.

The data obtained from the Affymetrix arrays were also used to create a gene list using analysis of variance (ANOVA) with a Benjamini-Hochberg False Discovery Rate multiple test correction for comparison with the list acquired from the Rosetta Resolver analysis.

To ensure the quality of the immunoprecipitation procedure, we tested the ability of the two serums to pull down the L3 protein. After the final NT2 buffer washing step, 100 μ L of a solution containing 3:1 phosphate buffered saline (PBS) and gel loading buffer was added to the beads from the anti-L3 antiserum and pre-immune serum immunoprecipitations. The samples were boiled for 5 min and western blot analysis was performed on 30 μ L of each sample, using the anti-L3 antiserum at a dilution of 1:2000 followed by a protein-A horseradish peroxidase (HRP) conjugate

(BioRad) at a dilution of 1:4000. Proteins were visualized with enhanced chemiluminescence (ECL) (Pierce).

3.2.2 Northern blotting for endogenous BNP mRNA

Placentas were collected from pregnant female Crl:CD1(CK) mice (Charles River Laboratories)(Appendix) at E9.5, E10.5, E12.5, and E14.5. Heart and liver were also collected to serve as positive and negative controls for BNP mRNA expression, respectively. Tissues were placed in RNAlater and were used for total RNA isolation with the RNeasy Mini Kit (Qiagen) following the manufacturer's protocol. RNA from each sample (20 µg) was fractionated on a 1.5% formaldehyde-agarose gel, transferred to an Amersham Hybond-N+ membrane (GE Healthcare), and hybridized with a random-primed, α -³²P-labeled probe. The probe used for detecting BNP transcripts consisted of nucleotides 188-553 of GenBank accession number NM_008726.4. The blot was also hybridized with a full length GAPDH cDNA probe to monitor gel loading. Hybridization was visualized using autoradiography.

3.2.3 In situ hybridization histochemistry

In situ hybridization histochemistry was performed by Eric Richfield at Rutgers University to examine BNP transcript expression in mouse placenta and control tissues. Heart, liver, spleen, and E15.5 placenta tissues from C57BL/6 mice (Appendix) were frozen in dry ice, cut into 15 µm sections on a cryostat, and mounted on

aminopropyltriethoxysubbed slides. The sections were then dehydrated at 25°C for several minutes and stored at -20°C until used for hybridization.

A BNP oligonucleotide anti-sense probe was designed as a reverse complement to 179-227 of the sense strand of GenBank accession number NM_008726.4. A sense probe complementary to the anti-sense strand of the BNP was also synthesized to the same portion of the gene. Each DNA probe had an approximate 50% GC ratio. Probes were designed for 100% similarity to mouse L3 and had minimal similarity to the transcripts for TTP, L1, and L2. The probes were 3' end-labeled with ³⁵S-dATP using terminal transferase (Roche) and were then purified with phenol/chloroform extraction and precipitation.

Sections were fixed for 5 min in 4% formaldehyde in 1X PBS at room temperature, washed three times for 10 sec in fresh 1X PBS, followed by acetylation in 0.1 M triethanolamine with 0.25% acetic anhydride, and finally dehydrated through graded ethanol solutions. The labeled probes were hybridized in a solution containing 50% formamide, 4X saline-sodium citrate (SSC), 500 µg/mL sheared single stranded DNA, 250 µg/mL yeast tRNA, 1X Denhardt's solution, 10% dextran sulfate, and 100 mM DTT. A total of 1 x 10⁶ cpm were applied to each section. Sections were hybridized overnight, washed in 2X SSC containing 50% formamide for 1 h, and then washed in 1X SSC for 1 h at room temperature before dehydration and drying. Hybridization was

visualized with autoradiography using ³⁵S-sensitive film (Kodak BiomaxMR). Staining with hematoxylin and eosin of adjacent sections was used for general visualization and orientation of the tissues.

3.2.4 Plasmids

Plasmid CMV2.EGFP.L3.BGH3'/BS⁺ was created by inserting the open reading frame of mouse *Zfp3613* (nucleotides 150-2327 of GenBank accession number NM_001009549.2) into the *Bam*HI and *Eco*RV restriction enzyme sites of CMV2.EGFP(c).BGH3'/BS⁺ (W.S. Lai, unpublished plasmid). This plasmid codes for the expression of a full length L3 protein (amino acids 1-725 of GenPept accession number NP_001009549.1) with an N-terminal green fluorescent protein (GFP) tag.

Site directed mutagenesis was performed on the plasmid CMV2.EGFP.L3.BGH3'/BS⁺ according to the QuikChange protocol (Stratagene). Cysteine 143 (from GenPept accession number NP_001009549.1) was mutated to arginine using the following primer set: 5'-GCAAGTATGGCCACAAGCGCCAGTTCGCGCATGGC-3' and 5'-GCCATGCGCGAACTGGCGCTTGTGGCCATACTTGC-3'. The sequence was confirmed by BigDye terminator cycle sequencing (Applied Biosystems). This plasmid, CMV2.EGFP.L3C143R.BGH3'/BS⁺, codes for the expression of a GFP-L3 protein with a mutation in the third zinc-coordinating cysteine residue in the first zinc finger of the

TZF domain. A similar mutation in TTP prevents RNA binding due to the disruption of the TZF structure (Lai et al., 2002); this mutation in L3 should also prevent RNA binding.

Plasmid FLAG-L3 was created by inserting the open reading frame of mouse *Zfp36l3* (nucleotides 150-2327 of GenBank accession number NM_001009549.2) into the recombination sites of the pDONR221 entry vector (Invitrogen) for cloning into the Gateway system. The resulting plasmid was subsequently recombined into the pDEST515 expression vector (Invitrogen). This plasmid codes for the expression of a full length L3 protein with an N-terminal FLAG tag.

A reporter construct using BNP transcript sequences was created for analysis of RNA degradation in the presence of L3 protein. Plasmid CMV2.BNP/SK⁻ was created by inserting the complete BNP mRNA sequence (nucleotides 112-797 of GenBank accession number NM_008726.4) from a full length cDNA clone (Open Biosystems) into the *Sall* and *XbaI* restriction enzyme sites of CMV2/SK⁻ (W.S. Lai, unpublished plasmid). This reporter was constructed for the expression of BNP protein and includes its entire 3'UTR, including the presumed endogenous polyadenylation signal at nucleotides 746-751 of GenBank accession number NM_008726.4.

A second reporter construct was created for analysis of RNA degradation in the presence of the L3 protein. Plasmid CMV2.EGFP.BNP/UTR/SK⁻ was created by inserting

the complete 3'UTR of BNP (nucleotides 554-772 of GenBank accession number NM_008726.4) into the *EcoRV* and *XbaI* restriction enzyme sites of CMV2.EGFP(SalIHindIII)/SK⁻ (W.S. Lai, unpublished plasmid). This plasmid expresses a GFP reporter RNA in which the coding region for GFP is followed by the whole BNP mRNA 3'UTR.

pEGFP-N1 (Clontech), which expresses GFP, was used in control experiments. pBS (Stratagene) was used in co-transfection experiments to bring the total amount of transfected DNA to 5 µg.

3.2.5 Cell culture and transfection

Maintenance of human embryonic kidney (HEK) 293 cells and transient transfections with FuGENE 6 Transfection Reagent (Roche Applied Science) were performed as described on page 35. Transient transfections were also performed using the standard calcium phosphate protocol.

3.2.6 Analysis of BNP mRNA binding

To prepare protein for RNA binding analysis, 0.7×10^6 HEK 293 cells were plated on 100 mm plates and transfected with 1 µg of pEGFP-N1, CMV2.EGFP.L3.BGH3'/BS⁺, or CMV2.EGFP.L3C143R.BGH3'/BS⁺ one day later. After 16-20 h, the medium was removed and the cells were washed twice with 10 ml of ice-cold phosphate buffered saline-calcium and magnesium free (PBS-CMF) (pH 7.4). A volume of 250 µl of cold,

fresh lysis buffer (50 mM Tris-HCl [pH 8.0], 1% [v/v] Nonidet-P40, 150 mM NaCl, 1X complete EDTA-free protease inhibitor cocktail [Roche Applied Science]) was added to the cells, which were then scraped and collected. The cells were incubated on ice for 15 to 20 min to complete cell lysis. Centrifugation at 18,000 x g for 20 min at 4°C was then performed to remove cell nuclei and debris. Glycerol was added to the supernatant to 20% total volume and the samples were stored at -80°C.

To check for recombinant protein expression, 10 µg of protein from the cell lysate was boiled in loading buffer, subjected to sodium dodecyl sulphate-polyacrylamide gel electrophoresis (SDS-PAGE) on a 10% acrylamide gel, and transferred to a nitrocellulose membrane. Western blot analysis was performed with an anti-GFP-HRP antibody (BD Biosciences) at a dilution of 1:3000. Proteins were visualized with ECL (Pierce).

RNA electrophoretic mobility shift assays were performed to evaluate direct binding of L3 to the ARE of the BNP mRNA transcript. Total protein (20 µg) from the HEK 293 cell lysate was incubated with a ³²P-labeled, synthetic BNP mRNA ARE oligonucleotide probe for 20 min at room temperature. The BNP mRNA ARE probe contained the sequence 5'-UAUUUAUUUAUUUAUUUAUAUUUAUU-3', corresponding to nucleotides 640-665 of GenBank accession number NM_008726.4. The presence of protein-probe complexes was determined by separation of each reaction on a 4% (w/v) non-denaturing polyacrylamide gel followed by autoradiography. In order

to analyze the large L3-RNA complex, the 4% gel was run for 3 h at 150 V; consequently, the free probe migrated off the gel and could not be visualized.

3.2.7 Analysis of BNP mRNA degradation

For co-transfection experiments of the GFP control or the GFP-L3 fusion construct with a BNP mRNA reporter, 0.5×10^6 HEK 293 cells were plated on 100 mm plates. The next day, cells were fed with supplemented Minimal Essential Medium (MEM)(Invitrogen) and then transfected with 10 ng pEGFP-N1 or 2.5 ng, 5 ng, or 10 ng CMV2.EGFP.L3.BGH3'/BS⁺, as well as 1 μ g CMV2.BNP/SK⁻ and 4 μ g pBS, using the calcium phosphate method. After 16 h, the medium was removed; cells were washed twice with incomplete MEM, and then fed with supplemented MEM. RNA was isolated 24 h later; the cells were washed twice with 10 ml ice-cold PBS-CMF, and the illustra RNAspin Mini Kit (GE Healthcare) was used according to the manufacturer's instructions.

For co-transfection experiments of the FLAG-L3 construct with the GFP-BNP mRNA reporter, cells were plated, fed, and transfected with 0 ng, 2.5 ng, 5 ng, 10 ng, 20 ng, 40 ng, or 80 ng plasmid FLAG-L3 as well as 1 μ g CMV2.EGFP.BNPUTR/SK⁻ and 4 μ g pBS. RNA was isolated as describe above.

To check for reporter mRNA degradation, 10 μ g of total RNA was analyzed by northern blotting as described previously. In the BNP reporter experiment, the probe

used for detecting BNP reporter transcripts consisted of nucleotides 112-787 of GenBank accession number NM_008726.4. This blot was also hybridized with a full length GFP cDNA probe, containing the entire EGFP sequence from pEGFP-N1 (Clontech), to monitor expression of GFP-L3. In the GFP-BNP reporter experiment, the same GFP probe was used for detecting GFP-BNP reporter transcripts. This blot was also hybridized with a Marcks-like protein (MLP) cDNA probe, containing nucleotides 182-786 of GenBank accession number NM_010807, to monitor gel loading. Hybridization was visualized using autoradiography.

3.3 Results

3.3.1 Identification of potential physiological targets of L3

RNA was isolated from immunoprecipitates of mouse placenta extracts at the time of maximal L3 protein expression (E14.5) (Fig. 13A). These immunoprecipitations were performed using an immune serum containing a highly specific antibody directed against the N-terminal 16 amino acids of the L3 sequence, or its corresponding pre-immune serum. The strength of this approach is that we were able to perform experiments in parallel, exposing the same placental lysates to either the immune or pre-immune antiserum under otherwise identical conditions. To minimize false positives, we used five biological replicates, i.e., five separate paired immunoprecipitations using immune and pre-immune serum, followed by RNA isolation, conducted on

different days. It is important to note that these assays not only identify transcripts that are directly bound by L3, but may also identify indirect binders that are associated with L3 in a complex.

The quality of the immunoprecipitation protocol was ensured by western analysis of proteins precipitated in both the pre-immune and anti-L3 samples. The pre-immune serum was unable to pull down the L3 protein, while the anti-L3 antiserum was effective in binding L3 (Fig. 13B).

Each RNA sample was analyzed for the presence of ~34,000 genes using ~45,000 probe sets on Affymetrix microarrays. Comparisons of RNA isolated from pre-immune and anti-L3 immunoprecipitations revealed RNA transcripts that were preferentially enriched in the anti-L3 samples; these candidate mRNAs are likely to bind to the L3 protein under physiological circumstances and in the physiologically relevant tissue.

Analysis of data from each of the five pairs of replicates was performed separately using Rosetta Resolver. Only transcripts that (1) were present in either the pre-immune sample, the anti-L3 samples, or both and (2) had an enrichment of at least 2-fold in the anti-L3 sample compared to the pre-immune sample with a $p < 0.001$ were

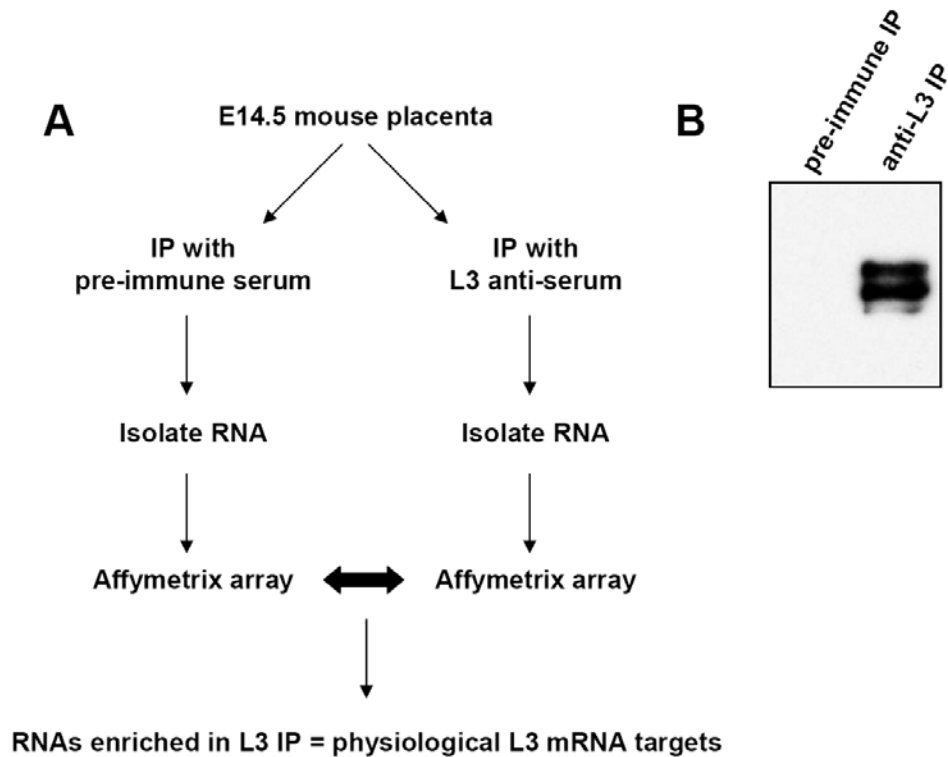


Figure 13: Design of L3 RIP-Chip experiment

(A) E14.5 placentas were collected, homogenized, and incubated with either pre-immune serum as a control or an anti-serum containing a specific L3 antibody at a dilution of 1:100. L3-mRNA complexes were isolated by immunoprecipitation and the L3-associated RNA was extracted. Each RNA sample was exposed to a whole mouse genome array. Transcripts that were selected as putative L3 targets were enriched greater than 2-fold in the L3 sample as compared to the control with a p-value < 0.001 in all five replicates. (B) The ability to pull down L3 through this immunoprecipitation (IP) method was confirmed by western blot analysis with the L3 anti-serum at a dilution of 1:2000 by followed by a protein A-HRP conjugate at a dilution of 1:4000. The IP using the L3 antiserum was able to pull down L3 protein, while the IP using the corresponding pre-immune serum was not.

considered. After these initial comparisons were performed, a list of 383 potential targets was assembled. This list contained only transcripts that were selected from comparisons of all five pairs of replicates. Data analysis was repeated using ANOVA and resulted in a similar list of potential targets, confirming that the initial Resolver analysis was accurate.

The thirty most enriched transcripts were then analyzed for the presence of TTP family RNA binding sequences in their 3'-UTRs, specifically for the pentamer AUUUA, the heptamer UAUUUAU, and the nonamer UUAUUUAUU. The thirty most enriched RNA transcripts identified in this study are listed in (Table 1) and are ranked in order of fold enrichment.

Table 1: Potential physiological RNA targets of L3 identified by RIP-Chip analysis of mouse placenta

Accession number	Sequence name	Average fold enrichment	Pentamer	Heptamer	Nonamer
NM_008726	Natriuretic peptide precursor type B	8.33	1	3*	2*
NM_183389	Double homeobox B-like	6.66	1	0	0
NM_173746	Predicted gene OTTMUSG00000004461	5.89	1	0	0
NM_026738	RIKEN cDNA 1110007C09 gene	5.87	0	1	0
NM_001033297	Gene model 561	5.86	4(3*)	0	0
NM_001113424	Antagonist of mitotic exit network 1 homolog	5.29	2	1*	1*
NM_009434	Pleckstrin homology-like domain, family A, member 2	5.28	0	1	0
AY047360	Chemokine-like factor	5.17	0	1	0
BC018472	COBW domain containing 1	5.13	1	1	0
NM_010415	Heparin-binding EGF-like growth factor	4.93	2	2	0
NM_018784	ST3 beta-galactoside alpha-2,3-sialyltransferase 6	4.92	0	0	0
AK003573	RIKEN cDNA 1110008H02 gene	4.88	-	-	-
AY047360	Chemokine-like factor	4.83	0	1	0
NM_025564	Mago-nashi homolog B	4.65	1	1	0
NM_054071	Fibroblast growth factor receptor-like 1	4.63	1*	1*	0
NM_172595	ADP-ribosylation factor related protein 2	4.50	5	2	1
NM_009497	Vesicle-associated membrane protein 2	4.46	1	1	0
NM_027998	Claudin 23	4.45	1	3	0
NM_026068	Mediator of RNA polymerase II transcription	4.43	1	0	0
NM_001143776	Family with sequence similarity 13, member C	4.39	6	0	0
NM_025600	DET1 and DDB1 associated 1	4.36	1	2	0
NM_019660	C-myc binding protein	4.35	1	0	1
NM_028943	Sphingomyelin synthase 2	4.34	0	1	0
NM_026744	Mitochondrial ribosomal protein L53	4.25	0	0	0
NM_026933	TP53 regulated inhibitor of apoptosis	4.23	0	0	0
NM_001039710	Coenzyme Q10 homolog B	4.22	2	1	0
NM_001127191	Sorting nexin 16	4.21	5	0	0
NM_021296	GrpE-like 2, mitochondrial	4.21	3	1	1
NM_145977	Solute carrier family 45, member 3	4.20	3(2*)	0	1*
NM_028394	Heat shock protein family B, member 11	4.13	0	1	0

The accession numbers and sequence names of the thirty most enriched RNAs are listed with their average fold enrichment values. The number of ARE sequences in the available sequence data for their 3' UTRs is also included. The presence of an ARE cluster is denoted by an asterisk (*). The 3' UTR sequence for RIKEN cDNA 1110008H02 gene was unavailable.

The transcript encoding BNP exhibited the greatest fold enrichment in the anti-L3 sample in each of the pairs of replicates (Fig. 14A), with an average of more than eight fold enrichment. The BNP mRNA sequence contains five overlapping ARE sequences in its 3'UTR (three heptamers and two nonamers) as well as a single pentamer further downstream (Fig. 14B). Consequently, BNP was judged to be an excellent candidate for post-transcriptional regulation by L3.

A

replicate	fold enrichment	p-value
1	12.562	1.47E-24
2	7.8735	2.22E-26
3	6.9522	3.87E-20
4	8.0096	1.74E-12
5	6.2663	1.70E-22

B

GAAGACCTCCTGGCTGCAGGAGACTCCAGTTTCTGACTCTGCCTGGGTCTCTTTCCCCAGCTCTGGG
ACCACCTTTGAAGTGATCCTATTTATTTATTTATTTATTTATTTTTATTTTTATTTTAAATTTATTTTGT
TGTTTTTCTACAAGACTGTTTCTTATCTTGGAGCACAACTTGCCACAACATAATTAACATAGCGTTTT
CCTGCTTTTAAAAGGAAAAAAAAAAAAAAAAAAAAA

Figure 14: BNP as a target of L3

(A) BNP was the most enriched RNA in the L3 immunoprecipitates. The enrichment value as compared to the control immunoprecipitation is listed for each biological replicate, along with its associated p-value. (B) The sequence of the BNP 3'UTR (GenBank accession number NM_008726.4) is shown with the polyA motif in italics. The BNP 3'UTR contains multiple, overlapping AREs. The cluster of ARE heptamers and nonamers as well as a single pentamer are in red and each single ARE unit in the cluster is underlined.

While we focused our study on the verification of one potential mRNA target of L3, BNP, the RIP-Chip experiment identified many other potential targets. Each of these candidates was enriched at least two-fold in the anti-L3 immunoprecipitates, and many contain ARE sequences within their 3'UTRs. The list of 383 candidate transcripts may contain many more true physiological targets that will need to be confirmed.

3.3.2 Analysis of BNP mRNA expression in mouse placenta

The natriuretic peptide family of hormones consists of A-type natriuretic peptide (ANP), BNP, and C-type natriuretic peptide (CNP). ANP and BNP are highly expressed in cardiomyocytes, with greatest expression in atria and ventricles, respectively. CNP is primarily expressed in the brain and in vascular endothelial cells [reviewed in (Potter et al., 2009)]. Although intensive studies have been completed on the expression and function of these hormones in adults, less is known about the natriuretic peptide family in embryos and extra-embryonic tissues. In situ hybridization histochemistry revealed both BNP and CNP mRNA expression within the decidua of mouse placenta, while no expression of ANP transcripts was detected (Cameron et al., 1996). ANP, while not found in mouse placenta to date, has been detected in cytotrophoblasts in human placenta (Lim and Gude, 1995).

To confirm that BNP mRNA is expressed in mouse placenta, we performed northern blots of placenta RNA at various timepoints during gestation. Total RNA from

E9.5, 10.5, 12.5 and 14.5 placentas, as well as from heart and liver, was isolated and subjected to northern analysis. BNP was detected at low levels in placenta, while heart showed high levels and liver showed no detectable expression (Fig. 15A).

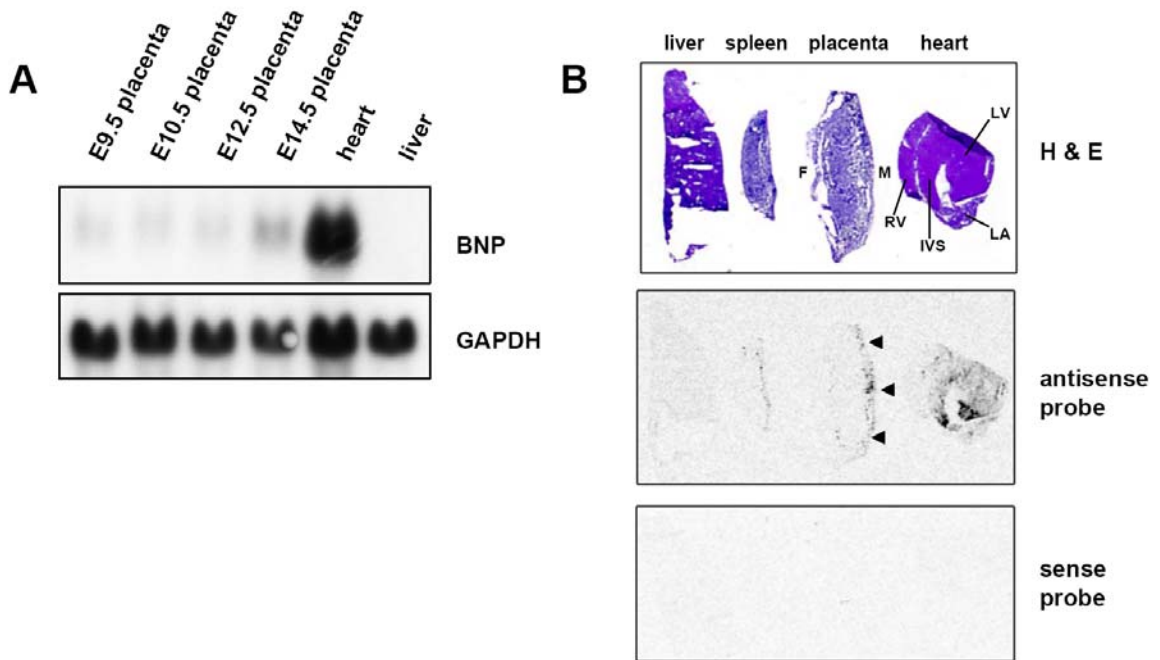


Figure 15: Expression of BNP RNA in mouse placenta

(A) Total RNA was isolated from the indicated mouse tissues and was analyzed for the presence of BNP mRNA by northern blotting. BNP was observed at low levels in placenta tissues from E9.5-E14.5. Heart and liver RNA were used as positive and negative controls for BNP expression, respectively. GAPDH is included in the lower panel as a loading control. (B) In situ hybridization histochemistry with BNP probes was performed on an E15.5 placenta section, along with heart, spleen, and liver as controls. The fetal (F) and maternal (M) sides of the placenta are denoted in the hematoxylin and eosin (H & E) stained section. The right and left ventricles (RV and LV), left atrium (LA), and intraventricular septum (IVS) of the heart are also indicated. BNP mRNA is expressed in the maternal decidua of the placenta, as well as in the heart, but is minimally expressed in the spleen and not in the liver.

We also performed in situ hybridization histochemistry with a radiolabeled BNP antisense probe to further examine the sites of BNP transcript expression in E15.5 mouse placenta. BNP was detected in the placenta in the region of the maternal decidua (Fig. 15B). BNP was also detected at high levels in the heart and low levels in the spleen, but not in liver, as expected (Fig. 15B). Hybridization with a BNP sense probe yielded no detectable signal, even after extended exposure times.

3.3.3 Binding of L3 to the BNP ARE

TTP family members are able to bind class II AREs, such as the ARE of TNF, the physiological target of TTP. The conserved TZF domain is required for binding and any mutation that drastically disrupts the structure of one of the zinc fingers also disrupts its ability to bind RNA (Lai et al., 2002). Binding to the ARE is necessary for the subsequent degradation of the targeted message.

In order to evaluate the ability of L3 to bind the ARE of BNP, we performed gel electrophoretic mobility shift assays. GFP or GFP-L3 fusion proteins were over-expressed in HEK 293 cells. Lysates from these cells were incubated with a radiolabeled RNA oligonucleotide containing the sequence of the BNP ARE (Fig. 16A). These reactions were analyzed for the presence of protein-probe complexes by separation with non-denaturing PAGE followed by autoradiography. The GFP-L3 fusion protein was able to shift the BNP ARE probe, while GFP alone and a GFP-L3 zinc finger mutant,

C143R, did not produce a shift (Fig. 16B). In comparison to other TTP family members, L3 yields substandard gel shifts due to aggregates that are unable to enter the gel. Nonetheless, the presence of the L3-RNA complex is apparent. Expression levels of the native GFP-L3 protein and the zinc finger mutant were relatively comparable in these assays (Fig. 16C). This study shows that L3 is able to bind the BNP ARE and mutation of its conserved TZF domain prevents this binding.

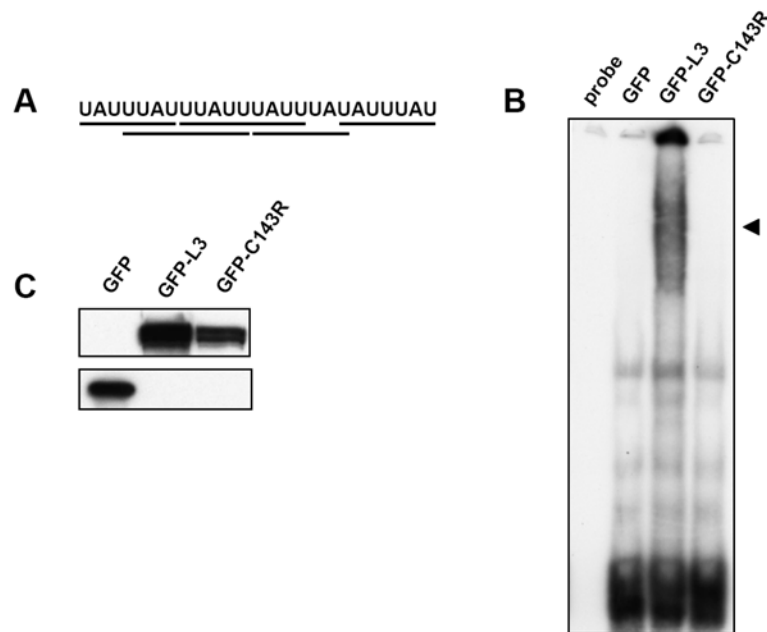


Figure 16: Binding of L3 to a BNP ARE probe

HEK 293 cells were transfected with constructs encoding GFP or GFP-L3 fusion proteins. Cytosolic extracts from these cells (20 μ g total protein) were incubated with a BNP ARE RNA probe (sequence shown in A). The reactions were separated with non-denaturing PAGE and analyzed with autoradiography. An arrowhead (\blacktriangleleft) indicates the L3 RNA complex in B. Note that GFP alone and the GFP-L3 zinc finger mutant, C143R, do not bind to the BNP ARE probe. Western analysis using a GFP antibody (C) shows relatively equal expression levels of GFP and its fusion proteins used in this study.

3.3.4 Effect of L3 on the degradation of BNP RNA

TTP family members act by promoting the degradation of ARE-containing mRNAs. This stimulated decay involves TTP-promoted deadenylation of the message, followed by nucleolytic decay.

The ability of L3 to promote the degradation of the ARE-containing BNP transcript was examined using co-transfection experiments. GFP or a GFP-L3 fusion protein and a reporter RNA were co-expressed in HEK 293 cells. Total RNA was isolated and the level of the reporter RNA was examined by northern blotting. The reporter RNA construct contained the entire BNP transcript, including its 3'UTR. The BNP reporter was degraded in the presence of the GFP-L3 fusion protein (Fig. 17A, lanes 4-6), as compared to reporter co-expressed with GFP alone (Fig. 17A, lanes 1-3). Increased concentrations of transfected GFP-L3 plasmid exhibited enhanced degradation of the reporter transcript along with the appearance and increased intensity of a smaller band that corresponds to the deadenylated form of the reporter. Similar deadenylated species have been noted in other studies using TTP family members and similar reporter constructs, such as in (Lai et al., 2003).

Another co-transfection experiment using different constructs was conducted to confirm these results. A FLAG-L3 fusion protein and a different reporter RNA were co-expressed in HEK 293 cells, and the total RNA isolated from these cells was subjected to

northern analysis. The reporter RNA construct contained the coding region for GFP followed by the whole BNP 3'UTR. The GFP-BNP reporter was not degraded in control transfections (Fig. 17B, lanes 1-3), but was degraded in the presence of FLAG-L3, with increased levels of decay in the presence of increased concentrations of the transfected FLAG-L3 construct (Fig. 17B, lanes 4-9).

These studies demonstrate that L3 is able to promote the degradation of mRNA targets containing BNP ARE sequences. Similar L3-promoted mRNA decay was previously demonstrated with an artificial target transcript containing TNF-based ARE sequences (Blackshear et al., 2005).

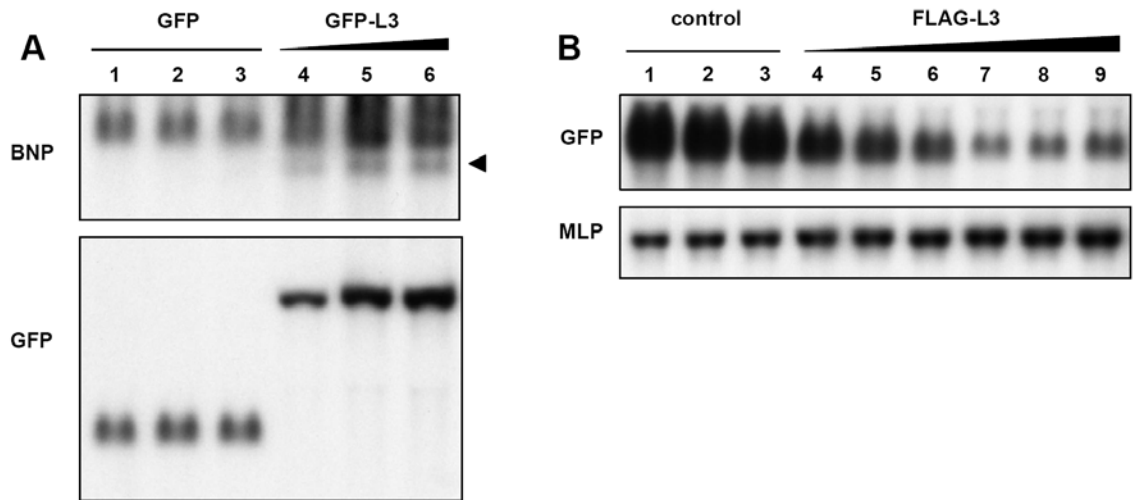


Figure 17: L3-promoted degradation of BNP RNA

(A) HEK 293 cells were co-transfected with 1 μ g of a full length BNP reporter RNA and either 10 ng of a GFP plasmid (lanes 1-3) or 2.5 ng (lane 4), 5 ng (lane 5), or 10 ng (lane 6) of a GFP-L3 plasmid. The amount of total transfected DNA was brought to 5 μ g with the addition of pBS. Total RNA was isolated and the level of reporter RNA was analyzed via northern blotting (top panel). The expression of GFP and GFP-L3 was also analyzed via northern blotting (bottom panel). GFP-L3 promotes the degradation of a BNP reporter RNA that contains the 3'UTR of BNP. The deadenylated products are indicated with an arrowhead (\blacktriangleleft). (B) A similar experiment was performed with different constructs to corroborate this data. In this assay, HEK 293 cells were co-transfected with 1 μ g of a GFP reporter RNA that contains the 3'UTR of BNP and 0 ng (lanes 1-3), 2.5 ng (lane 4), 5 ng (lane 5), 10 ng (lane 6), 20 ng (lane 7), 40 ng (lane 8), or 80 ng (lane 9) of a FLAG-L3 plasmid. Northern blotting with a GFP probe showed decreased levels of the GFP-BNP reporter mRNA upon increasing transfection amounts of FLAG-L3 (upper panel). Expression of endogenous MLP mRNA was also analyzed by northern blotting as a loading control (lower panel).

3.4 Discussion

The biological roles of the members of the TTP family of CCCH tandem zinc finger proteins are currently being elucidated. TTP, L1, L2, and L3 may act to regulate different RNA targets and, consequently, have distinctive functions within the organism while maintaining similar mechanisms of action. The relevance of each of these proteins to the intact animal will become clearer through identification of their physiological mRNA targets.

A number of physiological RNA targets have been identified for TTP to date, in many cases implicating this family member in mediation of the inflammatory response. For example, TTP binds to transcripts such as those encoding TNF- α , granulocyte macrophage-colony stimulating factor (GM-CSF), immediate early response 3 (Ier3), and interleukin-10 (IL-10).

The identities of these targets have been ascertained through a variety of methods, particularly including the use of TTP knockout cells, as well as over-expression experiments in which the stability of putative target transcripts was evaluated. TNF- α and GM-CSF transcripts were identified as physiological TTP targets through generation of TTP knockout mice and analysis of their mRNA stability in cells derived from these animals (Carballo et al., 1998, 2000; Lai et al., 1999). The Ier3 transcript was identified as a TTP target through a global microarray analysis of RNA

decay in cells from wild type and TTP-deficient mice (Lai et al., 2006). RIP-Chip analysis of macrophages stimulated with lipopolysaccharide allowed for the identification and verification of the IL-10 mRNA as a TTP target (Stoecklin et al., 2008).

The TTP family members L1 and L2 are both able to bind TNF- α and GM-CSF transcripts, as well as other ARE-containing mRNAs, and promote their decay in cell co-transfection experiments. However, their true physiological targets have not yet been identified. In the case of L1, (Duan et al., 2009) have recently revealed in knockdown and binding experiments that the mRNA encoding steroidogenic acute regulatory protein may be targeted for regulation by this family member. In the case of L2, no mRNA targets have been identified to our knowledge. The L3 protein represents an intriguing candidate protein for this type of study because of the availability of a specific antibody against this protein (Frederick et al., 2008) and its apparent abundant expression in placenta throughout development.

Because of the specific and abundant nature of this expression, we hypothesized that L3 can bind to and promote the turnover of a set of placental mRNAs. We utilized RIP-Chip analysis of E14.5 placenta to begin to test this hypothesis. The top candidate mRNA, that encoding BNP, contains five, overlapping AREs within an extremely AU-rich and conserved portion of its 3'UTR. We further demonstrated that L3 was able to

directly bind the BNP ARE and to promote the degradation of RNA containing the BNP ARE.

BNP, a member of the natriuretic peptide family, is highly expressed in and secreted from ventricular myocytes. BNP is well-known for its role in control of blood pressure and body fluid homeostasis. However, this hormone has been proposed to have other important functions in tissues such as the placenta (Cameron et al., 1996). These functions may be similar to those of a similar secreted peptide vasodilator, adrenomedullin (AM). AM has well-described roles as a vasodilator in the systemic and pulmonary circulation [reviewed in (Yanagawa and Nagaya, 2007)] but is also required for the establishment and maintenance of pregnancy and normal fetal growth. AM is expressed in the maternal decidua as well as in the trophoblast giant cells of the placenta (Yotsumoto et al., 1998). Its function in this tissue has been determined to be the promotion of branching of the labyrinth and remodeling of maternal spiral arteries, instead of an expected role in vasodilation of placental blood vessels. Placentas of AM knockout mice exhibit defects in branching of the labyrinth and maternal artery remodeling (Li et al., 2006), both of which are characteristic traits of pre-eclampsia in humans.

The physiological role of BNP in the placenta, if any, requires further study. BNP transcripts, along with those encoding other natriuretic peptides, are expressed in

placental tissue. We found that BNP mRNA is expressed in the placenta between E9.5 and E14.5. BNP mRNA has also been detected in E15.5 placenta in the maternal decidua through in situ hybridization histochemistry (Cameron et al., 1996), as well as in the current study. It seems possible that BNP mRNA may be expressed in other placental cell types, but may not be seen in these cells due to downregulation by L3.

In humans, administration of BNP into the fetal placental circulation has been demonstrated to inhibit the effects of the vasoconstrictor agent angiotensin II (Holcberg et al., 1995). Therefore, BNP may act as a vasodilator that can regulate the fetal-maternal blood flow in placental vessels. BNP has also been shown to be upregulated at the protein level in the placenta of pre-eclamptic human patients (Resnik et al., 2005). The complete spectrum of BNP action in the placenta remains to be determined. BNP may play a role in vasodilation or roles similar to those of AM, such as in vessel branching or in other critical developmental aspects of placenta physiology.

BNP is a secreted hormone and could act in either a paracrine or endocrine fashion. It could act locally to affect placenta physiology, as previously described, and it could also travel through the blood to affect distant cells. BNP could travel to the fetus and/or the mother to exert its effects on their tissues. A number of hormones that are expressed in and secreted from placental cells perform their roles far from their cells of origin. For example, human placental lactogen, a hormone secreted by the trophoblast

cells, enters the maternal circulation to inhibit maternal insulin and, thus, increases the glucose supply to the fetus [reviewed in (Walker et al., 1991)].

Both BNP knockout and over-expression mice have been created. BNP knockout mice were noted to be fertile, although a description of their placentas has not been published to date. Analysis of these knockout mice reveals the significance of BNP in cardiovascular regulation. These animals exhibit cardiac fibrosis, implicating BNP as a regulator of ventricular remodeling (Tamura et al., 2000). BNP over-expressing mice, in which BNP is over-expressed only in the liver after birth, exhibit endochondral ossification defects leading to skeletal overgrowth; no information was provided about the placentas of these animals (Suda et al., 1998).

Future investigations are required to validate other potential RNA targets of L3. While our work only focused on one candidate transcript, 382 other possible L3 mRNA targets were identified in this study. It should be relatively straightforward to demonstrate that the ARE regions of the selected transcripts can bind directly to L3, and that L3 is able to promote their deadenylation and degradation. When L3 knockout mice are generated, it will be necessary to evaluate levels of BNP mRNA and the other candidate target transcripts in the placentas from these animals as compared to those from wild type littermates. However, these data may be difficult to interpret since L3

deficiency may result in gross anatomical abnormalities, or even failure of development, of placentas in these animals.

The ever-changing nature of placental physiology during gestation demands continuous regulation of many genes in this organ. L3 may play an important role in this process by regulating gene expression at the level of mRNA decay. As an example, L3 may target BNP mRNA for degradation in rodent placenta, and consequently, downregulate BNP expression at critical periods during gestation.

4. Identification of phosphorylation sites and functional analysis of the conserved C-terminus of ZFP36L3

4.1 Introduction

ZFP36L3 (L3) is the placenta-specific member of the tristetraprolin (TTP) family of RNA-binding CCCH tandem zinc finger proteins. The proteins of the TTP family function to downregulate certain AU-rich element (ARE)-containing transcripts by binding to them and promoting their decay. We expect that L3 will ultimately be shown to regulate a number of placental mRNAs in order to control aspects of the development or physiology of this organ.

Because L3 is the most recently discovered member of the TTP family, not much is known about its characteristics and functions. In the course of our study on this unique TTP family member, we observed that both over-expressed and endogenous L3 appeared as two distinct species of approximately equal abundance when analyzed by denaturing polyacrylamide gel electrophoresis (PAGE). These two species exhibit a M_r of ~90,000 and ~100,000.

A protein can be detected as multiple species for a variety of reasons. Differential splicing may create different isoforms depending on the arrangement of exons and introns in its gene. Translation from alternative translation initiation sites could create species that differ in their amino (N)-terminal regions. Conversely, premature truncation could produce species that lack portions of the carboxyl (C)-

terminal region. Intracellular or post-homogenization proteolysis could result in any number of species that contain fragments of the original protein. Because post-translational modifications can add mass and charge to a protein, differing modifications could also result in the appearance of multiple protein species.

Post-translational modifications, particularly the addition of functional groups to proteins, are critical factors in the life of a protein and its action within the cell. For example, in glycosylation, the covalent attachment of oligosaccharides to cell surface and secreted proteins can affect surface receptor binding and immune recognition (Varki, 1993). In acetylation, reversible addition of acetyl groups to proteins such as histones can influence the overall condensation of chromatin and the level of gene transcription (Munshi et al., 2009). In ubiquitination, the addition of one or more ubiquitin moieties can target the modified protein for proteosomal degradation (Hochstrasser, 2009).

Phosphorylation, the addition of a phosphate group to a serine, threonine or tyrosine residue, is one of the most common post-translational modifications and plays a critical role in the regulation of protein function. Phosphorylation has previously been shown to regulate the activity, localization, and stability of TTP, the first discovered member of the TTP protein family. TTP binds to and promotes the decay of certain mRNAs whose protein products are involved in the innate immune response, such as

those encoding certain inflammatory cytokines. The reversible phosphorylation of TTP, therefore, provides another potential level of control over its regulation of the decay of its target mRNAs, and the innate immune response in general.

The phosphorylation of TTP does not create two distinct species upon separation with denaturing PAGE, as is observed with L3. Instead, TTP from tissues and stimulated cells migrates as a smear comprised of six to eight individual bands at a larger than predicted M_r . A number of phosphorylation sites have been identified for TTP and have been studied with respect to their effect on TTP function [reviewed in (Sandler and Stoecklin, 2008)]. For instance, during immune activation, a signaling cascade leads to the phosphorylation of TTP by mitogen-activated protein kinase-activated protein kinase 2 (MK2) at Ser52 and Ser178. This phosphorylation reduces the mRNA destabilizing activity of TTP and prevents decay of TTP by the proteasome while also increasing transport from the nucleus to the cytoplasm. In this way, when cytokines must be produced for an immune response, phosphorylation causes TTP to be inactivated but available and stable in the cytoplasm. When cytokine production must be turned off, TTP is accessible for activation by dephosphorylation by protein phosphatase 2A.

In this study, we investigated the molecular basis for the two observed species of L3: V1, the faster-migrating species, and V2, the slower-migrating species. We first

tested whether the faster-migrating species, V1, was a shorter version of the full length protein due to alternative translation initiation, premature truncation, or proteolysis, using a panel of anti-peptide antibodies. We then analyzed L3 for post-translational modification, specifically for phosphorylation. We hypothesized that the slower-migrating species, V2, could be a modified version of L3 that contained one or more additional phosphates. We were able to demonstrate that L3 was phosphorylated, and then identified five phosphorylation sites through mass spectrometry. We next analyzed deletion mutants and serine mutants to assess the significance of the C-terminus and the serine residues within the C-terminus in creating one of the species and influencing the phosphorylation state of the protein. We also tested the importance of the C-terminus and, hence, the phosphorylation of Ser721, to the mRNA binding and destabilizing functions of L3.

4.2 Methods

4.2.1 Plasmids

Plasmid GFP-L3 [page 31, (Frederick et al., 2008)] and plasmid CMV2.EGFP.L3.BGH3'/BS⁺ (page 66) both express an N-terminal green fluorescent protein (GFP) fused to the full length mouse L3 protein, amino acids 1-725 of GenPept accession number NP_001009549.1, corresponding to nucleotides 150-2327 of GenBank accession number NM_001009549.2. We found that use of plasmid

CMV2.EGFP.L3.BGH3'/BS⁺ results in much higher expression of the fusion protein as compared to plasmid GFP-L3; the basis for this difference in expression is unknown.

Four L3 deletion mutant constructs that were made previously [(page 33), (Frederick et al., 2008)] were used in this study. Plasmid GFP-TZF-RD-NES expresses GFP fused to amino acids 116-725 of GenPept accession number NP_001001806.1. Plasmid GFP-TZF-RD expresses GFP fused to amino acids 116-711. Plasmid GFP-RD-NES expresses GFP fused to amino acids 193-725. Plasmid GFP-RD expresses GFP fused to amino acids 193-711. These plasmids are diagrammed in (Fig. 19A).

A fifth GFP-L3 deletion mutant was newly created for this study. Plasmid GFP-L3trunc was created by inserting nucleotides 150-2282 of GenBank accession number NM_001001806.2 into the *Bam*HI and *Eco*RV restriction enzyme sites of CMV2.EGFP(c).BGH3'/BS⁺ (W.S. Lai, unpublished plasmid). This plasmid codes for the expression of a C-terminal truncated L3 protein (amino acids 1-711 of GenPept accession number NP_001001806.1), in which the 14 C-terminal amino acids of the wild type protein are omitted, with an N-terminal GFP tag. This deletion mutant is also diagrammed in (Fig. 19A).

Plasmid FLAG-L3, which was constructed earlier (page 67), was used to express protein for the mass spectrometry analysis and deadenylation experiments. We also created FLAG-L3trunc by inserting a stop codon at nucleotide 2283 of GenBank

accession number NM_001001806.2 in plasmid FLAG-L3. We used site-directed mutagenesis following the Stratagene QuikChange protocol with the primer set: 5'-CGACAACACCAACTCCAGCTGACGTCTGCCCATCTTCAGC-3' and 5'-GCTGAAGATGGGCAGACGTCAGCTGGAGTTGGTGTGTCG-3'. This plasmid also codes for the expression of a L3 protein in which the C-terminal 14 amino acids are deleted, although this time with an N-terminal FLAG tag.

We further employed the Stratagene site-directed mutagenesis protocol to produce ten serine mutants for study of possible L3 phosphorylation sites. The primers used and the mutants created are listed in (Table 2). All mutant sequences were confirmed by BigDye terminator cycle sequencing (Applied Biosystems).

Table 2: Primers used in site-directed mutagenesis to create serine mutants

mutants	template plasmid	primers
S710A	GFP-L3	5'-CGACAACACCAACGCCAGCCGCCGTCTGCC-3' 5'-GGGCAGACGGCGGCTGGCGTTGGTGTGTCG-3'
S711A	GFP-L3	5'-CGACAACACCAACTCCGCCCGCCGTCTGCC-3' 5'-GGGCAGACGGCGGGCGGAGTTGGTGTGTCG-3'
S710A/S711A	GFP-L3	5'-CGACAACACCAACGCCCGCCCGCCGTCTGCC-3' 5'-GGGCAGACGGCGGGCGGCGTTGGTGTGTCG-3'
S718A	GFP-L3	5'-CTGCCCATCTTCGCCCGTTCTCAGAC-3' 5'-GTCTGAGAAGCGGGCGAAGATGGGCAG-3'
S721A	GFP-L3	5'-CTTCAGCCGCTTCGCAGACTCTG-3' 5'-GACAGTCTGCGAAGCGGCTGAAG-3'
S723A	GFP-L3	5'-CGCTTCTCAGACGCTGAAAAATGAGACAA-3' 5'-GGGTCTCATTTTTTCAGCGTCTGAGAAGCG-3'
S718A/S721A	GFP-L3/S718A	5'-CTTCGCCCCGCTTCGCAGACTCTG-3' 5'-CAGAGTCTGCGAAGCGGGCGAAG-3'
S718A/S723A	GFP-L3/S718A	5'-CGCTTCTCAGACGCTGAAAAATGAGACAA-3' 5'-GGGTCTCATTTTTTCAGCGTCTGAGAAGCG-3'
S721A/S723A	GFP-L3/S721A	5'-CGCTTCGCAGACGCTGAAAAATGAGACCC-3' 5'-GGGTCTCATTTTTTCAGCGTCTGCGAAGCG-3'
S718A/S721A/S723A	GFP-L3/S718A/S723A	5'-CTTCGCCCCGCTTCGCAGACGCTG-3' 5'-CAGCGTCTGCGAAGCGGGCGAAG-3'

We used plasmid pMLP.TNF-3'UTR for analysis of ARE-containing mRNA degradation in the presence of the L3 protein (Blackshear et al., 2005). This reporter codes for Marcks-like protein (MLP) followed by the 3' untranslated region (UTR) of tumor necrosis factor (TNF).

Plasmid TNF- α 1309-1332 (A)50/SK- was created for use in deadenylation assays by inserting 50 base pairs from double-stranded oligonucleotides into the *XbaI* and *EagI* cloning sites of pTNF- α 1309-1332. Plasmid pTNF- α 1309-1332 was constructed previously and contains nucleotides 1309-1332 of GenBank accession number X02611.1 (Lai et al., 1999).

pEGFP-N1 (Clontech), which expresses GFP, was used in control experiments. pBS (Stratagene) was used in co-transfection experiments to bring the total amount of transfected DNA to 5 μ g.

4.2.2 Cell culture and transfection

Maintenance of human embryonic kidney (HEK) 293 cells and transient transfections with FuGENE 6 Transfection Reagent (Roche Applied Science) were performed as described on page 33. Transient transfections were also performed using the standard calcium phosphate protocol.

4.2.3 Preparation of cell lysates

To prepare cell lysates, 0.7×10^6 HEK 293 cells were plated on a 100 mm plate. After 24 h, the cells were transfected with 1 μg of the appropriate L3 construct using FuGENE 6 Transfection Reagent. The cells were harvested for protein 16 h later; the plate was washed twice with ice-cold phosphate buffered saline, calcium and magnesium free (PBS-CMF) and cells were scraped in 250 μL lysis buffer (50 mM Tris-HCl [pH 8.0], 1% [v/v] Nonidet-P40, 100 mM NaCl, 50 mM NaF, 1X complete EDTA-free protease inhibitor cocktail [Roche Applied Science]). The extract was left on ice for 20 min to complete cell lysis and was then centrifuged at $18,000 \times g$ for 20 min at 4°C to pellet debris.

4.2.4 Detection of L3 protein by immunoblotting

Total protein from cell lysates was separated on a sodium dodecyl sulphate (SDS)-polyacrylamide gel and transferred to a nitrocellulose membrane. To determine whether V1 is a shorter version of the full length protein, western blot analysis of a GFP-L3 fusion protein was performed with four antibodies that recognize L3, each at a dilution of 1:2000. The sequences of L3 to which the antibodies are directed against are illustrated in (Fig. 4-1A). A protein A-horseradish peroxidase (HRP) secondary antibody (Zymed) was used at a dilution of 1:16,000. For analysis of deletion mutants, serine mutants, and phosphatase-treated samples, western blot analysis was performed

with anti-GFP-HRP conjugate (BD Biosciences) at a dilution of 1:3000. In all cases, the proteins were visualized with enhanced chemiluminescence.

4.2.5 Phosphatase treatment of native L3 and serine mutants

HEK 293 cells were plated, transfected with 1 μ g GFP-L3 or serine mutants with FuGENE transfection reagent, and harvested as described above. Phosphatase reaction buffer (50 mM Tris HCl [pH 7.5], 1 mM MgCl₂) was added to 50 μ g of total protein from each lysate and the samples were incubated at 30°C for 10 min. Half of the samples were treated with 20 U calf intestinal alkaline phosphatase (CIAP)(Invitrogen). All samples were then incubated for 1 h at 30°C. The reactions were analyzed by immunoblotting with a GFP-HRP antibody as described above.

4.2.6 Purification of FLAG-L3 fusion proteins

HEK 293 cells were plated at a density of 0.7×10^6 cells per 100 mm plate. Each of 20 plates was transfected with 1 μ g FLAG-L3 or FLAG-L3trunc constructs using FuGENE 6 Transfection Reagent. Cell lysates were prepared as described above. Each FLAG fusion protein was purified by batch column with ANTI-FLAG M2 Affinity Gel (Sigma Aldrich) according to the manufacturer's instructions. After preparation of the resin with 0.1 M glycine HCl (pH 3.5), the cell lysate was incubated with 250 μ L resin, rotating overnight at 4°C. The resin was washed three times with ice-cold Tris buffered saline (TBS) and pelleted by centrifugation (8000 \times g, 30 sec, 4°C). FLAG fusion proteins

were eluted five consecutive times with 250 μ L of 100 μ g/mL 3X FLAG peptide (Sigma Aldrich) in TBS.

4.2.7 Mass spectrometry

In order to identify L3 post-translational modifications, extensive mass spectroscopy experiments of purified FLAG-L3 were performed by Jason Williams in the mass spectrometry core of the National Institute of Environmental Health Sciences. Both species of L3 were analyzed simultaneously in solution using the first elution from the FLAG-L3 purification. Also, each species of L3 was analyzed individually; the first elution (15 μ L) from the FLAG-L3 purification was separated by SDS-PAGE, followed by staining with SYPRO Ruby (BioRad).

4.2.8 Analysis of mRNA binding

To prepare protein for RNA binding analysis, HEK 293 cells were plated, transfected with 1 μ g of pEGFP-N1, CMV2.EGFP.L3.BGH3'/BS⁺, or GFP-L3trunc with FuGENE 6 Transfection Reagent, and harvested as described. In this experiment, NaF was eliminated from the lysis buffer and the amount of NaCl was adjusted to 150 mM. Also, glycerol was added to each lysate to 20% total volume. Immunoblotting with a GFP-HRP antibody was performed to check for recombinant protein expression.

RNA electrophoretic mobility shift assays were completed to evaluate direct binding of full length and truncated L3 to the ARE of TNF. Total protein (20 μ g) from

the HEK 293 cell lysates was incubated with a ^{32}P -labeled TNF ARE RNA oligonucleotide probe for 20 min at room temperature as described previously (Blackshear et al., 2005; Frederick et al., 2008). Each reaction was separated on a 4% (w/v) non-denaturing polyacrylamide gel and the presence of protein-probe complexes was visualized with autoradiography.

4.2.9 Analysis of mRNA degradation

Co-transfection experiments were performed to evaluate the ability of a GFP control, full length GFP-L3, and truncated GFP-L3 to degrade an mRNA reporter. Plates (100 mm) of 0.5×10^6 HEK293 cells were prepared and the cells were fed 16 h later with supplemented Minimal Essential Medium (MEM) (Invitrogen). The cells were transfected with 10 ng pEGFP-N1 or 2.5 ng, 5 ng, or 10 ng CMV2.EGFP.L3.BGH3'/BS⁺ or GFP-L3trunc, as well as 3 μg plasmid pMLP.TNF-3'UTR and 2 μg pBS using the calcium phosphate method. After 16 h, the cells were washed twice with incomplete MEM and then fed with supplemented MEM. RNA was isolated 24 h later using the illustra RNAspin Mini Kit (GE Healthcare) according to the manufacturer's instructions.

To check for mRNA reporter degradation, 10 μg of each RNA isolate was fractionated on a 1.5% formaldehyde-agarose gel, transferred to a Hybond-N⁺ membrane (Amersham), and hybridized with a random-primed, α - ^{32}P -labeled probe. The probe used for detecting MLP reporter transcripts consisted of nucleotides 182-786

of GenBank accession number NM_010807.3. The blot was also hybridized with a full length GFP cDNA probe, containing the coding region of EGFP from the plasmid pEGFP-N1 (Clontech), to monitor expression of GFP, GFP-L3, and GFP-L3trunc. Hybridization was visualized using autoradiography.

4.2.10 *In vitro* deadenylation assay

The *in vitro* deadenylation assays were performed by Melissa Adkins at the National Institute of Environmental Health Sciences. A template for the RNA probe TNF ARE A₅₀ was polymerase chain reaction (PCR) amplified from plasmid TNF- α 1309-1332 (A)₅₀/SK⁻ with M13 Forward and T50Xba primers. The resulting double-stranded template was sequenced by dRhodamine terminator cycle sequencing to confirm that the TNF ARE was followed by 50 adenosines, and no other nucleotides. The RNA probe was transcribed in the presence of α -³²P-UTP (800 Ci/mmol). PCR amplification products were used as templates, and the Promega riboprobe *in vitro* transcription systems protocol was employed. The resulting products were separated from the free nucleotides using G50 columns (Roche).

The reaction mixtures were assembled on ice. Each reaction was initiated by adding 50 μ l of probe (5×10^4 cpm in an assay buffer consisting of 10 mM HEPES [pH 7.6], 40 mM KCl, and 5% glycerol) into a tube containing a titration of protein extracts in 50 μ l of assay buffer. MgCl₂ (3 mM final) and/or 20 mM EDTA was present in the assay

unless otherwise indicated. The mixtures were incubated at 37°C for 60 min, or over a time course of 0-120 min. EDTA was added to achieve a final concentration of 20 mM to terminate the reaction. The mixture was then extracted once with phenol-chloroform. An aliquot of 60 µl of the aqueous phase was mixed with 60 µl of 2X formamide stop solution (95% formamide, 0.05% bromophenol blue, 0.1% xylene cyanol) and then heated at 70°C for 5 min. Aliquots of reaction products were analyzed on a 6% acrylamide gel containing 7 M urea, followed by autoradiography.

4.3 Results

4.3.1 Detection of L3 with various L3 antibodies

Both over-expressed and endogenous L3 proteins are detected as two characteristic bands in denaturing PAGE. These species migrate at M_r of approximately 90,000 and 100,000. The two species do not correspond to two L3 isoforms; our lab previously determined that *Zfp36l3* generates a single transcript with no introns (Blackshear et al., 2005). In order to investigate other possibilities for existence of these two L3 species, we detected over-expressed L3 with four different antibodies.

We generated three new polyclonal antibodies for the detection of the L3 protein. Each was created with a synthetic peptide directed against a different short (15-17) amino acid sequence within L3. We also utilized an antibody that was designed to detect the C-terminus of the TTP family member ZFP36L2 (L2), but also recognizes L3

due to a high level of sequence conservation in this region. The sequences within L3 that are recognized by the antibodies used in this study are described in (Fig. 18A).

A GFP-L3 fusion protein was over-expressed in HEK 293 cells. Western blot analysis was conducted on the resulting lysate using each of the four antibodies. These antibodies are directed against [1] the extreme N-terminus, [2] the extreme C-terminus, [3] a region upstream of the TZF, and [4] a region downstream of the TZF. Each antibody detected both of the two characteristic bands corresponding to the L3 protein (Fig. 18A). Therefore, the full length protein is present in both bands, and the two species of L3 are not generated as a result of alternative translation initiation, premature truncation, or proteolysis.

4.3.2 Phosphatase treatment of full length L3

Post-translational modifications can change the size and charge of a protein and, in turn, alter its migration through a polyacrylamide gel. In particular, the addition of phosphate groups to serine, threonine, and tyrosine residues can affect the gel migration of a protein. In order to determine whether different phosphorylation states of L3 correspond to the two characteristic species, we treated over-expressed L3 with phosphatase.

A GFP-L3 fusion protein was expressed in HEK 293 cells. The cell lysate was incubated with or without CIAP and the reactions were quenched by boiling in SDS and

dithiothreitol. The reactions were then separated by denaturing PAGE, transferred to a nitrocellulose membrane, and the position of L3 was analyzed using a GFP antibody. The two characteristic L3 bands were detected in the untreated sample, while only one band was detected in the CIAP-treated sample (Fig. 18B); when L3 was treated with CIAP to remove all phosphate groups, the upper band disappeared while the lower band increased in intensity. This suggests that the slower-migrating species, V2, contains one or more phosphate groups that contribute to its Mr.

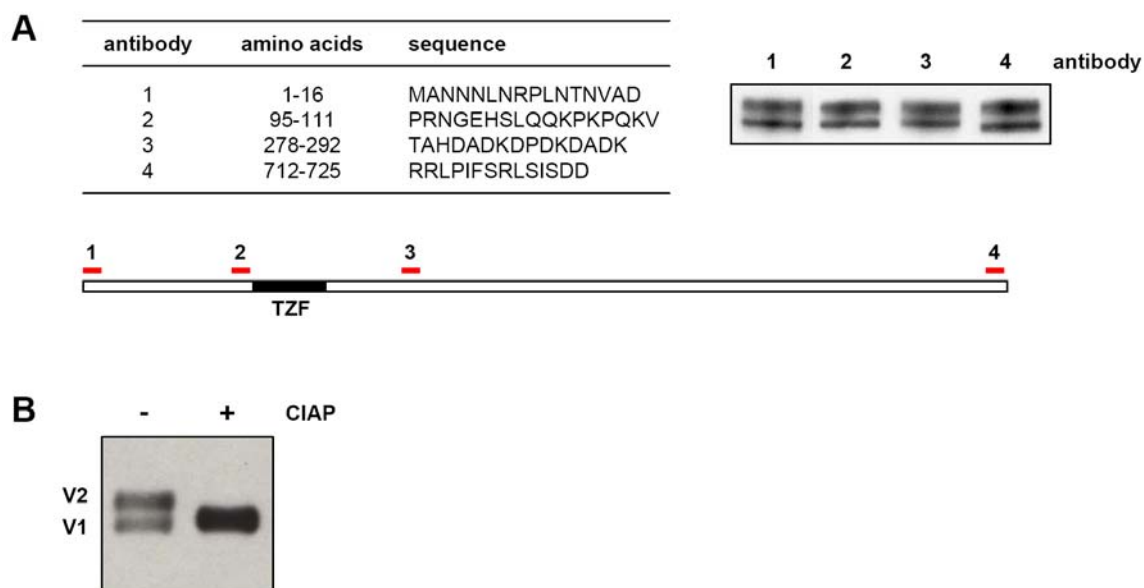


Figure 18: Analysis of the two characteristic species of L3

(A) GFP-L3 was over-expressed in HEK 293 cells. Lysates from these cells were subjected to western blot analysis with four peptide antibodies. The sequences of L3 recognized by each antibody are both listed and illustrated on a schematic representation of the L3 protein, in which TZF stands for the tandem zinc finger domain. Each antibody was able to recognize both L3 species, as shown in the western blot in the upper right panel. (B) Lysates from these cells were also incubated with or without CIAP and were then analyzed by western blotting with a GFP antibody. The top band, representing V2, collapses upon treatment with CIAP.

4.3.3 Analysis of deletion mutants

In order to identify the region of L3 that is required for the two different species to exist, we analyzed a number of L3 deletion mutants. Fusion proteins containing GFP linked to the N-terminus of either the full length L3 sequence or portions of the L3 sequence were over-expressed in HEK 293 cells. Lysates from these cells were subjected to western blot analysis using a GFP antibody.

Both species were detected for the full length protein (1-725) as expected, as well as for the deletion mutants containing amino acids 116-725 and 193-725 (Fig. 19). Only one species was observed for all proteins in which the C-terminal 14 amino acids are deleted; western analysis of the deletion mutants 1-711, 116-711, and 193-711 resulted in detection of one band (Fig. 19). The faint band detected for the deletion mutant 1-711 is not present on a SYPRO Ruby stained gel of the corresponding FLAG fusion protein after purification (not shown). Thus, the C-terminal 14 amino acids seem to be required for the existence of one of the two L3 species. Taken together with the data from our phosphatase experiment, it appears likely that the phosphorylation of the C-terminus might play a role in creating one of the species, possibly the slower-migrating species, V2.

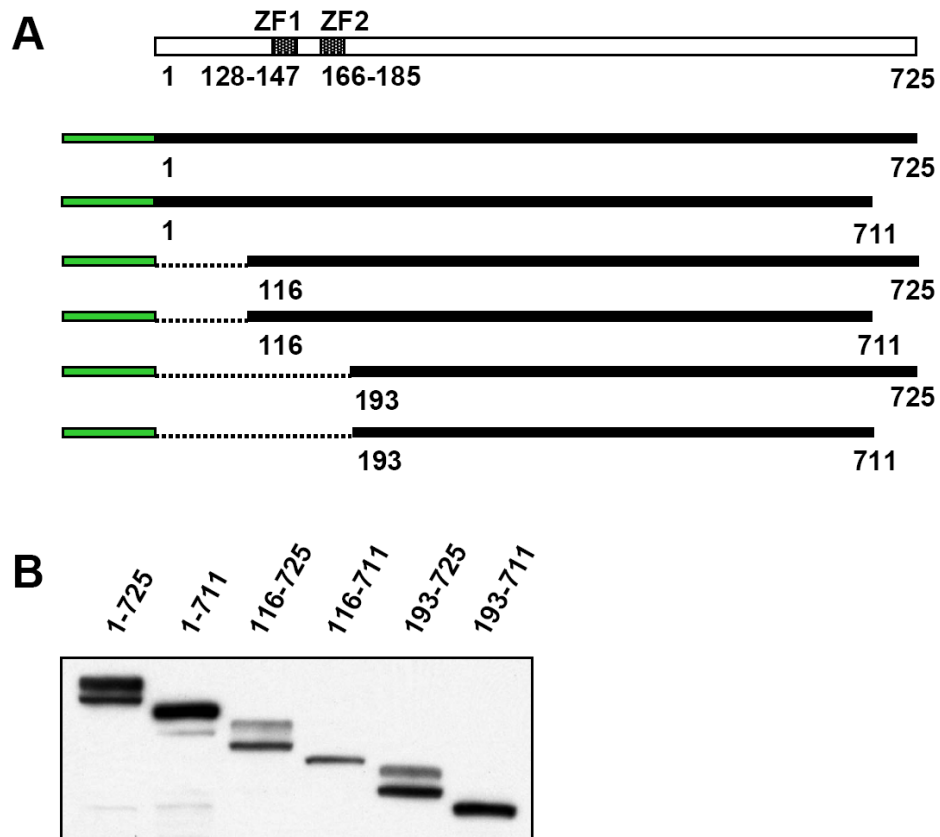


Figure 19: Analysis of L3 deletion mutants

(A) GFP-L3 deletion mutants are diagrammed, with GFP shown in green and the two zinc finger domains labeled ZF1 and ZF2. (B) The fusion proteins in A were over-expressed in HEK 293 cells and analyzed by western blotting with a GFP antibody. Only one species was detected when residues 712-725 are deleted, while both V1 and V2 (or their truncated versions) are detected when these residues were present.

4.3.4 Analysis of serine mutants

Mutants were created in order to identify the possible phosphorylation site or sites that could play a role in creating V2. Because the C-terminus could be essential to the existence of this band, we mutated all residues whose phosphorylation could be affected by deletion of the 14 C-terminal amino acids (Fig. 20A). Residues 712-725 contain serines that may be phosphorylated: Ser718, Ser721, and Ser723. Also, deletion of 712-725 could conceivably affect the kinase recognition motifs for Ser710 and Ser711 by disrupting downstream sequence. Because mutation of a phosphorylated residue can induce phosphorylation of adjacent residues that are normally not modified, multiple serine mutants were also created in this region.

GFP fusion proteins containing native or mutant L3 were over-expressed in HEK 293 cells and analyzed by western blotting with a GFP antibody. Single mutations of Ser710 (not shown), Ser711 (not shown), and Ser718 (Fig. 20B) to alanine did not affect the characteristic double banding pattern of L3, while mutation of Ser721 and Ser723 to alanine each resulted in the apparent loss of the lower band (Fig 20B). The S721A and S723A bands did not fully collapse into the lower band as one would expect for a non-phosphorylated protein. The presence of double and triple serine-to-alanine mutations did not further collapse the bands (Fig. 20C).

We treated native L3 and its serine mutants with phosphatase in order to better understand the unexpected migration changes seen with S721A and S723A. Lysates from cells over-expressing the single serine mutants, S718A, S721A, and S723A, were incubated with or without CIAP and were then analyzed by western blotting. The native L3 protein, as well as all three serine mutants, collapsed into a single, apparently lower M_r band upon addition of phosphatase (Fig. 20D). Hence, the single mutant proteins S721A and S723A appear to contain additional phosphates that slowed their migration through the gel and that could be removed with CIAP.

These data suggest that both Ser721 and/or Ser723 may be important for the double banding pattern that is characteristic of native L3. Phosphorylation of one or both of these residues may play a role in creating both bands, but other factors may come into play as well.

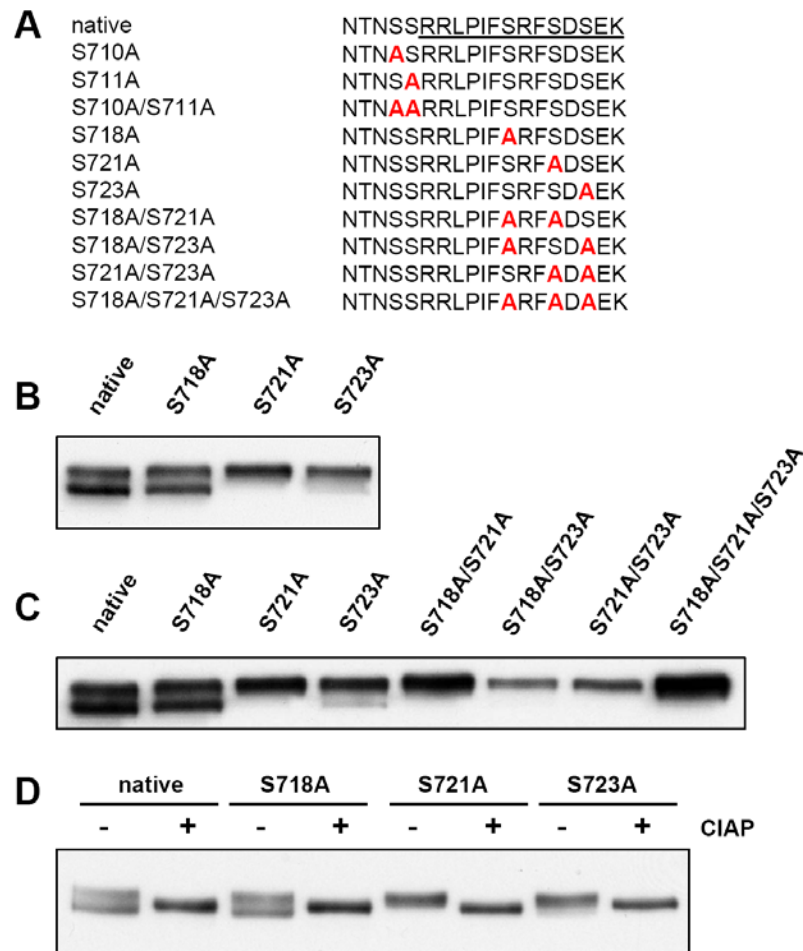


Figure 20: Analysis of L3 serine mutants

(A) The five serines whose phosphorylation state might be altered by deletion of 712-725 were mutated to alanine, both singly and in combination. The sequences of the L3 C-terminal region, including these mutants, are shown. Residues 712-725 are underlined. (B) Each mutant was expressed in HEK 293 cells and analyzed by western blotting with a GFP antibody. Both L3 bands were detected for all proteins containing the S710A (not shown), S711A (not shown), and S718A mutations. One major band was detected for the proteins containing the S721A and S723A mutations. (C) Proteins with multiple serine mutations were expressed and analyzed with the single mutants by western blotting as in B. The presence of multiple mutations did not affect the migration of the bands as compared to the single mutants. (D) Lysates from the cells expressing S718A, S721A, and S723A were incubated with or without CIAP and were then analyzed by western blotting with a GFP antibody. All bands from mutant proteins collapsed upon treatment with phosphatase, similar to the native L3 protein, which was used as a positive control.

4.3.5 Identification of phosphorylated residues via mass spectrometry

We applied mass spectrometry of purified, over-expressed L3 as another, more global approach to identify phosphorylated residues in each of the two species. A FLAG-L3 fusion protein was over-expressed in a large culture of HEK 293 cells and the lysate was subjected to batch column purification with a FLAG resin. The eluate was either analyzed for post-translational modifications as a liquid sample in which both species were present, or was separated by SDS-PAGE for analysis of the two species separately.

Five phosphorylated residues were identified by this means, and were concentrated within the C-terminal region. Some of the specific phosphorylated residues could not be distinguished within a peptide. Ser682, two serines between Ser694 and Ser697, Ser699, and either Ser718 or Ser721 were found to be phosphorylated in L3 (Table 3). Three of the five phosphorylation sites were identified in both species, while one phosphorylation site, on either Ser718 or Ser721, was only found in the upper band eluted from the gel, corresponding to V2. Also, the phosphorylation site on Ser682 was identified only in the liquid sample and, therefore, its presence in either one or both of the species could not be distinguished. Taken together with the aforementioned results, it seems likely that Ser721, not Ser718, is the phosphorylated residue in the C-terminal peptide. In addition, the data on Ser721 supports our results from the serine

mutant analysis, suggesting that the phosphorylation of Ser721 is important for the existence of the slower-migrating L3 species, V2.

Table 3: Phosphopeptides analyzed by mass spectrometry

sequence	residues of NP_001001806	phosphorylated residues
DSLLVpSDEDEDDFL	677-691	S682
<u>SSSS</u> SpSLNESEFDNTNSSR	694-712	S694/S695/S696/S697 S699
RLPIF <u>S</u> RF <u>S</u> DSEK	713-725	S718/S721

The phosphorylated residues identified in this study are indicated with (p) in the peptide sequence. Other residues that may be phosphorylated, but could not be distinguished within a peptide, are underlined.

4.3.6 Functional activity of full length and truncated L3

The C-terminus is highly conserved among TTP family members within an animal species and even across species (Fig. 21). Only the tandem zinc finger (TZF) domain, the vital RNA-binding domain, shows an equally high level of conservation to that of the C-terminus. This degree of sequence similarity implies that the C-terminus is important to some functional aspect of the TTP family proteins.

Mouse TTP	TPAPRRRLPIFNRI SVSE-
Mouse L1	TLDNSRRLPIFSRLSISDD
Mouse L2	SLDPGRRLPIFSRLSISDD
Mouse L3	NTNSSRRLPIFSRFS DSEK
Cow TTP	PPAAPRRRLPIFNRI SVSE-
Sheep TTP	PPAAPRRRLPIFNRI SVSE-
Human TTP	PVAAPRRRLPIFNRI SVSE-
Mouse TTP	TPAPRRRLPIFNRI SVSE-
Rat TTP	PPAPRRRLPIFNRI SVSE-
Frog TTP	PPPSNKRLPIFNRLSVSD-
Fish TTP	DGSTGKRLSVFARMSVSD-
	:**.:* *:* *:

Figure 21: Conservation of the C-terminus within the TTP family

Sequences of the C-terminal regions of all mouse TTP family members and of TTP orthologues from a variety of species were aligned to show strong sequence conservation in this region. Symbols (*), (:), and (.) indicate identical, conserved and semi-conserved residues, respectively.

To determine the relevance of the C-terminus to the function of L3, we evaluated the activity of truncated L3, which contained amino acids 1-711, as compared to the full length protein. Specifically, we compared their ability to bind RNA and to promote the degradation and deadenylation of ARE-containing mRNA. Because one of the L3 species, perhaps V2, does not exist upon deletion of the C-terminus, these experiments might also reveal the importance of this species to the function of L3.

In gel electrophoretic mobility shift assays, lysates from cells over-expressing GFP or GFP-fused full length or truncated L3 were incubated with a radiolabeled TNF ARE RNA probe. The reactions were separated on a non-denaturing gel. Both the full length and truncated L3 appeared to be able to shift the RNA probe, while GFP alone

did not shift the probe (Fig. 22). The deletion of residues 712-725 did not affect the ability of L3 to directly bind RNA. As previously seen with L3, this assay was somewhat unsatisfactory due to aggregation of L3-RNA complexes in the wells of the gel.

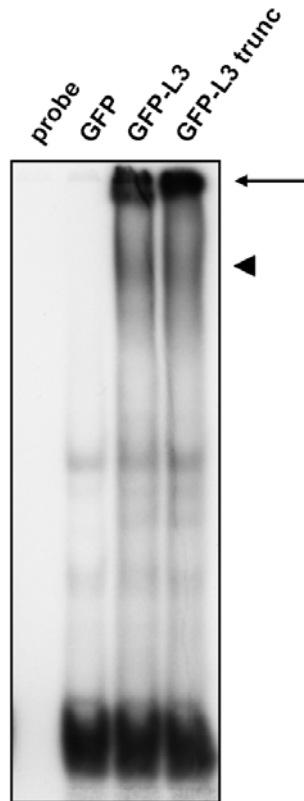


Figure 22: Binding activity of truncated L3

GFP and GFP fused to either full length or truncated L3 were over-expressed in HEK 293 cells. Total protein (20 μ g) from the resultant lysates was incubated with a RNA probe containing the ARE of TNF. The reactions were separated on a non-denaturing gel. L3-RNA complexes are denoted with an arrowhead (◄). Both full length and truncated L3 were able to bind and shift the TNF ARE RNA probe as compared to GFP alone, although in both cases most of the bound probe was trapped at the top of the gel (arrow).

In co-transfection assays, cells were transfected with a reporter RNA construct containing the protein coding region of MLP and the 3' UTR of TNF along with increasing amounts of full length and truncated L3 plasmids. Total RNA was isolated from these cells and was subjected to northern blotting using probes for MLP and GFP. The reporter RNA was degraded in the presence of both full length L3 and truncated L3 as compared to GFP alone (Fig. 23). Thus, it appeared that the C-terminus is not required for the ability of L3 to promote the degradation of ARE-containing mRNA in this assay.

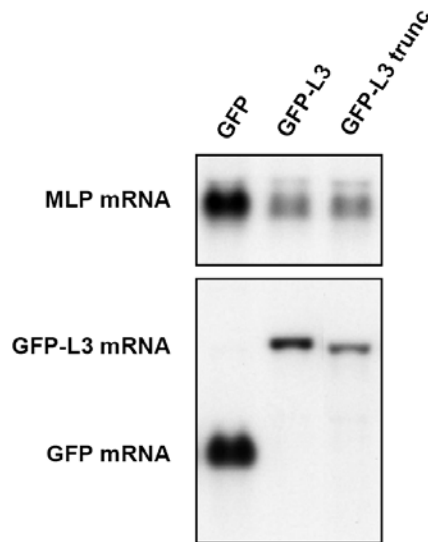


Figure 23: Ability of truncated L3 to promote mRNA degradation

GFP (10 ng DNA) and GFP fused to either full length L3 or truncated L3 (2.5 ng DNA) were co-transfected with 3 μ g of the MLP-TNF 3'UTR reporter in HEK 293 cells. Total transfected DNA was brought to 5 μ g with pBS. Total RNA was isolated and analyzed for the presence of MLP by northern blotting. Both full length L3 and truncated L3 promoted the degradation of the ARE-containing mRNA reporter, while GFP alone did not.

In cell-free experiments, lysates from cells over-expressing FLAG-tagged full length and truncated L3 were subjected to purification over a FLAG column. The purified proteins were incubated for 60 min with polyA ribonuclease (PARN) and a radiolabeled probe containing the TNF ARE followed by a polyA tail. The probes were then purified and subjected to electrophoresis. In reactions containing a low level of PARN, the amount of polyadenylated probe (ARE A₅₀) decreased and the amount of deadenylated probe (ARE A₀) increased upon addition of both full length L3 (Fig. 24A, lanes 3-7) and truncated L3 (Fig. 24B, lanes 3-7). The amount of PARN used in these experiments was, by itself, not sufficient to deadenylate the ARE A₅₀ probe (Fig. 24A and B, lane 2) and shows similar results to a control reaction in which EDTA is included to inhibit PARN (Fig. 24A and B, lane 1). Also, partially purified L3 alone could not deadenylate the probe (Fig. 24A and B, lane 8).

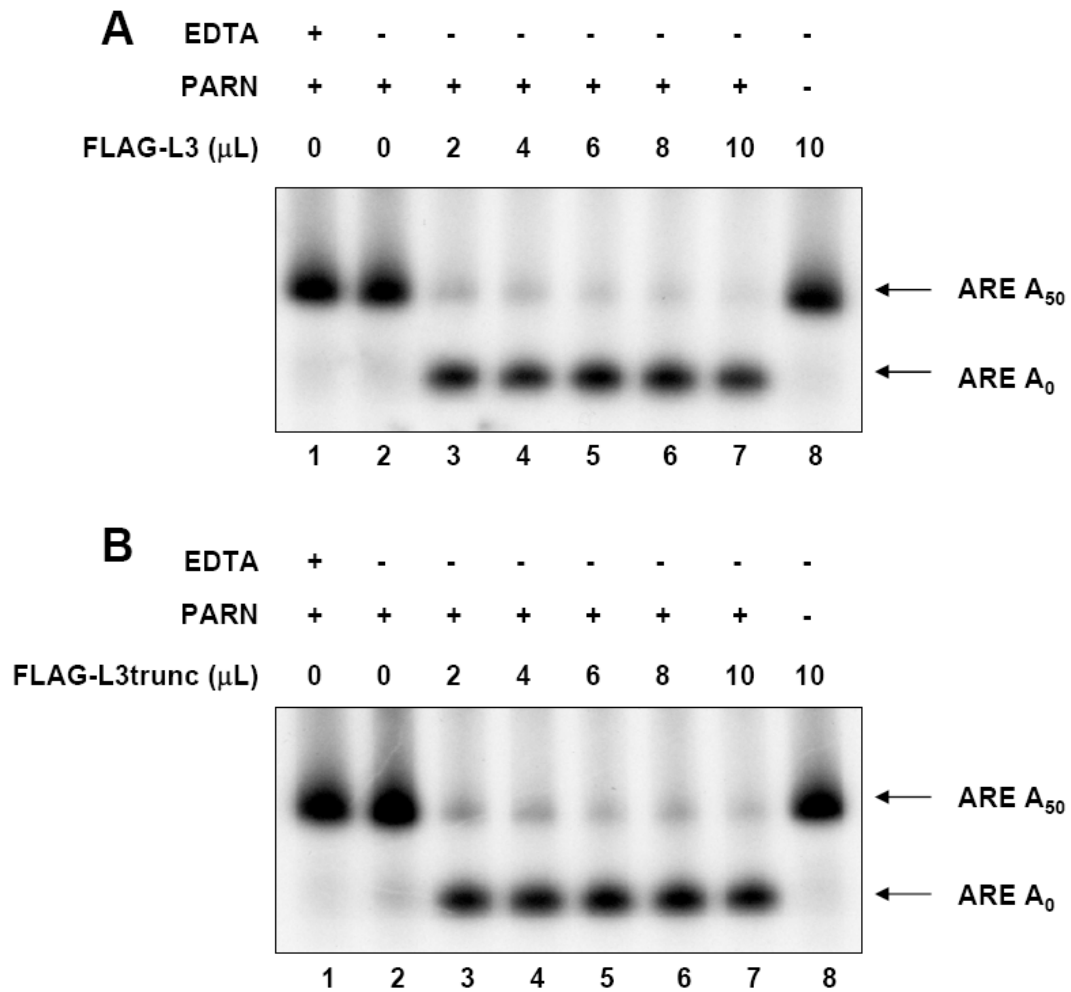


Figure 24: Ability of truncated L3 to promote mRNA deadenylation

FLAG-tagged full length and truncated L3 were expressed in HEK 293 cells and purified using a FLAG column. Increasing volumes of the first eluates were incubated with equal, low levels of PARN (lanes 3-7) and a TNF ARE A50 probe. Control incubations were also performed with PARN and EDTA (lane 1), PARN alone (lane 2), and L3 alone (lane 8). The reactions were terminated after 60 min and the probe was purified and subjected to electrophoresis. The deadenylated probe is indicated by the increased levels of ARE A0 and the decreased levels of ARE A50, only in the presence of full length L3 (**A**) or truncated L3 (**B**) and PARN together (lanes 3-8) and not in control reactions (lanes 1, 2, and 8).

A similar experiment was conducted in order to compare the rates of deadenylation between reactions containing full length or truncated L3. Reactions were analyzed at 15 min intervals over a period of 2 h. Reactions containing full length L3 (Fig. 25A) and truncated L3 (Fig. 25B) showed relatively equal rates of deadenylation. Collectively, these results suggest that the C-terminus is also not required for the ability of L3 to promote the deadenylation of the polyA probe in the presence of PARN.

In all of these functional assays, truncated L3 showed similar activity to that of full length L3, suggesting that the C-terminal 14 amino acids are not necessary for binding mRNA or promoting its deadenylation and degradation.

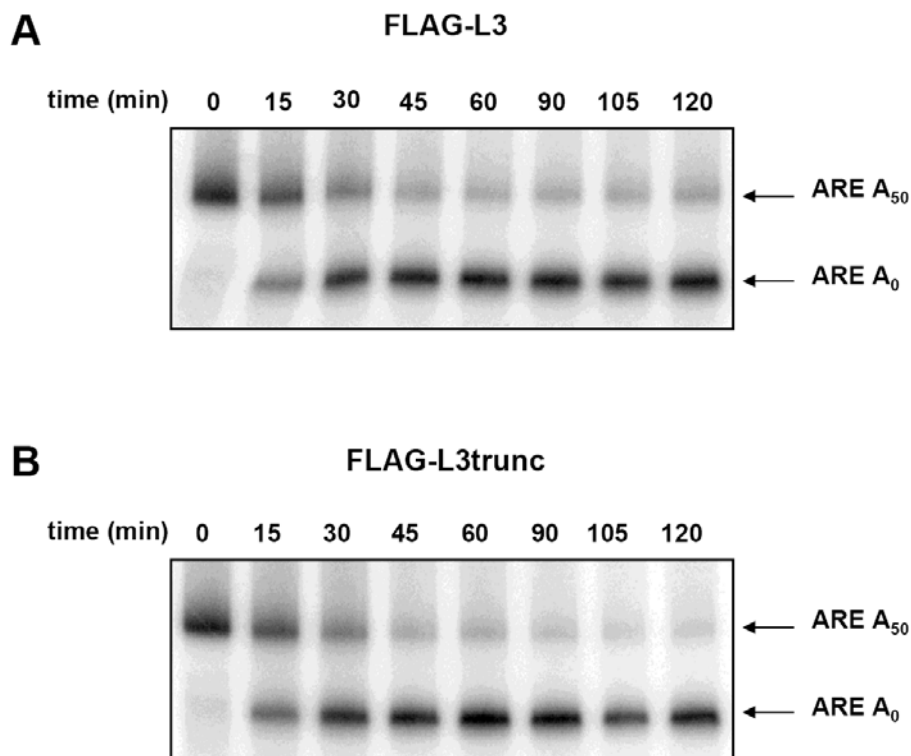


Figure 25: Analysis of reaction rate for deadenylation promoted by truncated L3

The ARE A₅₀ probe was incubated with PARN and similar amounts of either FLAG-purified full length or truncated L3. The amount of adenylated and deadenylated probe was analyzed every 15 min for a 2 h reaction by purifying the probe and subjecting it to electrophoresis. The rate of L3-promoted deadenylation in the presence of PARN was relatively equal in reactions containing full length L3 (A) and truncated L3 (B).

4.4 Discussion

In this study, we attempted to unveil the basis for the unique migration of the L3 protein in denaturing PAGE. We demonstrated that the faster-migrating species of L3, V1, does not exist as a result of alternative translation initiation, premature truncation, or proteolysis. Previous data from our lab revealed that the *Zfp36l3* gene does not have any introns (Blackshear et al., 2005); therefore, the two species do not exist as splicing isoforms.

We established the importance of both the overall phosphorylation status and the C-terminal region of L3 for the presence of both species. Our data suggest that L3 undergoes post-translational modifications, specifically phosphorylation within the C-terminal region, that affect the migration of the two species. Using mass spectrometry, we identified five novel phosphorylated residues: Ser682, two serines between Ser694 and Ser697, Ser699, and either Ser718 or Ser721. Although our analysis covered about 76% of the L3 sequence, it is important to note that we may not have identified all modified residues because we only analyzed over-expressed L3 in HEK 293 cells. The phosphorylation of L3 could differ in other cell types or in placental tissue in which it is normally expressed. Methylation sites were also identified through our mass spectrometry analysis, although future study is required to demonstrate their significance.

The post-translational modification of many proteins, including TTP, plays a critical role in regulating their activity. The phosphorylation state of TTP regulates its activity, localization, and stability by influencing its ability to bind other proteins, such as 14-3-3 (Hitti et al., 2006; Johnson et al., 2002; Stoecklin et al., 2004). The phosphorylation state of L3 may affect its function in a similar manner.

Our data suggest that phosphorylation of Ser721 alone affects the migration of the L3 protein in denaturing PAGE. Because the migration of the S721A mutant was unexpectedly slower than the normal lower band of L3, it is possible that the serine to alanine mutation in this position could lead to increased phosphorylation at one or more novel sites, resulting in an addition of size and charge. A preliminary mass spectrometry experiment on the S721A mutant has recently been conducted to test this possibility and, so far, we have no evidence for increased phosphorylation at another site.

It will also be important to identify the kinase responsible for phosphorylating this residue. Ser721 is in a sequence context compatible with phosphorylation by either protein kinase A or casein kinase 2, whose recognition motifs are RX(S/T)X and (S/T)XX(D/E), respectively. The invariant arginine residue two amino acids upstream of Ser721 in L3 as well as in other family members (see alignment in Fig. 6) supports the identity of this site as a protein kinase A site, but this has not been tested directly.

We hypothesize that the phosphorylation of Ser721 may influence the function of L3. This serine residue is conserved in all TTP orthologues from all vertebrates tested, as well as in the other family members. In fact, Ser336 in mouse TTP, which corresponds to Ser721 in L3, has been determined to be phosphorylated [noted in (Cao et al., 2006)], but the function of this modification in TTP is not known.

A potential role of the C-terminal region in the function of L3 was also examined in this study. Because the C-terminal sequences are highly conserved among TTP family members and within TTP across species, we hypothesized that this region may be important to the function of L3, as well all members of this family. The TZF domain, which is responsible for binding mRNA, is the only other region conserved to this degree across orthologues and related proteins. Mutation of the TZF in TTP results in the loss of the mRNA binding and destabilizing activity of the protein (Lai et al., 2002).

Here, we analyzed a deletion mutant that lacked the conserved C-terminus of L3 and, thus, also lacked species V2. Functional studies of this mutant compared to the wild type protein revealed that this region was apparently not necessary for binding mRNA or promoting its deadenylation and degradation. It is possible that the C-terminal region of L3 is important for the function of the protein but we were unable to uncover evidence for this in these specific experiments.

Further study is required to expand our knowledge of this region and its significance. A yeast two hybrid screen involving the C-terminal 14 amino acids of L3 is currently underway in attempt to identify proteins that bind to this conserved region. It is possible that L3 may recruit proteins involved in mRNA decay through binding to the C-terminus. By binding decapping enzymes, deadenylases, or nucleases, L3 could bring an mRNA in contact with decay machinery in order to be degraded. Because previous studies of TTP have suggested that the phosphorylation state of the protein is important for its stability , we are also investigating the possibility that the C-terminal domain and its phosphorylation state are important for the stability of the protein in cells.

In summary, the two species of L3 seen in denaturing PAGE likely exist due to phosphorylation of one or more serines in the conserved C-terminal domain, including Ser721. This phosphorylation event may regulate the interaction of L3 with other proteins, or may alter some behavior of the protein itself, such as its availability for proteolytic decay. Given its high degree of conservation with other TTP family members, we anticipate that this C-terminal domain will prove to be important for some function or behavior in the entire class of proteins.

5. Conclusions and future directions

Intricate control over gene expression is required for many cell functions, growth and response to extra- and intra-cellular signals. Although gene transcription has been the main focus of previous work, increasing attention is being paid to the regulation of gene expression at the post-transcriptional level.

The tristetraprolin (TTP) family of CCCH tandem zinc finger (TZF) proteins functions to downregulate certain subsets of genes at the post-transcriptional level in one type of AU-rich element (ARE)-mediated mRNA decay. The proteins of this family work in coordination with other ARE binding proteins and co-factors to control the stability of mRNA transcripts. TTP proteins exert their mRNA destabilizing activity by binding mRNAs at their AREs, and then promoting their deadenylation by mechanisms that remain unknown. More intricate regulation of gene expression is achieved through controlling the expression, activity, and localization of TTP family proteins themselves.

The mammalian members of the TTP family are TTP, ZFP36L1 (L1), ZFP36L2 (L2), and ZFP36L3 (L3). All of these proteins seem to use the same mechanism of action, but probably target different sets of mRNAs due to their differential expression. L3 is the most recently identified member of this family, with its initial description published in 2005 (Blackshear et al., 2005). The work included in this dissertation was performed

to further our understanding of this protein, with specific attention paid to its unique characteristics as compared to TTP, L1, and L2.

5.1 Contributions of the nuclear localization signal, nuclear export signal, and unique repeat domain to the subcellular localization of L3

TTP, L1, and L2 have been shown to shuttle between the nucleus and cytoplasm, using typical hydrophobic amino acid-rich nuclear export sequences, and nuclear localization sequences found within the TZF domain. In contrast, our lab previously demonstrated that green fluorescent protein (GFP)-labeled L3, expressed in HEK 293 cells, remained cytosolic, even in the presence of the nuclear export blocker leptomycin B (Blackshear et al., 2005).

In this work, we showed that the conserved tandem zinc finger domain of L3 contained an active nuclear localization signal (NLS), similar to those found in TTP, L1, and L2. The TZF domain alone was able to translocate into the nucleus. Mutation of two conserved inter-finger arginines affected the ability of the L3 NLS to direct nuclear import, but also affected the ability of L3 to bind mRNA. Thus, these mutations most likely altered the fundamental structure of the TZF domain and, therefore, can not be considered diagnostic of a functional NLS. Further study is required to pinpoint the critical NLS residues for all of the TTP family members. It will be necessary to identify residues that affect the nuclear import of these proteins but do not affect their mRNA

binding activity. In doing this, we can assume that the identities of the amino acids are solely responsible for the nuclear import of the protein.

We also demonstrated that the C-terminal sequence corresponding to the nuclear export signal (NES) in L1 and L2 was non-functional, and thus did not contribute to the cytosolic localization. The amino acid sequence of L3 did not contain any other NES-like sequences, which are characteristically leucine-rich with defined spacing, even at the site of the TTP NES at the N-terminus.

Because the NLS is functional and the NES is non-functional, L3 should localize to the nucleus. Instead, the L3 protein is cytoplasmic in both transfected cells and in tissue. We determined that the unique C-terminal repeat domain is a cytoplasmic localization domain. This unusual sequence, which is unique to L3 among TTP family members, could override the activity of the NLS, preventing the import of L3 into the nucleus. The mechanism by which the repeat domain exerts its cytoplasmic localization is presently unknown. This domain has some primary sequence similarities to the membrane spanning domain of mucin and has several predicted transmembrane helices. In our confocal microscopy study of endogenous L3, we did not detect membrane association although we were not explicitly investigating this possibility. Further study of the repeat domain will be necessary to determine if this region binds L3 to a membrane or anchors it in the cytoplasm through association with other proteins or

structures. The repeat domain also adds sheer size to L3 and could, possibly in this manner alone, prevent its transport through the nuclear pore.

The role of nucleocytoplasmic shuttling in the function of TTP, L1, and L2 is not well understood. These proteins have been hypothesized to facilitate the transport of mRNAs into the cytoplasm, but this activity has not yet been confirmed. The shuttling of TTP, L1, and L2 may also be a means to control their activity. They could be sequestered in the nucleus and then released into the cytoplasm when their mRNA destabilizing activity is needed.

In contrast to the other mammalian members of this protein family, our work has demonstrated that L3 is a “full-time” cytosolic protein, rather than a nucleocytoplasmic shuttling protein. The significance of this difference in subcellular localization to the physiology of placental trophoblast cells, where L3 seems to be specifically expressed, remains to be determined.

5.2 The role of L3 in placental mRNA decay

The integrity of the placenta, the site of exchange between the mother and fetus during gestation, is necessary for successful fetal development and survival. L3 has been implicated in rodent placenta physiology by virtue of its specific expression in this organ in mouse, rat, and hamster (Blackshear et al., 2005)(D.J. Stumpo, unpublished data). Our analysis of L3 mRNA and protein expression through northern blotting, and

immunoblotting with a specific L3 antibody, confirmed and supplemented this finding. We demonstrated that L3 mRNA and protein levels peak during mid-gestation, at the time that the placenta becomes mature. Through immunostaining of mouse placenta at maximum L3 protein expression, we demonstrated that L3 was located only in the cytoplasm of trophoblast giant cells and labyrinthine trophoblast cells. L3 mRNA expression has also been detected in the yolk sac (Blackshear et al., 2005), although its microscopic expression pattern in this tissue has not been examined.

As the fourth member of the TTP family to be discovered in rodents, L3 is presumed to function in a similar manner to its relatives by binding to AREs in the 3' untranslated regions (UTRs) of certain mRNAs, causing their deadenylation and accelerated degradation. In an attempt to identify physiological target transcripts for L3 in the placenta, we performed a microarray analysis of RNA isolated by immunoprecipitation of L3 from mid-gestation mouse placenta extracts. Approximately 400 transcripts were significantly enriched in immunoprecipitates with a specific anti-L3 antiserum compared to those obtained with a pre-immune serum. Many of these transcripts contained one or more typical TTP family member ARE binding sites with the canonical sequence UUAUUUAUU. However, a few transcripts did not contain ARE sequences; these could be false positives, or they could be brought down with L3 through indirect binding within a complex.

B-type natriuretic peptide (BNP) was the top candidate transcript identified by this analysis, with a mean enrichment of eight-fold in the anti-L3 immunoprecipitates. The 3'UTR of BNP contains multiple, overlapping AREs, which would support binding by L3. While BNP is a hormone well-known for its function in cardiac physiology, it has been proposed to function in placenta physiology as well, although this role is poorly defined. Natriuretic peptides have been previously reported to be expressed in mouse placenta and have been suggested to play a local role in dilation of placental vessels (Cameron et al., 1996). BNP expressed in the placenta could also act in an endocrine fashion, to control vasodilation in either the fetus or mother.

In this work, we detected BNP mRNA in the placenta through northern analysis and in situ hybridization histochemistry. We also demonstrated direct binding of L3 to BNP mRNA in gel electrophoretic mobility shift assays, and documented L3-stimulated decay of BNP mRNA in a cell co-transfection system. These data introduce the interesting possibility that L3 can regulate the stability of the BNP transcript in a physiological setting, resulting in changes in BNP synthesis and secretion, either locally in the placenta or even systemically.

Further work will be necessary to verify this and other potential physiological L3 targets identified through this study. An important validation experiment will involve the analysis of BNP mRNA stability, and the stability of other potential targets, in L3-

deficient cells as compared to wild type cells. A cultured cell line that endogenously expresses L3 has been elusive to date, and a knockout mouse has not yet been created. We recently found that L3 transcripts can be detected in a trophoblast stem cell line after differentiation in culture; these cells could be used in future L3 knockdown experiments. We expect that the ongoing development of the L3 knockout mouse will be completed within the next several weeks. This mouse line should provide invaluable information regarding the importance of L3 in physiology through its phenotype, as well as through study of L3 mRNA targets within its placental cells.

5.3 The conserved C-terminus and the phosphorylation of L3

Another unique characteristic of L3, along with its subcellular localization and specific expression, is its unusual migration in denaturing polyacrylamide gel electrophoresis (PAGE). The L3 protein migrates as two distinct bands of M_r ~90,000 and ~100,000. Through phosphatase treatment and analysis of a C-terminal truncation mutant, we determined that the slower-migrating species is phosphorylated and that the 14 C-terminal amino acids (712-725) are required for the formation of one of the species.

More detailed analysis of point mutants within the C-terminus revealed that phosphorylation of Ser721 and/or Ser723 could be significant for the existence of one of the species. The gel migration of the alanine mutants used in this study was perplexing. By preventing the phosphorylation of Ser721 and Ser723 through their mutation to

alanine, we expected these proteins to migrate more quickly in denaturing PAGE than the native, phosphorylated protein. Instead, the gel migration of these mutants matched the slower-migrating species of wild type L3. The mechanistic basis of this finding is currently unknown. It is possible that phosphorylation of Ser721 or Ser723 could lead to increases in the phosphorylation of other residues, or to the addition of other post-translational modifications, which could result in this unexpected migration.

In order to identify phosphorylation sites through a more global approach, we analyzed purified L3 from cultured cells through mass spectroscopy. We identified five phosphorylation sites, which were concentrated within the C-terminal region: Ser682, two serines between Ser694 and Ser697, Ser699, and either Ser718 or Ser721. The phosphorylation of L3 could function to regulate its mRNA destabilizing activity, localization, or expression, similar to TTP. Extensive studies are required to further describe the modifications of L3 and their consequences.

We also studied the effect of the conserved C-terminus on the function of L3. We found that a C-terminal truncated L3 protein was still able to bind an ARE RNA probe in gel electrophoretic mobility shift assays. The truncated protein could also promote the deadenylation and degradation of ARE-containing RNA reporters in cell-free assays and co-transfection experiments. The C-terminal region is highly conserved in the mammalian proteins of the TTP family. We expect the C-terminus to play an important

part in the function of TTP, L1, L2, and L3, but future study is required to determine this role. A possibility that we are currently investigating is that the C-terminus may be a binding domain for other proteins, such as mRNA decay enzymes, and could be used to bring these factors into contact with mRNAs that are targeted for degradation by TTP proteins.

5.4 Concluding remarks

Through this work, we have expanded our knowledge of the unique localization and expression of L3. In addition, we have identified potential physiological mRNA targets and phosphorylation sites. The next steps in the study of this TTP family member will most likely focus on experiments using its knockout mice. We suspect that L3 deficiency may cause embryonic lethality, due to developmental or functional defects in the trophoblast layers of the placenta. However, this hypothesis remains to be evaluated in the coming months.

The study of L3 is important, not only for understanding its mechanism of action and biological role, but also for understanding the functions and characteristics of the entire TTP protein family. Because these proteins are closely related, data from an individual member may be applicable to the entire family of proteins. Furthermore, because L3 is only expressed in rodents, one or more of the other TTP family members may assume its role in the placentas of non-rodent mammals. If we can apply our

knowledge of L3 to the relevant TTP family member in man, we may be able to better understand placental physiology and its perturbations in humans.

Appendix

All mouse experiments were conducted according to the U.S. Public Health Service policy on the humane care and use of laboratory animals. All animal procedures used in this study were approved by the National Institute of Environmental Health Sciences Institutional Animal Care and Use Committee.

References

- Anderson, P., and Kedersha, N. (2009). RNA granules: post-transcriptional and epigenetic modulators of gene expression. *Nat Rev Mol Cell Biol* 10, 430-436.
- Audic, Y., and Hartley, R.S. (2004). Post-transcriptional regulation in cancer. *Biol Cell* 96, 479-498.
- Bakheet, T., Williams, B.R., and Khabar, K.S. (2003). ARED 2.0: an update of AU-rich element mRNA database. *Nucleic Acids Res* 31, 421-423.
- Barreau, C., Paillard, L., and Osborne, H.B. (2005). AU-rich elements and associated factors: are there unifying principles? *Nucleic Acids Res* 33, 7138-7150.
- Blackshear, P.J., Lai, W.S., Kennington, E.A., Brewer, G., Wilson, G.M., Guan, X., and Zhou, P. (2003). Characteristics of the interaction of a synthetic human tristetraprolin tandem zinc finger peptide with AU-rich element-containing RNA substrates. *J Biol Chem* 278, 19947-19955.
- Blackshear, P.J., Phillips, R.S., Ghosh, S., Ramos, S.B., Richfield, E.K., and Lai, W.S. (2005). Zfp3613, a rodent X chromosome gene encoding a placenta-specific member of the Tristetraprolin family of CCCH tandem zinc finger proteins. *Biol Reprod* 73, 297-307.
- Bogerd, H.P., Fridell, R.A., Benson, R.E., Hua, J., and Cullen, B.R. (1996). Protein sequence requirements for function of the human T-cell leukemia virus type 1 Rex nuclear export signal delineated by a novel in vivo randomization-selection assay. *Mol Cell Biol* 16, 4207-4214.
- Bouchard, L., Tchernof, A., Deshaies, Y., Marceau, S., Lescelleur, O., Biron, S., and Vohl, M.C. (2007). ZFP36: a promising candidate gene for obesity-related metabolic complications identified by converging genomics. *Obes Surg* 17, 372-382.
- Boulikas, T. (1993). Nuclear localization signals (NLS). *Crit Rev Eukaryot Gene Expr* 3, 193-227.
- Brewer, B.Y., Malicka, J., Blackshear, P.J., and Wilson, G.M. (2004). RNA sequence elements required for high affinity binding by the zinc finger domain of tristetraprolin: conformational changes coupled to the bipartite nature of Au-rich MRNA-destabilizing motifs. *J Biol Chem* 279, 27870-27877.

Brook, M., Tchen, C.R., Santalucia, T., McIlrath, J., Arthur, J.S., Saklatvala, J., and Clark, A.R. (2006). Posttranslational regulation of tristetraprolin subcellular localization and protein stability by p38 mitogen-activated protein kinase and extracellular signal-regulated kinase pathways. *Mol Cell Biol* 26, 2408-2418.

Busse, M., Schwarzburger, M., Berger, F., Hacker, C., and Munz, B. (2008). Strong induction of the Tis11B gene in myogenic differentiation. *Eur J Cell Biol* 87, 31-38.

Cameron, V.A., Aitken, G.D., Ellmers, L.J., Kennedy, M.A., and Espiner, E.A. (1996). The sites of gene expression of atrial, brain, and C-type natriuretic peptides in mouse fetal development: temporal changes in embryos and placenta. *Endocrinology* 137, 817-824.

Cao, H., Deterding, L.J., Venable, J.D., Kennington, E.A., Yates, J.R., 3rd, Tomer, K.B., and Blakeshear, P.J. (2006). Identification of the anti-inflammatory protein tristetraprolin as a hyperphosphorylated protein by mass spectrometry and site-directed mutagenesis. *Biochem J* 394, 285-297.

Cao, H., Kelly, M.A., Kari, F., Dawson, H.D., Urban, J.F., Jr., Coves, S., Roussel, A.M., and Anderson, R.A. (2007). Green tea increases anti-inflammatory tristetraprolin and decreases pro-inflammatory tumor necrosis factor mRNA levels in rats. *Journal of Inflammation (London, England)* 4, 1.

Cao, H., Tuttle, J.S., and Blakeshear, P.J. (2004). Immunological characterization of tristetraprolin as a low abundance, inducible, stable cytosolic protein. *J Biol Chem* 279, 21489-21499.

Cao, H., Urban, J.F., Jr., and Anderson, R.A. (2008). Insulin increases tristetraprolin and decreases VEGF gene expression in mouse 3T3-L1 adipocytes. *Obesity (Silver Spring)* 16, 1208-1218.

Caput, D., Beutler, B., Hartog, K., Thayer, R., Brown-Shimer, S., and Cerami, A. (1986). Identification of a common nucleotide sequence in the 3'-untranslated region of mRNA molecules specifying inflammatory mediators. *Proc Natl Acad Sci U S A* 83, 1670-1674.

Carballo, E., Lai, W.S., and Blakeshear, P.J. (1998). Feedback inhibition of macrophage tumor necrosis factor- α production by tristetraprolin. *Science* 281, 1001-1005.

Carballo, E., Lai, W.S., and Blakeshear, P.J. (2000). Evidence that tristetraprolin is a physiological regulator of granulocyte-macrophage colony-stimulating factor messenger RNA deadenylation and stability. *Blood* 95, 1891-1899.

- Carrick, D.M., Chulada, P., Donn, R., Fabris, M., McNicholl, J., Whitworth, W., and Blackshear, P.J. (2006). Genetic variations in ZFP36 and their possible relationship to autoimmune diseases. *J Autoimmun* 26, 182-196.
- Carthew, R.W., and Sontheimer, E.J. (2009). Origins and Mechanisms of miRNAs and siRNAs. *Cell* 136, 642-655.
- Chen, C.Y., and Shyu, A.B. (1995). AU-rich elements: characterization and importance in mRNA degradation. *Trends Biochem Sci* 20, 465-470.
- Ciais, D., Cherradi, N., Bailly, S., Grenier, E., Berra, E., Pouyssegur, J., Lamarre, J., and Feige, J.J. (2004). Destabilization of vascular endothelial growth factor mRNA by the zinc-finger protein TIS11b. *Oncogene* 23, 8673-8680.
- Cuthbertson, B.J., Liao, Y., Birnbaumer, L., and Blackshear, P.J. (2008). Characterization of zfs1 as an mRNA-binding and -destabilizing protein in *Schizosaccharomyces pombe*. *J Biol Chem* 283, 2586-2594.
- De, J., Lai, W.S., Thorn, J.M., Goldsworthy, S.M., Liu, X., Blackwell, T.K., and Blackshear, P.J. (1999). Identification of four CCCH zinc finger proteins in *Xenopus*, including a novel vertebrate protein with four zinc fingers and severely restricted expression. *Gene* 228, 133-145.
- Dreyfus, M., and Regnier, P. (2002). The poly(A) tail of mRNAs: bodyguard in eukaryotes, scavenger in bacteria. *Cell* 111, 611-613.
- Duan, H., Cherradi, N., Feige, J.J., and Jefcoate, C. (2009). cAMP-dependent posttranscriptional regulation of steroidogenic acute regulatory (STAR) protein by the zinc finger protein ZFP36L1/TIS11b. *Mol Endocrinol* 23, 497-509.
- Fechir, M., Linker, K., Pautz, A., Hubrich, T., Forstermann, U., Rodriguez-Pascual, F., and Kleinert, H. (2005). Tristetraprolin regulates the expression of the human inducible nitric-oxide synthase gene. *Mol Pharmacol* 67, 2148-2161.
- Fischer, U., Huber, J., Boelens, W.C., Mattaj, I.W., and Luhrmann, R. (1995). The HIV-1 Rev activation domain is a nuclear export signal that accesses an export pathway used by specific cellular RNAs. *Cell* 82, 475-483.

- Frederick, E.D., Ramos, S.B., and Blackshear, P.J. (2008). A unique C-terminal repeat domain maintains the cytosolic localization of the placenta-specific tristetraprolin family member ZFP36L3. *J Biol Chem* 283, 14792-14800.
- Goldstrohm, A.C., and Wickens, M. (2008). Multifunctional deadenylase complexes diversify mRNA control. *Nat Rev Mol Cell Biol* 9, 337-344.
- Gomperts, M., Pascall, J.C., and Brown, K.D. (1990). The nucleotide sequence of a cDNA encoding an EGF-inducible gene indicates the existence of a new family of mitogen-induced genes. *Oncogene* 5, 1081-1083.
- Hitti, E., Iakovleva, T., Brook, M., Deppenmeier, S., Gruber, A.D., Radzioch, D., Clark, A.R., Blackshear, P.J., Kotlyarov, A., and Gaestel, M. (2006). Mitogen-activated protein kinase-activated protein kinase 2 regulates tumor necrosis factor mRNA stability and translation mainly by altering tristetraprolin expression, stability, and binding to adenine/uridine-rich element. *Mol Cell Biol* 26, 2399-2407.
- Hochstrasser, M. (2009). Origin and function of ubiquitin-like proteins. *Nature* 458, 422-429.
- Holcberg, G., Kossenjans, W., Brewer, A., Miodovnik, M., and Myatt, L. (1995). The action of two natriuretic peptides (atrial natriuretic peptide and brain natriuretic peptide) in the human placental vasculature. *Am J Obstet Gynecol* 172, 71-77.
- Hudson, B.P., Martinez-Yamout, M.A., Dyson, H.J., and Wright, P.E. (2004). Recognition of the mRNA AU-rich element by the zinc finger domain of TIS11d. *Nat Struct Mol Biol* 11, 257-264.
- Ji, Z., Lee, J.Y., Pan, Z., Jiang, B., and Tian, B. (2009). Progressive lengthening of 3' untranslated regions of mRNAs by alternative polyadenylation during mouse embryonic development. *Proc Natl Acad Sci U S A* 106, 7028-7033.
- Jing, Q., Huang, S., Guth, S., Zarubin, T., Motoyama, A., Chen, J., Di Padova, F., Lin, S.C., Gram, H., and Han, J. (2005). Involvement of microRNA in AU-rich element-mediated mRNA instability. *Cell* 120, 623-634.
- Johnson, B.A., Stehn, J.R., Yaffe, M.B., and Blackwell, T.K. (2002). Cytoplasmic localization of tristetraprolin involves 14-3-3-dependent and -independent mechanisms. *J Biol Chem* 277, 18029-18036.

- Kanoh, J., Sugimoto, A., and Yamamoto, M. (1995). Schizosaccharomyces pombe zfs1+ encoding a zinc-finger protein functions in the mating pheromone recognition pathway. *Mol Biol Cell* 6, 1185-1195.
- Keene, J.D., Komisarow, J.M., and Friedersdorf, M.B. (2006). RIP-Chip: the isolation and identification of mRNAs, microRNAs and protein components of ribonucleoprotein complexes from cell extracts. *Nat Protoc* 1, 302-307.
- Keene, J.D., and Tenenbaum, S.A. (2002). Eukaryotic mRNPs may represent posttranscriptional operons. *Mol Cell* 9, 1161-1167.
- Kohler, A., and Hurt, E. (2007). Exporting RNA from the nucleus to the cytoplasm. *Nat Rev Mol Cell Biol* 8, 761-773.
- Kornblihtt, A.R. (2007). Coupling transcription and alternative splicing. *Adv Exp Med Biol* 623, 175-189.
- Kudo, N., Matsumori, N., Taoka, H., Fujiwara, D., Schreiner, E.P., Wolff, B., Yoshida, M., and Horinouchi, S. (1999). Leptomycin B inactivates CRM1/exportin 1 by covalent modification at a cysteine residue in the central conserved region. *Proc Natl Acad Sci U S A* 96, 9112-9117.
- Kudo, N., Wolff, B., Sekimoto, T., Schreiner, E.P., Yoneda, Y., Yanagida, M., Horinouchi, S., and Yoshida, M. (1998). Leptomycin B inhibition of signal-mediated nuclear export by direct binding to CRM1. *Exp Cell Res* 242, 540-547.
- Lai, W.S., and Blackshear, P.J. (2001). Interactions of CCCH zinc finger proteins with mRNA: tristetraprolin-mediated AU-rich element-dependent mRNA degradation can occur in the absence of a poly(A) tail. *J Biol Chem* 276, 23144-23154.
- Lai, W.S., Carballo, E., Strum, J.R., Kennington, E.A., Phillips, R.S., and Blackshear, P.J. (1999). Evidence that tristetraprolin binds to AU-rich elements and promotes the deadenylation and destabilization of tumor necrosis factor alpha mRNA. *Mol Cell Biol* 19, 4311-4323.
- Lai, W.S., Carballo, E., Thorn, J.M., Kennington, E.A., and Blackshear, P.J. (2000). Interactions of CCCH zinc finger proteins with mRNA. Binding of tristetraprolin-related zinc finger proteins to Au-rich elements and destabilization of mRNA. *J Biol Chem* 275, 17827-17837.

- Lai, W.S., Kennington, E.A., and Blackshear, P.J. (2002). Interactions of CCCH zinc finger proteins with mRNA: non-binding tristetraprolin mutants exert an inhibitory effect on degradation of AU-rich element-containing mRNAs. *J Biol Chem* 277, 9606-9613.
- Lai, W.S., Kennington, E.A., and Blackshear, P.J. (2003). Tristetraprolin and its family members can promote the cell-free deadenylation of AU-rich element-containing mRNAs by poly(A) ribonuclease. *Mol Cell Biol* 23, 3798-3812.
- Lai, W.S., Parker, J.S., Grissom, S.F., Stumpo, D.J., and Blackshear, P.J. (2006). Novel mRNA targets for tristetraprolin (TTP) identified by global analysis of stabilized transcripts in TTP-deficient fibroblasts. *Mol Cell Biol* 26, 9196-9208.
- Lai, W.S., Stumpo, D.J., and Blackshear, P.J. (1990). Rapid insulin-stimulated accumulation of an mRNA encoding a proline-rich protein. *J Biol Chem* 265, 16556-16563.
- Li, M., Yee, D., Magnuson, T.R., Smithies, O., and Caron, K.M. (2006). Reduced maternal expression of adrenomedullin disrupts fertility, placentation, and fetal growth in mice. *J Clin Invest* 116, 2653-2662.
- Lim, A.T., and Gude, N.M. (1995). Atrial natriuretic factor production by the human placenta. *J Clin Endocrinol Metab* 80, 3091-3093.
- Ma, Q., Wadleigh, D., Chi, T., and Herschman, H. (1994). The *Drosophila* TIS11 homologue encodes a developmentally controlled gene. *Oncogene* 9, 3329-3334.
- Mangus, D.A., Evans, M.C., and Jacobson, A. (2003). Poly(A)-binding proteins: multifunctional scaffolds for the post-transcriptional control of gene expression. *Genome Biol* 4, 223.
- Matsuda, D., Sato, H., and Maquat, L.E. (2008). Chapter 9. Studying nonsense-mediated mRNA decay in mammalian cells. *Methods Enzymol* 449, 177-201.
- Moore, M.J. (2005). From birth to death: the complex lives of eukaryotic mRNAs. *Science* 309, 1514-1518.
- Munshi, A., Shafi, G., Aliya, N., and Jyothy, A. (2009). Histone modifications dictate specific biological readouts. *J Genet Genomics* 36, 75-88.

- Murata, T., Yoshino, Y., Morita, N., and Kaneda, N. (2002). Identification of nuclear import and export signals within the structure of the zinc finger protein TIS11. *Biochem Biophys Res Commun* 293, 1242-1247.
- Nigg, E.A. (1997). Nucleocytoplasmic transport: signals, mechanisms and regulation. *Nature* 386, 779-787.
- Ogilvie, R.L., Abelson, M., Hau, H.H., Vlasova, I., Blackshear, P.J., and Bohjanen, P.R. (2005). Tristetraprolin down-regulates IL-2 gene expression through AU-rich element-mediated mRNA decay. *J Immunol* 174, 953-961.
- Pemberton, L.F., and Paschal, B.M. (2005). Mechanisms of receptor-mediated nuclear import and nuclear export. *Traffic* 6, 187-198.
- Pennanen, P.T., Sarvilinna, N.S., and Ylikomi, T.J. (2009). Gene expression changes during the development of estrogen-independent and antiestrogen-resistant growth in breast cancer cell culture models. *Anticancer Drugs* 20, 51-58.
- Phillips, R.S., Ramos, S.B., and Blackshear, P.J. (2002). Members of the tristetraprolin family of tandem CCCH zinc finger proteins exhibit CRM1-dependent nucleocytoplasmic shuttling. *J Biol Chem* 277, 11606-11613.
- Pierrat, O.A., Mikitova, V., Bush, M.S., Browning, K.S., and Doonan, J.H. (2007). Control of protein translation by phosphorylation of the mRNA 5'-cap-binding complex. *Biochem Soc Trans* 35, 1634-1637.
- Potter, L.R., Yoder, A.R., Flora, D.R., Antos, L.K., and Dickey, D.M. (2009). Natriuretic peptides: their structures, receptors, physiologic functions and therapeutic applications. *Handb Exp Pharmacol*, 341-366.
- Puig, S., Vergara, S.V., and Thiele, D.J. (2008). Cooperation of two mRNA-binding proteins drives metabolic adaptation to iron deficiency. *Cell Metab* 7, 555-564.
- Ramos, S.B., Stumpo, D.J., Kennington, E.A., Phillips, R.S., Bock, C.B., Ribeiro-Neto, F., and Blackshear, P.J. (2004). The CCCH tandem zinc-finger protein Zfp3612 is crucial for female fertility and early embryonic development. *Development* 131, 4883-4893.
- Reppe, S., Olstad, O.K., Rian, E., Gautvik, V.T., Gautvik, K.M., and Jemtland, R. (2004). Butyrate response factor 1 is regulated by parathyroid hormone and bone

morphogenetic protein-2 in osteoblastic cells. *Biochem Biophys Res Commun* 324, 218-223.

Resnik, J.L., Hong, C., Resnik, R., Kazanegra, R., Beede, J., Bhalla, V., and Maisel, A. (2005). Evaluation of B-type natriuretic peptide (BNP) levels in normal and preeclamptic women. *Am J Obstet Gynecol* 193, 450-454.

Sachs, A.B., and Varani, G. (2000). Eukaryotic translation initiation: there are (at least) two sides to every story. *Nat Struct Biol* 7, 356-361.

Sandler, H., and Stoecklin, G. (2008). Control of mRNA decay by phosphorylation of tristetraprolin. *Biochem Soc Trans* 36, 491-496.

Shaw, G., and Kamen, R. (1986). A conserved AU sequence from the 3' untranslated region of GM-CSF mRNA mediates selective mRNA degradation. *Cell* 46, 659-667.

Sonenberg, N. (2008). eIF4E, the mRNA cap-binding protein: from basic discovery to translational research. *Biochem Cell Biol* 86, 178-183.

Stoecklin, G., Stubbs, T., Kedersha, N., Wax, S., Rigby, W.F., Blackwell, T.K., and Anderson, P. (2004). MK2-induced tristetraprolin:14-3-3 complexes prevent stress granule association and ARE-mRNA decay. *Embo J* 23, 1313-1324.

Stoecklin, G., Tenenbaum, S.A., Mayo, T., Chittur, S.V., George, A.D., Baroni, T.E., Blackshear, P.J., and Anderson, P. (2008). Genome-wide analysis identifies interleukin-10 mRNA as target of tristetraprolin. *J Biol Chem* 283, 11689-11699.

Stumpo, D.J., Byrd, N.A., Phillips, R.S., Ghosh, S., Maronpot, R.R., Castranio, T., Meyers, E.N., Mishina, Y., and Blackshear, P.J. (2004). Chorioallantoic fusion defects and embryonic lethality resulting from disruption of Zfp36L1, a gene encoding a CCCH tandem zinc finger protein of the Tristetraprolin family. *Mol Cell Biol* 24, 6445-6455.

Suda, M., Ogawa, Y., Tanaka, K., Tamura, N., Yasoda, A., Takigawa, T., Uehira, M., Nishimoto, H., Itoh, H., Saito, Y., *et al.* (1998). Skeletal overgrowth in transgenic mice that overexpress brain natriuretic peptide. *Proc Natl Acad Sci U S A* 95, 2337-2342.

Tamura, N., Ogawa, Y., Chusho, H., Nakamura, K., Nakao, K., Suda, M., Kasahara, M., Hashimoto, R., Katsuura, G., Mukoyama, M., *et al.* (2000). Cardiac fibrosis in mice lacking brain natriuretic peptide. *Proc Natl Acad Sci U S A* 97, 4239-4244.

- Taylor, G.A., Carballo, E., Lee, D.M., Lai, W.S., Thompson, M.J., Patel, D.D., Schenkman, D.I., Gilkeson, G.S., Broxmeyer, H.E., Haynes, B.F., *et al.* (1996a). A pathogenetic role for TNF alpha in the syndrome of cachexia, arthritis, and autoimmunity resulting from tristetraprolin (TTP) deficiency. *Immunity* 4, 445-454.
- Taylor, G.A., Thompson, M.J., Lai, W.S., and Blackshear, P.J. (1996b). Mitogens stimulate the rapid nuclear to cytosolic translocation of tristetraprolin, a potential zinc-finger transcription factor. *Mol Endocrinol* 10, 140-146.
- Thompson, M.J., Lai, W.S., Taylor, G.A., and Blackshear, P.J. (1996). Cloning and characterization of two yeast genes encoding members of the CCCH class of zinc finger proteins: zinc finger-mediated impairment of cell growth. *Gene* 174, 225-233.
- van der Velden, A.W., and Thomas, A.A. (1999). The role of the 5' untranslated region of an mRNA in translation regulation during development. *Int J Biochem Cell Biol* 31, 87-106.
- Varki, A. (1993). Biological roles of oligosaccharides: all of the theories are correct. *Glycobiology* 3, 97-130.
- Varnum, B.C., Ma, Q.F., Chi, T.H., Fletcher, B., and Herschman, H.R. (1991). The TIS11 primary response gene is a member of a gene family that encodes proteins with a highly conserved sequence containing an unusual Cys-His repeat. *Molecular and cellular biology* 11, 1754-1758.
- Walker, W.H., Fitzpatrick, S.L., Barrera-Saldana, H.A., Resendez-Perez, D., and Saunders, G.F. (1991). The human placental lactogen genes: structure, function, evolution and transcriptional regulation. *Endocr Rev* 12, 316-328.
- Wang, X., and Tanaka Hall, T.M. (2001). Structural basis for recognition of AU-rich element RNA by the HuD protein. *Nat Struct Biol* 8, 141-145.
- Weng, L., Dai, H., Zhan, Y., He, Y., Stepaniants, S.B., and Bassett, D.E. (2006). Rosetta error model for gene expression analysis. *Bioinformatics* 22, 1111-1121.
- Wilusz, C.J., Wormington, M., and Peltz, S.W. (2001). The cap-to-tail guide to mRNA turnover. *Nat Rev Mol Cell Biol* 2, 237-246.

Wu, F., Lee, S., Schumacher, M., Jun, A., and Chakravarti, S. (2008). Differential gene expression patterns of the developing and adult mouse cornea compared to the lens and tendon. *Exp Eye Res* 87, 214-225.

Xu, N., Chen, C.Y., and Shyu, A.B. (1997). Modulation of the fate of cytoplasmic mRNA by AU-rich elements: key sequence features controlling mRNA deadenylation and decay. *Mol Cell Biol* 17, 4611-4621.

Yanagawa, B., and Nagaya, N. (2007). Adrenomedullin: molecular mechanisms and its role in cardiac disease. *Amino Acids* 32, 157-164.

Yoneda, Y. (2000). Nucleocytoplasmic protein traffic and its significance to cell function. *Genes Cells* 5, 777-787.

Yotsumoto, S., Shimada, T., Cui, C.Y., Nakashima, H., Fujiwara, H., and Ko, M.S. (1998). Expression of adrenomedullin, a hypotensive peptide, in the trophoblast giant cells at the embryo implantation site in mouse. *Dev Biol* 203, 264-275.

Zubiaga, A.M., Belasco, J.G., and Greenberg, M.E. (1995). The nonamer UUAUUUAUU is the key AU-rich sequence motif that mediates mRNA degradation. *Mol Cell Biol* 15, 2219-2230.

Biography

Elizabeth Dawn Frederick

Born to Dana and Gerard Frederick on September 27, 1981 in Attleboro, MA.

Education

Ph.D. in Biochemistry, Certificate in Biological Chemistry
Duke University, Durham, NC, June 2009.

B.A. in Chemistry and Biology
Colby College, Waterville, ME, May 2003.

Publications

Frederick, ED, Ramos, SB, Blackshear, PJ. A unique carboxyl-terminal repeat domain maintains the cytosolic localization of the placenta-specific tristetraprolin family member ZFP36L3. *J Biol Chem.* 2008; 283: 14792-800.

Sawyer, GA, **Frederick, ED**, Millard, JT. Flanking sequences modulate diepoxide and mustard cross-linking efficiencies at the 5'-GNC site. *Chem Res Toxicol.* 2004; 17: 1057-63.

Millard, JT, Katz, JL, Goda, J, **Frederick, ED**, Pierce, SE, Speed, TJ, Thamattoor, DM. DNA interstrand cross-linking by a mycotoxic diepoxide. *Biochimie* 2004; 86: 419-23.

Honors and Awards

2008: NIEHS Laboratory of Signal Transduction Rodbell award

2003: Cum laude, Colby College

2003: American Institute of Chemists, top chemist in the Colby College class of 2003